A review of in situ real-time monitoring techniques for membrane fouling in the biotechnology, biorefinery and food sectors

Rudolph Gregor, Virtanen Tiina, Ferrando Montserrat, Güell Carmen, Lipnizki Frank, Kallioinen Mari

DOI: 10.1016/j.memsci.2019.117221

Manuscript Details

Manuscript number	MEMSCI_2019_1007_R2
Title	A review of in situ real-time monitoring techniques for membrane fouling in the biotechnology, biorefinery and food sectors
Article type	Review article

Abstract

Pressure-driven membrane processes are often used for the separation and purification of organic compounds originating from biomass. However, membrane fouling remains a challenge as these biobased streams have a very complex composition and comprise a high fouling tendency. Conventional, the fouling is monitored based on either a decrease in flux or an increase in pressure over time. Those conventional techniques provide no information on the location, composition or amount of fouling. As fouling is often cumulative, it will be detected as a loss of performance. Once fouling becomes irreversible, it is often not possible to clean the membrane without chemicals and the filtration/separation process has to be stopped eventually. In situ real-time monitoring of membrane fouling could provide dynamic information on the development of fouling, allowing optimization of the process. This paper reviews the state of the art in in situ monitoring techniques that could be applied to membrane processes in the biotechnology, biorefinery and food sectors and briefly reflects on the current awareness of in situ monitoring techniques among experienced industrial users of membrane processes. The physical principles as well as the strengths and weaknesses are addressed, and potentially, promising techniques are identified.

Keywords	Pressure-driven membrane processes; Organic fouling; Proteins; Polysaccharides; Online monitoring
Manuscript category	Fouling / Membrane characterization

Corresponding Author	Gregor Rudolph
Corresponding Author's Institution	Lund University
Order of Authors	Gregor Rudolph, Tiina Virtanen, Montserrat Ferrando, Carme Güell, Frank Lipnizki, Mari Kallioinen
Suggested reviewers	Thomas Schäfer, Alberto Figoli, Matthias Wessling, John Chew

Submission Files Included in this PDF

File Name [File Type]

Coverletter.docx [Cover Letter]

Comments of Reviewers 2.docx [Response to Reviewers]

Highlights.docx [Highlights]

GraphicalAbstract.pdf [Graphical Abstract]

rewari_TVGRvJMS.pdf [Manuscript File]

Submission Files Not Included in this PDF

File Name [File Type]

JMS.zip [LaTeX Source File]

To view all the submission files, including those not included in the PDF, click on the manuscript title on your EVISE Homepage, then click 'Download zip file'.

Dear Editor of the Journal of Membrane Science,

After consultation and agreement with Editor-in-Chief Prof. A. Zydney, we would hereby like to submit our invited review with the title “A review of in situ real-time monitoring techniques for membrane fouling in the biotechnology, biorefinery and food sectors” to the Journal of Membrane Science.

Our manuscript identifies and critically evaluates promising in situ real-time monitoring techniques for industrial membrane applications based on prior research done in the field. The technical principles and practical implementation of these techniques in membrane processes are explained; main strengths and weaknesses are discussed; and the type of information obtained and potential applications are effectively summarized. Future online monitoring opportunities and challenges related to membrane fouling control in the sectors biotechnology, biorefinery and food are considered.

We review the state of the art in in situ real-time monitoring of membrane fouling for the pressure driven membrane processes microfiltration, ultrafiltration, nanofiltration and reverse osmosis from 2004 until the present day (2018) with focus on membrane fouling in the food, biotech and biorefinery sectors. In contrast to previous work focusing on individual foulants or fouling phenomena, our manuscript highlights monitoring techniques and their potential applications in membrane processes with focus not only on proteins but also on polysaccharides and aromatic compounds. Moreover, we examine the use of monitoring techniques with reference to all membrane modules.
We include all relevant established and potential techniques for in situ real-time monitoring of membrane fouling based on the latest. However, monitoring techniques on biofouling especially for water treatment are beyond the scope of this manuscript.

Overall, we are strongly convinced that our manuscript is a very comprehensive and critical overview on existing in situ real-time monitoring techniques for membrane fouling - a topic of greatest importance for the further development of membrane technology in industrial applications.

On behalf of all of the authors, thank you for your consideration.
Sincerely,
Gregor Rudolph

Reviewer 1

I provided a review for the original submission and identified as Reviewer #1.

I feel that Table 2 is still incomplete and my previous comments were not fully addressed.

[From previous comments: “Basic requirement or Pre-requisite” should be a heading e.g. transparent membrane, flat, rigid etc. “Flow/Static/Pulse” should also be a heading]

The operability, type and choice of detection techniques strongly depends the basic requirement or pre-requisite information available for the system of interest.

The suitability of the techniques also depend on the operating condition i.e. whether it is suitable for cross flow / dead-end system.

The above two points provide an indication of the advantages and disadvantages of each technique. Therefore, these should be included in Table 2, not just in the text.

Response: We would again like to thank reviewer 1 for the valuable comments and the resulting improvements on our manuscript.

Regarding the basic requirement/ pre-requisite information, we checked each technique again and, to our knowledge, there is only on technique that would have such a basic requirement as it was mentioned by the reviewer, i.e. transparent membrane. Requirements such as the membrane module, i.e. flat-sheet membrane, are already covered by the category Membrane in Table 2. Other basic requirements such as e.g. fluorescence, low concentration or rigidity of the foulant/ fouling layer are, from our point, better considered as limitations/ weaknesses or disadvantage (as the reviewer wrote) instead of a pre-requisite and are therefore already presented in Table 3.

Regarding the operating mode, we realized that one can distinguish between static and flow mode but a specific operating condition such as cross flow or dead-end is not required for any technique. We therefore improved the manuscript and added this information under the section “In situ real-time monitoring techniques” on page 5 and added the category Operation in Table 2 which distinguishes between static or flow operation mode.

Highlights

- In the given sectors, adsorptive membrane fouling monitoring is the most needed
- Many monitoring techniques are available for use in fundamental and lab scale
- Majority of techniques offer monitoring of fouling layer thickness and distribution
- Limited amount of composition monitoring techniques are available
- Evaluation which technique to choose requires profound knowledge

In situ Real-time Monitoring of Membrane Fouling

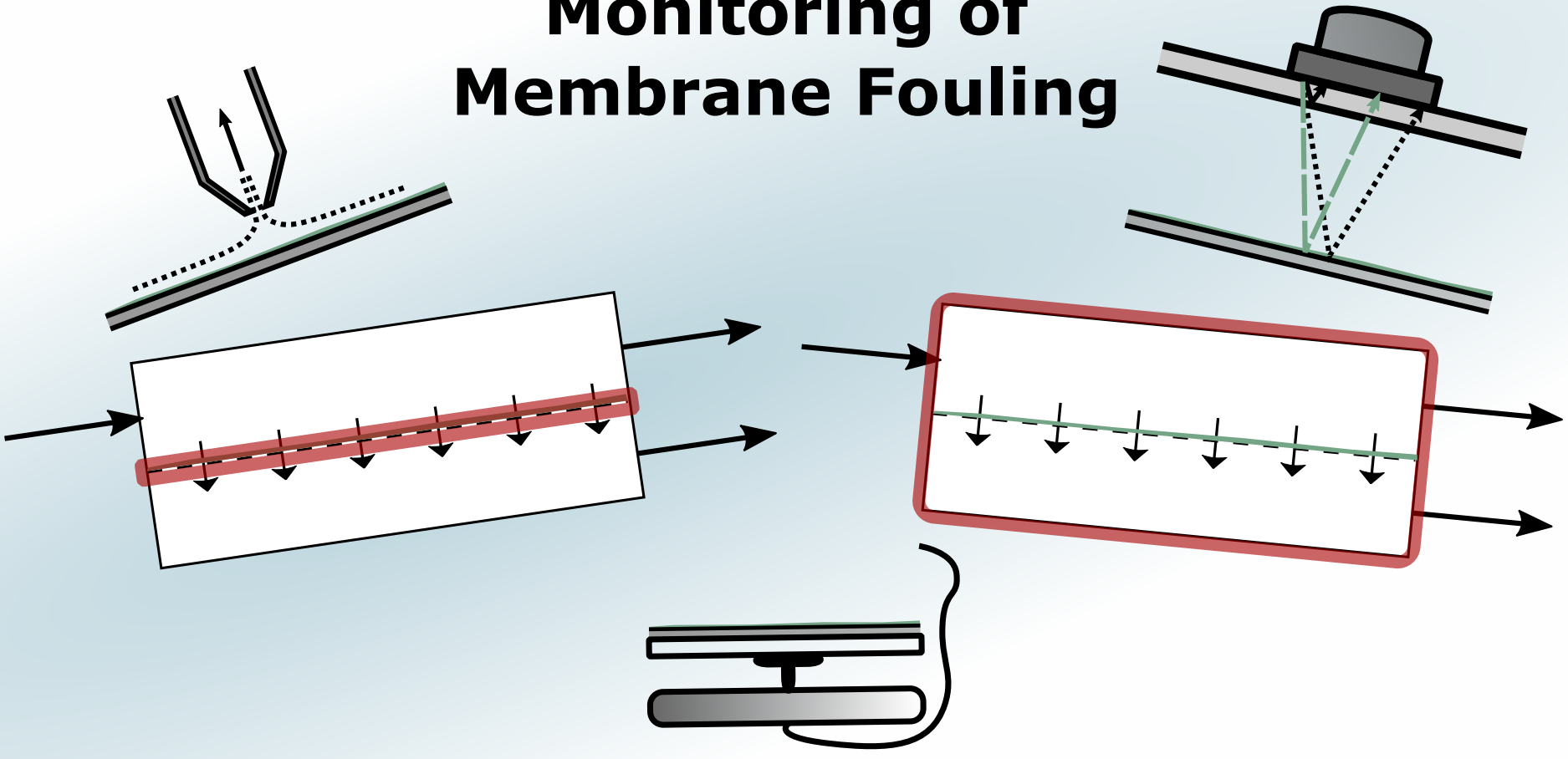

A review of in situ real-time monitoring techniques for membrane fouling in the biotechnology, biorefinery and food sectors

G. Rudolph[a,*,1], T. Virtanen[b,1], M. Ferrando[c], C. Güell[c], F. Lipnizki[a] and M. Kallioinen[b]

[a]Department of Chemical Engineering, Lund University, P.O.Box 124, SE-221 00 Lund, Sweden
[b]School of Engineering Science, LUT University, P.O.Box 20, 53851 Lappeenranta, Finland
[c]Departament d,Enginyeria Química, Universitat Rovira i Virgili Avda, Països Catalans 26, 45007 Tarragona, Spain

ARTICLE INFO

Keywords:
Pressure-driven membrane processes
Organic fouling
Proteins
Polysaccharides
Online monitoring

ABSTRACT

Pressure-driven membrane processes are often used for the separation and purification of organic compounds originating from biomass. However, membrane fouling remains a challenge as these bio-based streams have a very complex composition and comprise a high fouling tendency. Conventional, the fouling is monitored based on either a decrease in flux or an increase in pressure over time. Those conventional techniques provide no information on the location, composition or amount of fouling. As fouling is often cumulative, it will be detected as a loss of performance. Once fouling becomes irreversible, it is often not possible to clean the membrane without chemicals and the filtration/separation process has to be stopped eventually. In situ real-time monitoring of membrane fouling could provide dynamic information on the development of fouling allowing optimization of the process. This paper reviews the state of the art in in situ monitoring techniques that could be applied to membrane processes in the biotechnology, biorefinery and food sectors and briefly reflects on the current awareness of in situ monitoring techniques among experienced industrial users of membrane processes. The physical principles as well as the strengths and weaknesses are addressed, as well as potentially and promising techniques are identified.

Contents

1 Introduction 2
2 Organic membrane fouling 3
3 In situ real-time monitoring 3
4 In situ real-time monitoring techniques 5
5 Visual and microscopic observations 5
6 Direct observation 5
7 Laser-based techniques 7
8 Image analysis 7
9 Confocal laser scanning microscopy 7
10 Multiphoton microscopy 9
11 Light based spectroscopy 10
12 Surface plasmon resonance 10
13 Ellipsometry 11
14 Other light based methods 12
15 Acoustic techniques 13
16 Photoacoustic spectroscopy 13
17 Ultrasonic time-domain reflectometry 13
18 Quartz crystal microbalance with dissipation 14
19 Interferometry 15
20 Holographic interferometry 15
21 Optical coherence tomography 16
22 Magnetic resonance imaging 17
23 NMR/MRI 17
24 X-ray and neutron imaging 18
25 X-ray microimaging 18
26 Small-angle scattering techniques 19
27 Vibrational spectroscopy and microspectroscopy 20
28 Infrared spectroscopy 20
29 Raman spectroscopy 21
30 Other Raman-based microspectroscopic methods 22
31 Controlled-current techniques 22
32 Electrical impedance spectroscopy 22
33 Streaming potential 23

*Corresponding author
Gregor.Rudolph@chemeng.lth.se (G. Rudolph)
[1]Equal contribution

34 Voltammetry and chronopotentiometry **24**

35 Controlled stress techniques **25**

36 Fluid dynamic gauging **25**

37 Conclusions and future perspectives **26**

1. Introduction

Over recent decades, membrane technology has become established in several industrial areas. Despite the success of membrane processes in the separation and purification of organic compounds originating from biomass, membrane fouling is still a problem especially due to the complexity and high fouling tendency of bio-based streams. Membrane fouling is defined as "a process resulting in loss of performance of a membrane due to the deposition of suspended or dissolved substances on its external surfaces, at its pore openings, or within its pores" [1] and may decrease filtration capacity, change rejection cut-off, reduce membrane lifetime, and increase operational costs. Since membrane fouling is hindering the comprehensive implementation of membranes in the biotechnology, biorefinery and food sectors, the development of effective fouling monitoring and prevention strategies are urgently required. Hence, online monitoring techniques have the potential to achieve one of the most important goals in the development of membrane-based technologies, namely a non-fouling or controlled-fouling process with stable flux and retention [2].

Conventional fouling monitoring approaches are based on measuring the decrease in flux or the increase in pressure drop. However, these provide no information on the location, composition or amount of foulants. Related effects, such as concentration polarization, might also have significant effects on the flux or transmembrane pressure, which might lead to misinterpretation of data. Thus, membrane process operations, and strategies for the control and prevention of fouling are more or less based on trial and error [2, 3]. In addition, it is virtually impossible to detect early-stage fouling using conventional methods. By the time fouling is detected by a significant loss in performance, an irreversible fouling layer may have been developed [4, 5]. In contrast to reversible fouling, performance loss caused by irreversible fouling cannot be recovered easily. As a result, online monitoring techniques providing dynamic information on membrane fouling could have positive effects on membrane processes and hence reduce the overall costs [4].

Effective methods of monitoring and controlling fouling would not only reduce membrane fouling, but would also lead to improved membrane cleaning. Back-flushing or chemical cleaning is usually applied to recover the flux, but both lead to operational downtime. Moreover, the complex nature of organic process streams complicates the choice of cleaning agents, while the extensive use of chemical cleaning agents can reduce the lifetime of the membrane. Real-time monitoring tools would allow the timing of cleaning to be optimized and the most suitable sequence of cleaning agents to be used. Furthermore, lower quantities of cleaning agents could be used to remove less extensive fouling layers [5, 6]. Advanced process control could reduce operational downtime and minimize membrane damage, thus increasing the lifetime of the membranes and reducing costs.

A survey we conducted with selected relevant and experienced industrial users of membrane processes [7], revealed that a majority (>90 %) of the users see real-time monitoring as important for industrial membrane processes. None of the interviewees have permanently implemented real-time monitoring in their membrane processes. However, a quarter of the interviewees knew some of the existing techniques. Of them, 50 % are considering or have already conducted studies with tools belonging to light based spectroscopy, acoustic and controlled current techniques.

In this paper, we review the state of the art in in situ real-time monitoring of membrane fouling for the pressure-driven membrane processes microfiltration (MF), ultrafiltration (UF), nanofiltration (NF) and reverse osmosis (RO) from 2004 until the present day (2018). Three very comprehensive papers on the topic were presented in 2004, in which methods for the characterization of protein fouling [8] as well as monitoring of concentration polarization and cake layer build-up during pressure-driven membrane filtration [9, 10] were reviewed. The present paper should be seen as a continuation of these earlier reviews. A great deal of research has been carried out since 2004 on the characterization of fouling by proteins, peptides and amino acids [11], and more recently on methods of monitoring fouling of hollow-fiber membranes [12]. Furthermore, an extensive review of methods of probing solid/liquid surfaces at the molecular level has been presented by Zaera [13], and many of these methods can easily be applied to membrane technology. A paper on the use of molecular spectroscopy methods for studying membrane fouling [14] and a state-of-the-art review of methods for membrane surface characterization [15] have recently been published, both of which include aspects interesting for in situ real-time monitoring of organic membrane fouling.

A number of recent reviews have focused on biofouling in RO and fouling in membrane bioreactors, for example, [16] and [17, 18], as well as the characterization and in situ visualization of biofouling in spiral wound membranes [19] and the monitoring and control of biofouling during water treatment [20]. Drews [21] and Meng et al. [22] have also recently reviewed methods for the visualization and characterization of membrane fouling in membrane bioreactors. Therefore, these areas are not included in the present review.

Our paper includes well-established techniques, as well as novel techniques that have recently been developed or are still too sophisticated for broader applications. The presented techniques are structured according to their physical working principles. The most simple, visual and microscopic techniques are reviewed first and followed by light-based spectroscopic techniques and analogous sound wave-based acoustic techniques. Thereafter follows interferometric techniques which are also based on interaction between

waves and matter. It is than continued with techniques based on nuclear magnetic resonance, an overview of the use of X-rays and neutrons, as well as vibrational techniques. The last sections focus on the use of controlled current and controlled stress techniques.

Promising in situ real-time monitoring techniques for industrial membrane applications are identified. The technical principles, practical implementation in membrane processes, main strengths and weaknesses, the type of information obtained and potential applications are discussed. Future online monitoring opportunities and challenges related to membrane fouling control in the biotechnology, biorefinery and food sectors are considered.

2. Organic membrane fouling

Membrane fouling by organic compounds is a serious problem in membrane filtration in the biotechnology, biorefinery and food sectors [23, 24, 25], and can be reversible or irreversible. Although reversible fouling causes loss of permeability, affecting the filterability and productivity, it can be removed by rinsing. In contrast to this, irreversible membrane fouling is the result of the adsorption of foulants on or in the membrane, and, if at all, can only be removed by thorough membrane cleaning. Fouling in the biotechnology, biorefinery and food sectors is generally caused by macromolecules, organic colloids, adhesion of microorganisms (biofouling), and inorganic compounds (e.g scaling). Membrane fouling by proteins is a considerable problem in food applications [23], as both proteins and polysaccharides occur in macromolecular and colloidal forms. In pulp mill biorefineries, organic carbohydrates such as polysaccharides, as well as extractives such as phenolic compounds, aromatic carboxyl acids and fatty acids, and lignin are the main causes of membrane fouling [24, 25]. The understanding of the interactions between colloidal particles and dissolved organics on the fouling process in the biotechnology, biorefinery and food sectors is limited due to the complex nature of the streams involved. Table 1 gives an overview of the different types of fouling, fouling mechanisms and the main foulants in these sectors. The examples reported in the literature underrate the importance of adsorptive fouling. Especially in bio-based streams, adsorptive fouling is a major problem that occurs immediately after the process stream gets in contact with the membrane. A combination of the different fouling mechanisms affecting together the membrane performance severely. To understand the fouling development, the fouling layer composition and concentration as well as its thickness build-up, consistency, strength and distribution are the most essential parameters to be known.

A great deal of research has been performed on membrane fouling with model compounds. The most commonly used model protein foulants are bovine serum albumin (BSA) and β-lactoglobulin (LG), while common model polysaccharide foulants are sodium alginate (SA) and dextran. Extracellular polymeric substances (EPS) have been identified as another important contributor to membrane fouling. EPS are secreted by microorganisms, and contain various functional groups. EPS are commonly used to study more complex membrane fouling as they represent a mixture of proteins and polysaccharides. However, it has to be kept in mind that studies performed with model compounds can give only a limited understanding on the membrane fouling process as model compound solutions rarely represent the complex nature of bio-based process streams.

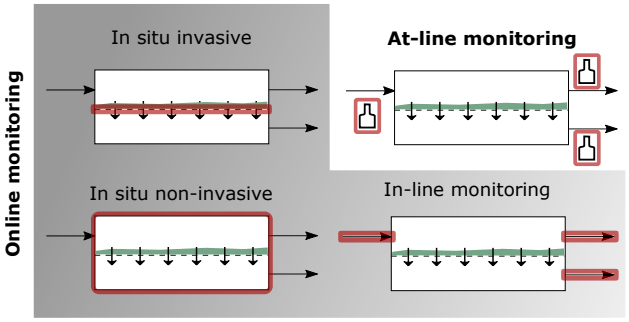

Figure 1: Schematic overview of various monitoring approaches. In the context of this work, online monitoring includes in situ monitoring as well as in-line monitoring. Whereas in situ monitoring comprises either of introducing a probe into the membrane module (invasive) or monitoring the process through the module (non-invasive), and in-line monitoring means to continuously analyze feed, retentate and/or permeate streams. Online monitoring is fundamentally different from at-line monitoring which necessitates sampling with subsequent sample analysis.

3. In situ real-time monitoring

Within the framework of this study, in situ real-time monitoring should be understood as online observation of a rapid response to a signal change without exposing the sample to the environment (see Fig. 1). Methods that can be used for real-time monitoring include optical methods and controlled-current methods. Spectroscopic methods, such as Raman spectroscopy, can be used to collect discrete data over a period of time, and their response time is so rapid that observations of dynamic phenomena are possible. Online monitoring eliminates the need to take samples from the process line, and data can thus be acquired in real time without interrupting the process. This review focuses on invasive and non-invasive in situ monitoring techniques rather than in-line or at-line monitoring techniques. Fouling can be measured at one spot as single-point measurement or over the whole membrane/module as an average measurement. Deciding which measurement mode to use highly depends on the process. However, in general, the knowledge on the development of the fouling layer on the membrane surface (in situ invasive) or in the membrane module (in situ non-invasive) will in contrast to in-line and at-line techniques be the most valuable techniques to understand the build-up of fouling, adjusting the process parameters, and tailoring suitable membrane cleaning protocols.

A common criticism of online analysis is its poor sensitivity compared to conventional analytical methods. Thus,

Table 1: Reported examples of fouling types, fouling mechanisms, and main foulants in the biotechnology, biorefinery and food sectors (modified from [25] and [26])

	Process	Membrane type	Fouling type	Mechanism	Main foulant
Biotechnology sector	Cell harvesting	MF	Organic		Cell particulates, proteins, lipids
	Sterile filtration	MF	Organic		Cells, proteins
	Virus filtration	UF	Organic	Gel layer, pore blocking	Protein aggregates
	Protein purification	MF, UF, NF	Organic	Gel layer, pore blocking, adsorption	Proteins, amino acids
Biorefinery sector	Lignin recovery	MF, UF, NF	Organic	Cake layer, gel layer, pore blocking, adsorption	Lignin, extractives
	Hemicelluloses recovery	MF, UF, NF	Organic	Cake layer, gel layer	Hemicelluloses
	Inhibitor removal	NF	Organic	–	Sugars or inhibitors
	Enzyme recovery	MF, UF	Organic	Cake layer, gel layer	Enzymes, lignocellulosic, particles
	Algae harvesting	UF	Biofouling	Cake layer	Algae
			Organic	Adsorption	Algogenic organic matter
	Acetic acid production	MF, UF	Biofouling	Deposition	Microorganisms and fermentation broth
			Organic	Pore blocking	
	Biogas production	MF, UF	Biofouling		
	Bio-oil production	MF	Inorganic	Cake layer	Char
	Biodiesel production	MF, UF, NF	Organic	Pore blocking	Glycerol agglomerates
	Effluent, sludge and wastewater treatment	MBR	Biofouling		EPS, SMP, flocs, bacteria
			Organic	Cake layer, gel layer, pore blocking	Colloidal particles, proteins, polysaccharides, humic acids
			Inorganic	Cake layer	Ca, Al, Ba and Fe salts
Food sector	Dairy processing	MF, UF	Biofouling	Gel layer, adsorption	Microorganisms
			Organic		Proteins, carbohydrates, fats
			Inorganic	Scaling	Minerals (Ca, Mg, phosphate)
	Vegetable protein production	UF	Organic		Fats, proteins, polysaccharides
			Inorganic	Deposition	Minerals
	Vegetable oil processing	MF, UF, NF, RO	Organic	Adsorption	Pigments, wax, lipids, fatty acids, glycerides
	Clarification of sugarcane juice	MF, UF	Organic	Gel layer, adsorption	Sucrose, polysaccharides, lipids, proteins, starches, phenolics
	Fruit juice treatment	MF, UF, NF, RO	Organic	Gel layer	Suspended solids, pectin, cellulose, starch, proteins, polyphenols
	Wine and beer treatment	MF, RO	Organic	Pore blocking	Proteins, polyphenols, yeast
	Polyphenol recovery	MF, UF, NF, RO	Organic	–	Suspended solids, pectin

MF: Microfiltration, UF: Ultrafiltration, NF: Nanofiltration, RO: Reverse osmosis, MBR: Membrane bioreactor,
EPS: Extracellular polymeric substances, SMP: Soluble microbial products

online sensors should be at least as sensitive as, or even more sensitive than, sensors used for at-line or in-line measurements. Therefore, the specificity and sensitivity of sensors must be improved [27]. The reliability of single-point measurements can also be questioned. The representativeness can be improved, for example, by using a flexible multi-probe system that enables independent concurrent measurements at different control points [28]. In addition, motion between the probe and the monitored surface may complicate data analysis. As cleanliness of observation windows and probe tips is essential for the collection of reliable data, self-cleaning materials and anti-fouling probe designs are also desirable.

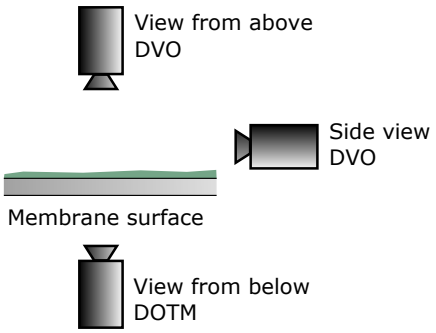

Figure 2: Schematic illustration of the DO techniques direct visualization on the membrane (DVO) and direct observation through the membrane (DOTM) for in situ real-time monitoring of membrane fouling.

4. In situ real-time monitoring techniques

Fouling processes in the biotechnology, biorefinery and food sectors are usually rather complex due to the heterogeneity of bio-based streams. Therefore, methods of monitoring fouling must be tailored to each individual case [24]. Ideally, fouling monitoring methods should be able to provide deep insight into fouling mechanisms, i.e., the chemical composition, structure and interactions of the foulants during the membrane filtration processes [14].

Table 2 provides an overview of the in situ real-time monitoring techniques for membrane fouling that are discussed in more detail in this review. The table, shows the type of information the techniques provide, such as the foulants concentration or fouling layer thickness, distribution or composition. The scale of application for each technique is categorized as fundamental, lab, pilot or industrial scale. Fundamental means that it is useful in gaining an understanding of adsorption/ desorption processes, using model solutions and model membrane films. Industrial indicates that the technique has either already been applied, or has the potential to be applied, on the industrial scale in the very near future. Furthermore, each technique was assigned to at least one type of membrane module, namely: flat-sheet, hollow-fiber, tubular or spiral wound, that has been investigated, or has the potential to be investigated, with the specific technique in the future. The operation mode is given but not differentiated in e.g. cross-flow or dead-end as the literature research showed that this is not a requirement. However, the operation mode can be distinguished in static or flow.

5. Visual and microscopic observations

6. Direct observation

Direct observation (DO) includes a variety of techniques for the visualization of fouling deposition and removal in real time [29]. DO can be applied to membranes by monitoring the surface of the membrane from above or from the side (direct visualization on the membrane, DVO) or through the membrane (direct observation through the membrane, DOTM) (Fig. 2). If the observation window is on the feed side of the module, parallel to the membrane, the top of the fouling layer can be observed [30], while if it is perpendicular to the membrane, the thickness of the cake layer can be observed. The determination of the cake layer thickness is limited by the precision of the viewing angle. In order to determine the uniformity of the cake layer, a larger area of the membrane must be studied by imaging different parts of it separately [31]. Images can be acquired using a light microscope and/or a camera, to capture still images or videos at locations or times of interest. Observations are made through a glass window, which limits the maximal feed pressure that can be applied. [32, 33, 34] DO techniques can be used to visualize fouling on the micrometer scale. Observation of fouling caused by foulants of smaller sizes, including macromolecules such as polysaccharides and proteins, is usually not possible with DO [30].

Direct observation through the membrane is only possible with membranes that are transparent when wet, which rules out industrial membranes. Deposition of foulants on the surface of the membrane can be observed by placing the observation window on the permeate side of the membrane module, provided the contrast between the deposition and the membrane is sufficiently high. However, the contrast can be improved by fluorescent labeling. DOTM only allows the initial stages of deposition to be monitored as the view is immediately blocked by only a monolayer of particles on the surface of the membrane [31]. Zamani et al. [35] studied the effect of surface energy of particulate foulants on the extent of fouling. Polystyrene and glass particles with negative and positive Gibbs free energy, respectively, and with diameters of $\sim$10 µm were used as foulants and DOTM was used to characterize the critical flux and to assess the initial deposition of particles onto Al_2O_3 membrane disks. The monitoring of hollow-fiber membranes is also possible with DO, and is achieved by mounting a single membrane in a cross-flow module with an out-in flow configuration [29, 34]. DO of hollow-fiber membranes has been performed to monitor fouling deposition and the detachment of bentonite suspensions [29], and to visualize the influence of the particle surface charge of monodisperse polymer model particles on filter cake growth, thickness, structure, compression, relaxation back-wash and cross-flow shear [34]. Le-Clech et al. applied DO to hollow-fiber membranes to observe the formation of fouling by SA [36, 37]. They found that it was

Table 2: Overview of in situ real-time techniques that can be used for monitoring membrane fouling in the biotechnology, biorefinery and food sectors

Monitoring technique	Type of information	Scale	Membrane	Operation	Area	Detection limit	Section
Direct observation	Composition, distribution, thickness	Lab	Flat, tubular, hollow	Flow	Module	<10 μm	6
Laser-based techniques	Thickness	Lab	Flat	Flow	Spot	<5 μm	7
Image analysis	Concentration, distribution	Lab, pilot	Flat	Flow	Spot	ppm	8
Confocal laser scanning microscopy	Composition, distribution	Fundamental, lab	Flat	Static	Spot	20 μM	9
Multiphoton microscopy	Composition, distribution	Fundamental, lab	Flat	Static	Spot	20 μM	10
Surface plasmon resonance	Thickness	Fundamental	Flat	Flow	Spot	<10 nm	12
Ellipsometry	Thickness	Fundamental, lab	Flat	Flow	Spot	μm - nm	13
UV/Vis reflectance spectroscopy	Composition, concentration	Lab	Flat, hollow, tubular	Flow	Spot	1 mol%	14
Photointerrupt sensor	Thickness, distribution	Lab, pilot	Flat	Flow	Spot	10 μm	14
Photoacoustic spectroscopy	Thickness, composition	Fundamental, lab	Flat	Flow	Spot	<10 μm	16
Ultrasonic time-domain reflectometry	Thickness, distribution	Pilot, industrial	Flat, tubular, hollow, spiral	Flow	Module	<10 μm	17
Quartz crystal microbalance with dissipation	Thickness	Fundamental	Flat	Flow	Spot	<10 nm	18
Holographic interferometry	Concentration, thickness	Lab	Flat	Flow	Module	μm, mol	20
Optical coherence tomography	Distribution	Fundamental, lab	Flat	Flow	Spot	10 μm	21
Magnetic resonance imaging	Thickness, distribution	Fundamental, lab	Flat, tubular, hollow, spiral	Flow	Spot, module	μm - nm	23
X-ray microimaging	Distribution	Fundamental	Flat, tubular, hollow, spiral	Flow	Spot	<1 μm	25
Small-angle scattering	Distribution	Fundamental	Flat, tubular, hollow, spiral	Static	Spot	1 nm	26
Infrared spectroscopy	Composition, concentration	Fundamental, lab	Flat	Flow	Spot	1 μg/ cm^2	28
Raman spectroscopy	Composition, concentration	Lab, pilot	Flat	Flow	Spot	100 μg/ cm^2	29
Electrical impedance spectroscopy	Thickness, composition	Lab, pilot, industrial	Flat, tubular, hollow	Flow	Module	10 μm, 1 μm	32
Streaming potential	Thickness	Fundamental, lab	Flat, tubular, hollow	Flow	Module	<20 μm	33
Voltammetry and chronopotentiometry	Concentration	Lab	Flat	Flow	Spot	1 mol	34
Fluid dynamic gauging	Thickness, cohesive and adhesive strength	Lab, pilot, industrial	Flat	Flow	Spot	10 μM	36

difficult to observe the transparent hydrogel layer formed by SA directly through a microscope. Therefore, they added bentonite particles to the feed solution to make the SA layer visible. Small quantities of bacteria were also added to SA to study the interactions occurring in membrane bioreactors [36, 37]. DO using light microscopy has been applied to monitor the development of biofilm fouling on carriers with different geometries and under different aeration rates [38].

Altogether, direct observation methods provide an easily accessible, simple and low cost option for membrane fouling monitoring, but suffer from inherent, low resolution, which disable detection of foulants of smaller sizes.

7. *Laser-based techniques*

Laser-based techniques, including laser triangulometry, laser refractometry and laser sheet at grazing incidence (LSGI) utilize reflections of an incident laser beam (Fig. 3). Deflections of the laser beam from the original path and the angle at which the reflected laser light impinges on a detector can be used to study the variation in the surface of a cake layer [31, 39]. Characterization with LSGI can be performed at several locations along the length of the module channel, but the location is fixed during the experiment. The resolution is about 3 µm and the standard deviation is 2.5 µm [40]. The main requirements are that the cake surface must reflect laser light and should not be composed of photosensitive material. Possible changes in the refractive index of the solution being filtered resulting from concentration changes should also be considered [39]. LSGI has been applied to study the morphological properties of deposits of clay suspensions [40] and to study the growth kinetics of cake layer formation by monodispersed melamine particles [41].

Laser-based techniques are able to make precise distance measurements through transparent media, and due to this possess multiple applications outside the field of membrane technology. However, membrane fouling measurements have been limited so far cause the techniques suffer from accuracy problems stemming from undesirable refractions occurring at interfaces.

8. *Image analysis*

Image analysis and color descriptors can be used to quantify fouling that produces color changes on the surface of a membrane by taking digital images of the membrane surface and analyzing the red-green-blue (RGB) values of the color pixels. These techniques are applicable for the evaluation of the changes in a membrane surface by adsorption, color-developing molecules, bioactive compounds and contrast agents (Fig. 4). Palencia et al. [42] implemented a surface color index (I_{sc}) based on a RGB-color model describing the changes in the amount of color on the membrane surface during the filtration of aqueous extracts of plant leaves. The weakness of this method is that adequate fouling descriptor experiments must be designed for each case. Image processing and analysis can be used to correct for illumination artifacts and to achieve better contrast, for example, in biofouling monitoring. Moreover, images can be converted into a binary form, and the resulting gray scale intensity can be used in automatic calculations for quantification of the extent of the fouling [38].

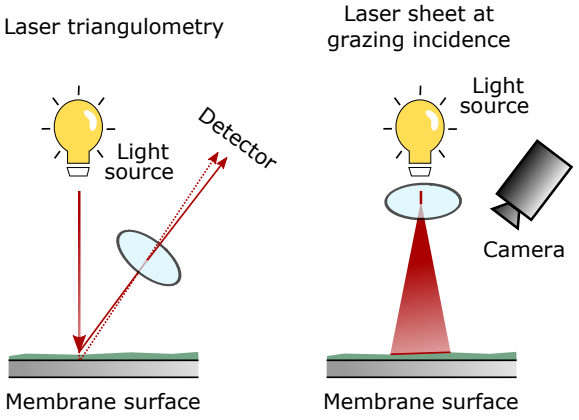

Figure 3: Schematic illustration of the laser setups laser triangulometry and laser sheet at grazing incidence used for in situ real-time monitoring of membrane fouling.

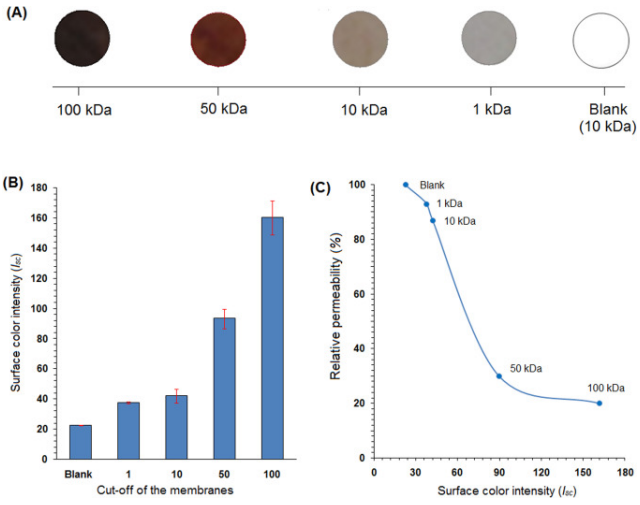

Figure 4: Example of the use of a color index in the analysis performed by Palencia et al. A) Images of fouled cellulose membranes with different MWCOs after filtration of aqueous extracts of plant leaves, B) variation of I_{sc} for each membrane and C) relative permeability as a function of I_{sc} [42]. Copyright 2016. Adapted with permission of Elsevier Science Ltd.

Digital image analysis enables easy and simple description of membrane surface changes, but requires that observable color changes occur as the result of the fouling.

9. *Confocal laser scanning microscopy*

Confocal laser scanning microscopy (CLSM) is an optical microscopic technique that has better axial resolution than conventional optical microscopy, and provides high-resolution images at different depths in a three-dimensional object, avoiding the need for invasive sample preparation. Although CLSM has been used for twenty-five years to char-

acterize membranes and membrane fouling, its application to online visualization has been limited. There is, however, a growing interest in the use of CLSM for biofilm characterization in water and wastewater treatment. Most of the recent publications involving CLSM report its use to visualize and/or differentiate the components of biofilms using multi-staining protocols.

CLSM images allow visualizing of membrane structures, foulant deposition inside the pores and on the membrane surface, and the identification of individual groups of foulants and microorganisms. Image analysis is a very powerful tool that can provide information on pore size, membrane and cake thickness, roughness, the size of defects, and the porosity of the cake, among other things. However, one of the drawbacks of CLSM is the short penetration depth. Marroquin et al. [43] developed a methodology to overcome this limitation by sectioning the membrane samples parallel to the z-axis, to give flat cross-section layers that could be analyzed with CLSM. This method has been used to obtain information on fouling caused by a protein (casein) and a polysaccharide (dextran) filtered with a MF polyethersulfone (PES) membrane [44]. Off-line CLSM membrane characterization has also been used by Gao et al. [45] in an attempt to understand the mechanisms governing the adsorption of organic matter on aged polyvinylidene fluoride (PVDF) membranes. In a more recent study, CLSM has has been used to characterize the retention of nanoparticles (1.5 and 10 nm) by UF PES hollow-fiber membranes [46].

The first reported studies on the use of CLSM for online characterization of membrane processes were performed by Kromkamp et al. [47] and Brans et al. [48]. The same experimental setup was used in both studies, and consisted of a parallel-plate device with a transparent upper plate and particle deposition was monitored. Kromkamp et al. [47] focused their study on the behavior of bidisperse suspensions (mixtures of dyed polystyrene particles) under shear-induced diffusive back-transport in MF with PES membranes. Particle deposition was monitored by obtaining images at different depths, and the particle deposition on the membrane was expressed as the volume of particles per unit surface area of the membrane. Brans et al. [48] studied the deposition of particles on the surface of the membrane and inside the pores during dead-end and cross-flow filtration with polymeric membranes and microsieves. CLSM was used to investigate the interaction of fluorescent polystyrene microspheres and fluorescent sulfate microspheres with the different membranes, by online monitoring of particle transmission. Their results showed a different fouling behavior depending on the type of membrane. In the case of the polymeric membrane, small particles were adsorbed at random places in its tortuous structure, or became trapped in the pores, while for the microsieves, in-pore fouling and adhesion of the particles to the membrane pore edges were observed. The images obtained with CLSM allowed the percentage of the membrane surface area covered by particles at different times to be quantified.

Online microbial cell visualization has been performed by Bereschenko et al. [49] and Beaufort et al. [50] using a different approach. Bereschenko et al. [49] studied membrane fouling of RO membranes during an actual process filtration of a full-scale water purification plant. Sampling at different processing times allowed pseudo-online monitoring of the filtration process. Analysis of the CLSM data allowed the build-up of the biofilm to be followed. Beaufort et al. [50], on the other hand, used two self-fluorescent microorganisms (a yeast and a bacterium) to study the organization of complex structures during MF. They designed a dead-end filtration module to fit into the confocal microscope, and performed online characterization of the yeast, the bacterium and mixed microbial deposits as well as some off-line characterization of bacterial deposits. They were able to observe the organization of these microbial deposits down to a depth of 30 μm, and image analysis allowed the filtration performance to be correlated with some properties of the cake layer, such as void fraction and cake composition.

Vanysacker et al. [51] developed a high-throughput system for online visualization of microbial fouling. The system consisted of six parallel flow cells, each of them equipped with three glass observation windows, allowing simultaneous comparison of different experimental conditions. Fouling of a PVDF MF membrane with labeled *P. aeruginosa* was used to test the performance of this set-up and to assess the possibility of obtaining reliable and comparable information. It was necessary to stop filtration, in order to obtain high-quality CLSM images, but the effect of this was minimized by running the filtration tests for more than 24 h. The results showed a decrease in permeability during the first 5 h of filtration, which was related to the adherence of bacteria on the membrane and cake layer build-up.

Online particle deposition (monodispersed dyed fluorescent microspheres) and cake growth were studied by Hassan et al. [52] on two silicon nitride microsieves (0.8 and 2 μm) using a custom-made filtration chamber with a glass observation window. Cake growth was monitored during successive injections of the spheres, which resulted in layer-by-layer cake formation. However, it was clear from this study that the main limitations of CLSM are the inability of the laser to penetrate the deposit, and limited resolution in all three directions. Their study combined online observation of particle deposition and measurement of permeability reduction, providing a better understanding of the influence of particle size, pore size and pore pitch of microsieves on the formation and morphology of the cake. In a continuation of this work, the same authors [53] analyzed cake build-up during the filtration of a bidisperse suspension, using the layer-by-layer cake growth approach. They also studied the possible protective effect of a layer of large particles on the surface of the membrane during the filtration of small (1 μm) particles using the same online CLSM setup. Moreover, the results of 3D visualization of cake build-up, particle arrangement and cake thickness obtained using this online characterization setup were used to develop a model to simulate MF [54].

CLSM has also been used for online characterization during UF. The deposition of model polystyrene particles on UF

PES membranes was monitored online with CLSM using a custom-built microfluidic system [55]. The novelty of this approach is the possibility of studying particle deposition in the submicron range on UF membranes with a molecular weight cut-off of 10 kDa. Membrane pores cannot be visualized with this setup, but the deposition of 0.4 μm polystyrene particles was monitored under different filtration conditions. They found that individual particles on the membrane surface acted as seeds for the deposition of more particles as reported previously [52, 53, 54]. The same custom-built microfluidic system was used for later studies on UF membrane fouling over a range of pH, ionic strength and feed concentration [56]. It was found that, regardless of the experimental conditions, membrane-particle interactions had a greater influence on the initial deposition behavior, while particle-particle interactions governed long-term deposition.

CLSM images provide both qualitative and quantitative information. Sample preparation for CLSM is minimal, allowing in situ and online experiments to be performed, however, its main limitations are related to resolution. The lack of commercial confocal objectives with appropriate working distances for measurements in miniaturized filtration modules is the most important problem preventing the wider use of CLSM for online characterization. It should also be remembered that online monitoring of very fast processes is limited by the time taken to acquire an image. CLSM is becoming a complementary method of characterization, together with common microscopic techniques, to provide information that can be used to improve membrane manufacturing and process performance.

10. Multiphoton microscopy

Multiphoton microscopy (MPM) is an alternative technique to confocal microscopy. As in the case of CLSM, the fluorophores are excited by laser light, which allows 3D imaging of fluorescent species. However, the working principles are different since multiphoton microscopy is based on the phenomenon of two-photon excitation (Fig. 5). Multiphoton microscopy utilizes infrared (IR) light or near-infrared pulsed lasers that enable the almost simultaneous absorption of two photons. Absorption of the first photon leads to excitation to a virtual energy level, while the almost simultaneous absorption of the second photon excites the molecule to an allowed energy level that is the same as that in one-photon excitation. The wavelength of the photons is thus twice that in normal one-photon excitation. Photons with longer wavelengths scatter less, and can thus penetrate deeper into the sample. In addition, multiphoton excitation can extend the imaging region into the UV and special UV optics and expensive UV lasers are not needed to excite fluorophores that absorb in the UV region. The third advantage of MPM over CLSM is the localized nature of multiphoton absorption, which occurs only at the focal point and not in the optical path [2]. The resolution is typically 0.27 μm, but can be as low as 0.1 μm [2, 57].

Real-time monitoring of membrane processes with MPM has certain limitations. The distance between the objective

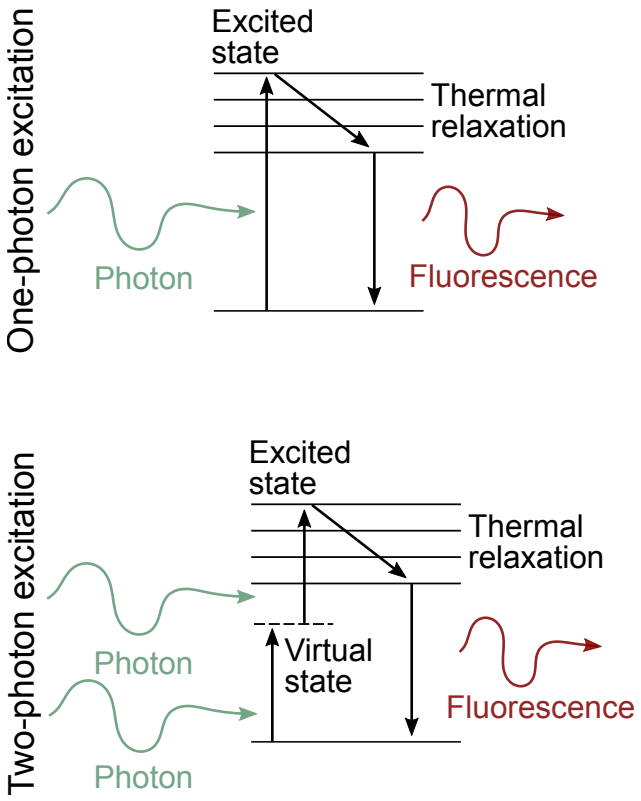

Figure 5: Schematics of one-photon and two-photon excitation processes. (After [2])

and the sample should not exceed 1 mm, and the path between the objective and sample should contain only transparent materials with known refractive indices [2, 58]. In addition, the filtration process must be stopped during imaging to avoid motion artifacts. The acquisition of an image takes 1–5 min, and any movement during imaging will result in blurring [57].

Hughes et al. have studied fouling caused by protein suspensions (unlabeled and fluorescent labeled proteins) [58], yeasts (fluorescent labeled yest) [59] and yeast-protein mixtures (fluorescent labeled yeast) [57, 60]. They found that MPM imaging could be used to distinguish deposited ovalbumin and BSA aggregates providing visual confirmation of a two-stage fouling mechanism. The side-view images obtained at the beginning of the fouling process showed alternating vertical bands of fluorescence and darkness. Thus, it was evident that the fouling caused by the proteins was initially internally dominated (pore blocking). After the initial phase, fouling became externally dominated as the aggregates were deposited on the surface of the membrane (cake layer formation). The whole membrane appeared fluorescent as the result of cake layer formation [58]. In the yeast fouling study, the gradual development of the filter cake was imaged in situ and it was found that the technique offered good submicron resolution when imaging patchy, thin and thick cakes up to a thickness of 45 μm. The fine structural details of the yeast cakes were best captured by 3D image reconstruction, or by the montage of individual slices side by side [59].

When the membrane was fouled with yeast-protein mixtures, the MPM images provided visual confirmation of the deposition of protein aggregates, and confirmed aggregate capture by the yeast cake [57]. Imaging of the deposition of both yeast cells and protein aggregates was achieved simultaneously. It was shown that the yeast cake was effective in screening out BSA aggregates, but was too thin to capture ovalbumin aggregates, and thus failed to reduce the fouling caused by ovalbumin [60].

Imaging in the UV-region is problematic for conventional microscopes and CLSM because specialized optics and high cost lasers are required. Thus the capability of MPM to image UV-excited fluorophores is its greatest advantage.

11. Light based spectroscopy

12. Surface plasmon resonance

Surface plasmon resonance (SPR) is a surface-sensitive analytical method based on waves propagating along the interface of two media, usually a metal and a dielectricum such as an aqueous solution [61]. Monochromatic laser light is focused onto the underside of the metal interface and adjusted so that total internal reflection occurs. Sufficiently thin metal films at a certain incident beam angle (resonance angle) produce surface plasmons. Matching them with the change in momentum of the incoming laser beam leads to resonance excitation. Molecules adsorbing on the metal surface change the local refractive index, and hereby the resonance conditions of the surface plasmon waves. The resonance angle thus depends strongly on the thickness and dielectric constant of the layer on the upper surface of the metal (Fig. 6). SPR experiments are commonly carried out in one of three modes: (1) using light of a fixed wavelength and measuring the angle of minimum reflection (maximum absorption), which can change by approximately 10 % during thin-film adsorption; (2) following the changes in absorption with wavelength; or (3) imaging mode (mapping all of the local changes over the surface) [13].

SPR can be easily implemented and is sensitive to nanometer scale changes in thickness, density fluctuations, and molecular adsorption. It thus provides information on the very early stages of adsorption that lead to membrane fouling. It allows the detection of monolayer and multilayer adsorption, as well as the spatial distribution of the layer and interfacial roughness. SPR provides no information on the molecular level, but allows the study of surfaces with specific chemical properties by modifying the sensor surface. However, it cannot be used to study membranes, but by creating a sufficiently thin model surface out of membrane polymer on top of the sensor, adsorption processes can be investigated. Common methods of producing thin layers are self-assembled monolayers (SAMs) [62, 63, 64, 65, 66] and spin-coating [67]. In order to obtain a good signal, the model surface must be flat and placed within the penetration depth of the evanescent wave, typically less than 1 µm.

SPR has been applied to investigate the effect of the surface properties on the adsorption behavior of proteins in general, and on competitive protein adsorption. When BSA was

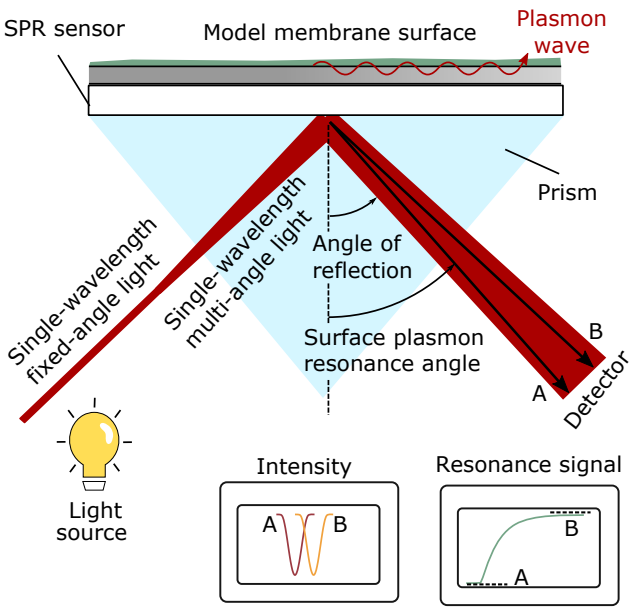

Figure 6: Schematic illustration of SPR for in situ real-time monitoring of membrane fouling on a model layer.

adsorbed onto chemically homogeneous and heterogeneous SAMs, the presence of chemical heterogeneity changed the initial rate of adsorption of globular BSA proteins, and changed the morphology of the adsorbed proteins [66]. Conformational changes in proteins have also been investigated during the adsorption of avidin and BSA onto polysulfone (PS) and gold surfaces. Compared to BSA, large conformational changes were observed for avidin, which formed a thicker, more diffuse and viscoelastic layer on PS [67]. Investigations on the influence of the chemical heterogeneity of surfaces have also shown that the surface chemistry effectively governs protein adsorption for single-, binary and ternary protein solutions of human serum albumin, fibrinogen and fibronectin as well as human plasma [63]. The analysis of competitive protein adsorption revealed that results from single-protein adsorption studies cannot be used to predict the composition of the protein adsorption layer during multi-protein adsorption.

The fouling properties of polyacrylamide coatings have been studied by the adsorption of BSA, fibrinogen, lysozyme and complex media [65]. In general, the adsorption behavior of the proteins changed depending on the polymerization time of the polyacrylamide. However, in comparison to gold surfaces, polyacrylamide surfaces resisted protein adsorption from single-protein solutions and were well below the commonly accepted ultra-low fouling surface criteria. Hook et al. [68] analyzed protein-polymer interactions in high-throughput experiments with SPR imaging. In an attempt to improve the resistance to polysaccharide and protein adsorption, Minehara et al. [69] qualitatively assessed model membrane surfaces of various polymer blends of PVDF and poly(methyl methacrylate) with polyethylene glycol, and compared them to common polymeric membrane surfaces by monitoring the adsorption of BSA and dextran.

A correlation was found between the fouling resistance and the hydrophilicity of the polymer for both model foulants. Filtration with activated sludge revealed a good correlation between the rate of increase of differential pressure and the amount of adsorbed BSA, but no correlation for dextran adsorption onto the investigated model membrane surfaces.

Combinations and comparison of SPR with other tools, such as atomic force microscopy (AFM), surface acoustic waves, quartz crystal microbalance with dissipation (QCM-D) or Raman spectroscopy [63, 66, 62, 70] have provided more insight into adsorption processes and have helped to verify findings. The combination of SPR with QCM-D allowed the differentiation between dry absorbed protein mass and wet adsorbed protein mass [71], while the displacement of one protein in the adsorption layer by another was determined by the combination of SPR and AFM [63].

Peiris et al. developed a novel fluorescence-based technique for the characterization of colloidal/ particulate-protein interactions at a physical level and corroborated the developed technique with SPR [64]. This technique was compared to various others by monitoring the adsorption of α-lactalbumin and colloidal/ particulate- and protein-like matter onto SAMs. The results indicated a possible reduction in signal in the SPR measurements due to inter-molecular or inter-particle physical-level interactions between colloidal/ particulate- and protein-like matter and α-lactalbumin.

In conclusion, SPR is reasonably easy to use and is widely used for real-time monitoring of mainly protein fouling. However, it is until now only applicable to model membrane surfaces. The presented studies highlight the potential of high-throughput analysis for improving the understanding of the interaction between polymers and biomolecules, as well as the complex behavior of biomolecules at surfaces.

13. Ellipsometry

Ellipsometry is an optical technique that can be used to detect, quantify and derive information about adsorption processes on a wide range of surfaces. In ellipsometry, the phase change and the ratio of the amplitude of the incident and reflected, polarized light reflected from the investigated surface are monitored (Fig. 7). Reflections at the interfaces of the different scatterers are combined to form a reflected light wave with a changed state of polarization. The most common application of ellipsometry is in the measurement of film thickness, from 0.01 nm to several µm [8]. The technique has been widely used to analyze the structure of multilayer components. The results obtained can also provide insight into other properties of films, including their morphology, chemical composition and electrical conductivity [72]. The review by Ogieglo et al. [73] provides an extensive overview of the use of in situ ellipsometry in investigations of the interactions between thin films and penetrants.

The application of ellipsometry is generally limited to interfaces with a changing refractive index during adsorption/fouling over time. Moreover, it provides no specific chemical information. Hence, ellipsometry can usually not differentiate between adsorbates and surfaces, or individual

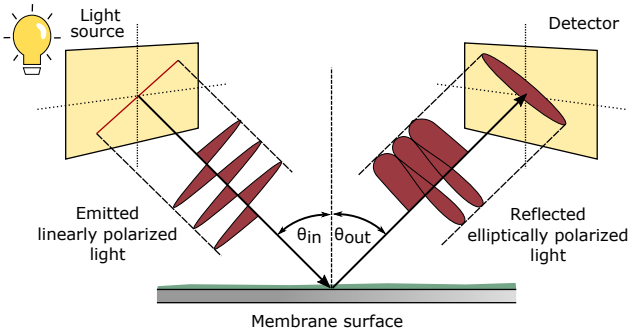

Figure 7: Schematic illustration of ellipsometry for in situ real-time monitoring of membrane fouling.

adsorbates that have similar refractive indices. As the data analysis relies on mathematical models of the studied surfaces, the calculations can be complex, and the validity of the results depends strongly on the theoretical model. If the light beam travels through a liquid phase during the measurements, the properties of the liquid must be taken into account due to possible interference or attenuation [13, 8].

As surface structures on different scales and heterogeneous materials have different optical properties, the nature of membrane samples is optically complex since a membrane is a porous material that scatters light in all directions when irradiated. The different scattering sources can be differentiated by ellipsometry of angle-resolved scattering (EARS). EARS measures the polarization state of scattered waves with high angular resolution, which enables the separation of surface from volume effects. In this way, it is possible to obtain information on the geometrical properties of a sample, as long as the angular scattering pattern is associated with the electromagnetic model.

In situ ellipsometry has been applied to study the adsorption of surfactants to modified MF membranes, to measure the thickness of fouling layers before and after cleaning, and to investigate the morphology of ceramic and polymeric UF membranes. Adsorption studies of surfactants on MF membranes modified via surface grafting of polyelectrolyte brushes showed swelling of the polyanionic brushes by 280 % in water, and a reduction of the adsorption of anionic sodium dodecyl sulfate occurred [74]. Rückel et al. [75] initially applied ellipsometry to develop and analyze a model fouling layer consisting of SA, BSA and humic acid in order to find an effective cleaning strategy for the removal of marine biofouling in desalination membranes. They later used it to measure the layer thickness before and after cleaning [76]. EARS has been applied to investigate the morphology of porous ceramic membranes [72] and polymeric UF membranes [77] with different molecular weight cut-offs. These investigations showed that it is possible to determine a membrane bulk volume distribution by EARS without contacting or altering the membrane itself. Furthermore, an increase in the angular variations of the polarimetric phase shift with an increasing porosity was observed. This kind of non-destructive technique for the characterization of the

variation in porosity, and thus the molecular weight cut-off, might be useful in studying the influence of membrane fouling on the separation performance.

Using IR light instead of visible light, ellipsometry offers the possibility to acquire noninvasive, structural and chemical information at the liquid/solid interface simultaneously. For example, in situ IR spectroscopic ellipsometry allowed the assessment of the ionization of a thin film made of mixed polyelectrolyte brushes as a function of pH by using the intense absorption of the carboxyl group and the carboxylate ion [78].

Ellipsometry is limited by the refractive index of the surface, surface scattering and light depolarization. The method requires good mathematical modeling, which limits its applicability. However, it generally allows monitoring of the early stage of membrane fouling, theoretically, even in real membrane filtration.

14. Other light based methods

UV/Vis reflectance spectroscopy UV/Vis reflectance spectroscopy employs light in the ultraviolet-visible spectral region, and is based on the interaction between electromagnetic radiation and opaque surfaces. The energy of photons from the light promotes or excites a molecular electron to a higher energy orbital. This is in contrast to fluorescence spectroscopy, which is based on the transition of a molecular electron from an excited state to the ground state. UV/Vis reflectance spectroscopy can be applied to characterize the membrane-solution interface. The light reflected from the opaque surface can be recorded by a fiberoptic probe positioned above the membrane (Fig. 8). The measured reflectance from the layer being studied can be related to absorption, as the light that is not absorbed is reflected. The wavelengths of the absorption peaks give qualitative information on the functional groups present in the foulants, and the method can thus be applied to determine the composition of the fouling layer. The absorbance is directly proportional to the concentration and path length of the absorbing component in the sample, and is usually determined using the Beer-Lambert law. An increase in the absorption at a chosen wavelength, or in a spectral area, can be applied to monitor changes in the concentration of a compound in the foulant layer.

Combining UV/Vis spectroscopy with other techniques allows the qualitative analysis of foulant deposition during filtration. Gao et al. [79] showed how UV/Vis spectroscopy synchronized with electrochemical impedance spectroscopy can be used to study the role of ionic strength on protein fouling by BSA during UF. The fouling potential of BSA was found to be greatly affected by the ionic strength of the feed water. A salting-out effect due to the concentration of salt ions near the membrane surface was also observed.

UV/Vis reflectance spectroscopy is a simple, fast and affordable technique that has recently been developed for real-time monitoring, and promises to provide information that will lead to a better understanding of membrane fouling [79].

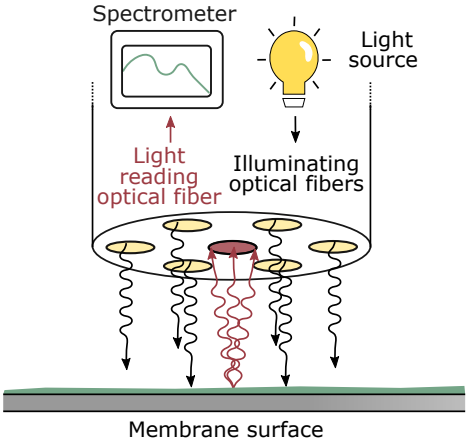

Figure 8: Schematic illustration of UV/Vis reflectance spectrophotometry for in situ real-time monitoring of membrane fouling.

Photointerrupt sensor array A photointerrupt sensor array consists of a light emitter and a light receiver element that are either placed facing each other, or on the same surface in a way, so that the transmitted or reflected light can be detected. The technique can be used to measure fouling layer thickness and distribution based on the absorption of the fouling layer. The cake layer thickness can be estimated by measuring the intensity of the output signal and applying the modified Beer-Lambert law. The resolution is limited to around 10 μm, but the method has the advantages of easy installation and low costs. The sensitivity of the measurement is affected by the intensity of the light and the transparency of the surrounding medium. High particle concentration and color of the medium may reduce the transparency, and hereby reduces the penetration depth of the sensor signal. To a certain degree, this problem can be overcome by reducing the distance between the sensor and the membrane being studied [80].

Tung et al. [80] applied sub-miniature (diameter 4 mm, thickness 3 mm) reflector-type IR light emitting diode photointerrupt sensors to monitor the growth of the fouling layer during the filtration of a high-turbidity feed stream of TiO_2 suspension on a submerged membrane filtration system. Sensors were placed inside a glass test-tube to prevent their corrosion. The sensor module could be moved up and down over the submerged flat sheet membrane by a variable-speed stepping motor (Fig. 9). The range of measurement distance for which the results were valid was determined to be 0.25 to 4.25 mm. Visual observations of polytetrafluoroethylene and PVDF membranes revealed that the absorbance properties of the membrane material might affect the sensitivity of the measurements. Overall, the photointerrupt sensor array is a promising tool for fast scanning of membrane surfaces, even on pilot-scale submerged membrane filtration units [80].

Photointerrupt sensors provide a simple, effective and low costs solution for evaluation of the fouling layer thickness in the range of 10 to 5000 μm, but their use is limited

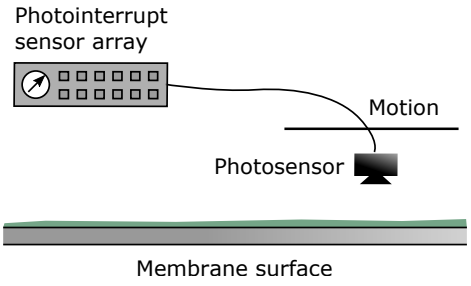

Figure 9: Schematic illustration of a photointerrupt sensor array for in situ real-time monitoring of membrane fouling.

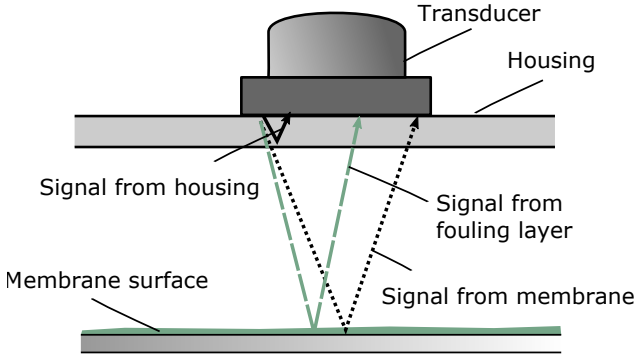

Figure 10: Schematic illustration of UTDR for in situ real-time monitoring of membrane fouling. (After [85])

to diluted feeds due to scattering problems at higher concentrations [2].

15. Acoustic techniques

16. Photoacoustic spectroscopy

Photoacoustic spectroscopy (PAS) is based on the absorption of electromagnetic radiation inside a sample, and combines the features of optical spectroscopy and ultrasonic tomography. Energy from the absorption of radiation is converted into heat by non-radiative relaxation of excited molecules. Depth-resolved analysis of both optical and acoustical inhomogeneous media is achieved by measuring the pressure waves originating from the thermal expansion of the medium resulting from heat production with microphones or piezoelectric transducers. PAS allows optical absorption measurements of highly adsorbing samples, even in strongly scattering or optically opaque media [81]. The technique is simple, and causes only minimal disturbance in the sample.

Schmid et al. [81] used PAS to monitor the growth and detachment of biofilms under the influence of various biocides. The biofilm thickness was determined and the detachment mechanism during hydrogen peroxide and isothiazolinone treatment elucidated. Segal et al. [82] combined offline Fourier transform infrared PAS (FTIR-PAS) with partial least-squares analysis to quantitatively investigate protein fouling on UF membranes in the presence of polysaccharides. SA was found to have no effect on the adsorption of BSA on the membrane, and this result was successfully validated by indirect estimations using a mass balance approach.

PAS has been used to monitor biofouling, but has not yet been applied in research in the biotechnology, biorefinery or food sectors. However, the work of Segal et al. [82] using FTIR-PAS shows that monitoring of membrane fouling caused by proteins or polysaccharide could be possible in the future.

17. Ultrasonic time-domain reflectometry

Ultrasonic time-domain reflectometry (UTDR) is an acoustic technique that utilizes the transmission and reflection of ultrasonic waves to provide information on the medium through which the waves travel. When an ultrasonic wave encounters an interface between two media, reflection, transmission and mode conversion of the incident wave relative to the reflected wave occur, and the magnitudes of the reflected and transmitted waves can be detected as a function of the acoustic impedances of the two media [18]. This makes it possible to obtain information on the fouling layer such as its thickness or density. Data analysis is often combined with Fourier wavelet transformation of the UTDR signal to enhance the resolution. It is important to consider that the sonic velocity of the waves is dependent on temperature, pressure, concentration and the medium. It is therefore difficult to separate the fouling layer from the membrane, if the density of the fouling layer is similar to, or lower than the membrane density (Fig. 10). A way to gain high precision UTDR measurements (0.6 to 2 μm) is the compensation of the sonic velocity by using for example a reference transducer [83] or a double transducer [84].

UTDR offers an alternative to optical techniques as the medium can be opaque. Different membrane module types can be investigated as long as the investigated membrane area is larger than the sensor surface. UTDR has therefore already been applied to a broad variety of modules, including flat-sheet [86, 87, 88, 89, 90, 91, 92, 93, 94], tubular [95] hollow fiber [96, 97, 98, 99] and even spiral wound [100, 101] membrane modules. Depending on the frequency, some ultrasonic waves are unavoidably attenuated by the module housing before they arrive at the interface of interest. The penetration at low frequencies is much greater than that at higher frequencies, however, the resolution is greater at higher frequencies, requiring a trade-off between the attenuation and the resolution of the acoustic waves [91].

UTDR has been widely studied with both model solutions and real process solutions. Protein fouling has been investigated by studying BSA adsorption on several commercial polymeric MF membranes under cross-flow conditions [89, 90]. BSA adsorption on a tubular UF membrane has successfully been distinguished from the various curved surfaces, housing holder, steel support and the module [95].

Membrane fouling caused by lipids has also been widely investigated. Xu et al. [97] investigated the fouling of hollow-fiber membranes during the MF of oily wastewater from offshore oil platforms. Concentration polarization and fast oil adsorption near the inlet of the module were identified as

the cause of an instantaneous flux decline at the start of filtration. A 3D ultrasonic imaging technique based on UTDR was developed by monitoring lipid adsorption on PES UF membranes [91]. In this study, the sequential events during fouling, and the internal structures of the membrane were determined as a function of time. Chen et al. [93] developed an automated UTDR monitoring system to obtain information on the spatial and statistical features of fouling while microfiltrating phospholipids. They later developed the system further for direct and unambiguous diagnosis under practical operating conditions [94].

Li et al. [98, 99] investigated fouling of PES hollow-fiber membranes by yeast solutions. They found that fouling could not be prevented by using sub-critical conditions, aeration or shorter fiber length, but it was slowed down [98]. Interestingly, double-end submerged hollow-fiber membranes showed a better filtration performance than the one-end module [99]. They also used UTDR for sensitive and rapid evaluation of the fouling layer thickness and distribution during the MF of humic acids [88]. The flow conditions were found to be the main factor influencing the spatial and temporal distribution of humic acid fouling on the membrane. Tung et al. [101] combined UTDR with computational fluid dynamics (CFD) simulations to characterize membrane fouling in UF and RO spiral wound modules, and found that gravity and membrane curvature influenced the distribution of humic acid fouling. Sim et al. [100] developed an early warning system for quantitative monitoring of fouling under controlled hydrodynamics and flux conditions in a RO spiral wound module (a so-called canary cell) using UTDR. They found that it was possible to follow the change in density of a silica colloid fouling layer and to create qualitative images of it. UTDR has also been used to investigate fouling during the filtration of paper mill wastewater [86]. By employing Fourier wavelet transformation, the signal from a thin fouling layer has also been successfully separated from that originating from a porous MF membrane and other surfaces. Skider et al. [87] also applied a Fourier wavelet transformation together with UTDR to visualize fouling resulting from MF of natural brown water.

UTDR is thus a novel, versatile and very promising technique. As a result of many successful applications involving various solutions and membrane module types, it is likely that this technique will soon be applied in industrial applications.

18. *Quartz crystal microbalance with dissipation*

Quartz crystal microbalance with dissipation (QCM-D) is a mass sensing technique based on acoustic waves. Information on mass adsorption is generated by constantly measuring the shift in resonance frequency of a piezoelectric quartz crystal sensor (Fig. 11), allowing determination of the thickness of the adsorption layer, density-viscosity changes in a solution, viscoelastic changes in a boundary layer and changes in the surface free energy. QCM-D is a simple and cost-efficient technique over a broad detection range, extending from the adsorption of small molecules such as heavy

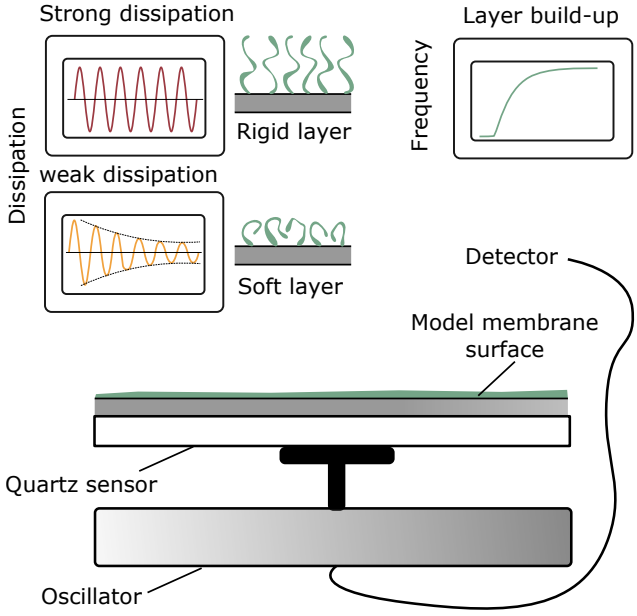

Figure 11: Schematic illustration of QCM-D for in situ real-time monitoring of membrane fouling on a model layer.

metal ions, to much larger molecules such as complex biopolymers or bio-macromolecules. It can be run without reference measurements, requires only small sample volumes in the range of several mL, and can detect subtle changes at a solution-surface interface. However, surface interface effects are difficult to separate from volume effects [102, 67].

QCM-D functions well in complex, optically opaque solutions. Although it is not possible to mimic an actual membrane filtration process, adsorption of diverse types of solutions on model membrane surfaces can be examined. However, changes in the solution density or temperature and electrical effects can cause changes in the oscillation frequency [103]. External pressure degrades the sensitivity of the sensor. Manipulation of the surface towards specific chemical properties is possible by modifying the sensor surface. To create a thin layer, the same methods as for SPR can be applied such as spin-coating [67, 104, 105, 106, 107, 108, 75]; SAMs [109, 110]; but also other layer deposition techniques [102, 103, 111].

Many studies have focused solely on protein adsorption [105, 107, 108, 110, 111, 62]. It has been found that BSA adsorbed less onto a zwitterionic copolymer with high 4-vinylpyridine-content coatings [111]. Differences in the rigidity of the fouling layer were found depending on the model membrane surface and the amount of BSA adsorbed. A rigid layer was initially formed during the adsorption of BSA onto a PVDF film, which became softer with an increasing amount of adsorbed BSA [105], whereas a soft layer was formed directly upon the adsorption of BSA onto poly(ethylene-co-vinyl alcohol) and PES films, which remained soft regardless of the amount of BSA adsorbed [105]. At low concentrations, LG has been found to be irreversibly adsorbed onto PES films forming a complete, rigid fouling layer; while at higher concentrations it was reversibly adsorbed as a soft

fouling layer [107, 108]. Continuous, complete adsorption over time has been reported for LG on PES films [108], and for BSA on hydrophilic and hydrophobic alkane-terminated surfaces, with a preference towards the hydrophilic surface [110]. In their study, Roach et al. [110] reported a stepwise adsorption rate for bovine fibrinogen during adsorption at high concentration onto hydrophilic and hydrophobic alkane-terminated surfaces, with an initial rapid adsorption stage followed by a slower stage, and then a second rapid adsorption stage, and slowing over a longer period. Contreras et al. [109] found good correlation between the adsorption rate of SA and the water contact angle. However, a mismatch was found between the adsorption rate of BSA and the water contact angle, as well as the zeta potential of the investigated surfaces [109]. Overall, they showed that irreversible fouling by polysaccharides and proteins is mainly caused by hydrogen bonding and specific electrostatic interactions between the foulants and the surface; nonspecific electrostatic and hydrophobic interactions are less important for the adsorption process.

High adsorption rates have been observed for BSA and low adsorption rates for SA during adsorption onto silica surfaces and cellulose acetate butyrate films [112, 106]. Furthermore, differences have been reported between the adsorption of BSA and SA onto SAMs, with the highest initial adsorption rate for both compounds onto -COOH surfaces and the rapid formation of irreversible fouling caused by BSA on -$CONH_2$ and -NH_2 surfaces. In contrast, similar rates have been reported for the adsorption of BSA and SA on clean sensor surfaces [109].

Another research focus tackled with QCM-D is the investigation of fouling by EPS. QCM-D has been used by Rückel et al. [75] to develop a model fouling layer consisting of a mixture of polysaccharides, proteins and humic acids. They found that the concentration of SA in an EPS matrix influenced the adsorption behavior significantly. Ferrando-Chavez et al. [104] found that high concentrations of the polysaccharide Psl reduced the adsorption of EPS onto the negatively charged aromatic polyamide surface, while the shear modulus and shear viscosity of the fouling layer were increased. A comparison between the adsorption of effluent organic matter and EPS on a polyamide surface revealed inhibited swelling of the polyamide surface and a lower adsorption rate of effluent organic matter, presumably due to cross-interactions between the various components included in the process [113]. Wang et al. [114] extracted EPS from a membrane bioreactor after three different hydraulic retention times and studied its adsorption onto PVDF coated sensors. A loose and soft fouling layer was found for EPS extracted after the shortest hydraulic retention time. This EPS also adsorbed much faster than the two other. A study by Piatkovsky et al. [115] investigated the effect of an anti-fouling coating consisting of a zwitterionic block-copolymere on the adsorption behavior of EPS and found a positive effect of the hydration of the coating regarding the anti-fouling properties of the coating. However, the presence of calcium during the EPS adsorption affected the anti-fouling effects negatively.

The combination of QCM-D with other techniques such as ellipsometry, SPR and AFM can offer further insights. The combination of QCM-D with SPR revealed differences in the amounts of BSA and avidin adsorbed onto PS films [67]. This was attributed to hydrodynamically coupled water in the protein fouling layer that was detectable with QCM-D but not with SPR [67]. Zhou et al. [62] applied QCM-D together with SPR and surface acoustic wave to study the adsorption of human immunoglobulin G onto hydrophobized surfaces. Also the adsorption of human immunoglobulin G onto cellulose based membranes for virus removal has been studied by the combination of QCM-D and SPR [116]. Mierczynska-Vasilev et al. [102] combined QCM-D with AFM to investigate the adsorption behavior of the constituents of white, rosé and red wine on functional plasma-polymerized coatings. QCM-D gave a higher adsorbed mass of the wine constituents than suggested by the AFM images, due to the exclusion of attached hydration water in the images. Furthermore, the same combination has been applied to study if blending of SiO_2 nanoparticles (NPs) together with PVDF effects the adsorption of effluent organic matter. It was found that the effluent organic matter adsorbed lower and attached non-rigid onto the SiO_2-terminated polymer layer [117]. Moreover, two stages of adsorption have been detected: an initial stage with a rapid adsorption and a second stage, where the frequency had reach equilibrium but the dissipation was still changing and the adsorption layer tended to rearrange itself. The AFM results revealed a repulsion between a SiO_2-terminated PVDF membrane and a probe coated with effluent organic matter.

Only few studies have compared results from QCM-D with results from conventional membrane fouling monitoring methods such as flux or pressure measurements. However, the studies that have been performed, found good agreement between fouling on the model surfaces and fouling during the filtration process [105, 107, 113]. Pore plugging has been identified by comparing QCM-D measurements and flux decline measurements [106].

QCM-D thus appears to be a promising technique that is easy to use and provides useful information with comparably small monetary efforts. There is even an open 3D printing project that offers the possibility to print one's own device [118]. However, it only gives information on model surfaces, and will likely be of the greatest value in the early development of new membranes and new membrane processes.

19. Interferometry

20. Holographic interferometry

Holographic interferometry is a non-invasive optical technique that measures changes in the refractive index of a solution based on interference rings. The technique has been used to visualize concentration polarization over UF, NF and RO membrane surfaces [119, 9]. Concentration polarization increases the probability of fouling. The formation of a concentration gradient causes a change in the refractive index of the solution, which can be seen as a pattern of interfer-

ence fringes [120]. The use of holographic interferometry is restricted to low flow rates due to the inherent physical limitations of the technique [119]. Therefore, it is easier to study concentration polarization in an unstirred batch process than in a crossflow processes, as the thickness of the boundary layer is limited by the flow parallel to the membrane [121].

Holographic interferometry is usually performed through a transparent window in the filtration module. The use of a window limits the maximum pressure that can be applied [121]. Two steps are necessary: First, the reference state must be recorded without applied pressure to obtain an image of the non-concentration-polarized system. The sample is then illuminated using a coherent light source, e.g. a laser. The holographic light field of the area close to the membrane surface can then be recorded and rendered using holographic films or digital sensor arrays. During the second step, the light beam passes through the filtration module and the light field is online recorded. As the online light fields differs from the reference light field, the phases of the light fields will interfere producing fringes containing information on the concentration gradient [9, 120, 121]. Each interference fringe corresponds to a certain change in concentration and the amount of fringes increases as the thickness of the boundary layer increases. Interference fringes are not observed at greater distances from the surface of the membrane when the bulk solution maintains its initial concentration [122].

Fernández-Sempere et al. [123] monitored the reversible adsorption of PEG-10000 on the surface of a cellulose acetate membrane indirectly through the appearance, evolution and disappearance of the polarization layer. When the solute mass balance in the polarization layer was calculated, it was found that the amount of solute provided by the feed solution was greater than the amount accumulated in the polarization layer. It was therefore assumed that the amount of solute that was not present in the polarization layer was adsorbed on the membrane surface. When the pressure was removed, new interference fringes appeared as the solute accumulated on the membrane returned to the polarization layer. Fernández-Sempere et al. [120] also studied the influence of variables that can cause the physical adsorption of PEG-10000. They found that pressure did not cause the deposition of solute on an inert control surface. However, the adsorption of the solute on the membrane surface dependes on the pressure applied and on the membrane saturation adsorption capacity. Adsorption occurred simultaneously with the accumulation of solute in the polarization layer. The main weakness of monitoring fouling by holographic interferometry is the need for mathematical modeling of the system. Various models can be used to explain and simulate the adsorption process, some of which are better than others. Light deflection is a source of experimental error. A refractive index gradient within a concentration polarization layer deflects the light beam towards the membrane, and the interference fringes may be significantly distorted depending on the system [119, 124]. It has been shown by Rodrigues et al. [119] that light deflection can be neglected if the difference

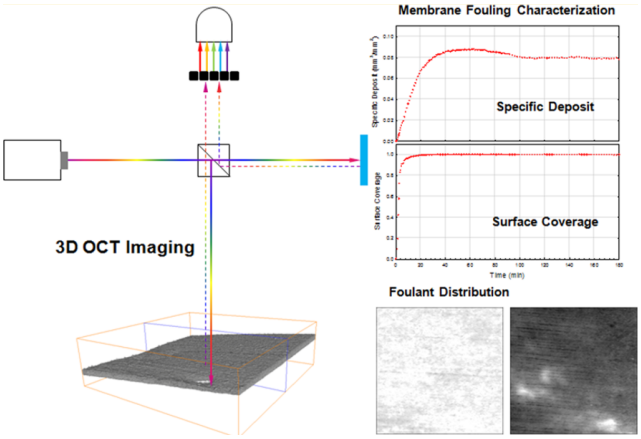

Figure 12: Schematic illustration of OCT in in situ real-time monitoring of membrane fouling [3].
Copyright 2016. Adapted with permission of Elsevier Science Ltd.

in the refractive index between the membrane surface and the aqueous solution is sufficiently small. They developed a numerical ray tracing model that improved the precision of the measurements. Holographic interferometry has been an important method in nondestructive testing of materials in various fields of industry, and thus simple and efficient, low cost, real-time commercial tools are already available [125] and adaptation of the method to the suitable, industrial membrane-based applications may be seen in the future.

21. Optical coherence tomography

Optical coherence tomography (OCT) enables the detection of 2D and 3D structures by generating a series of images from scans at different depths, combined with information on back-scattering, and the location and intensity of the interference signal [126, 127, 128]. OCT is similar to acoustic tomographic techniques, but instead of acoustic waves IR light is used. It penetrates the sample and is partially reflected when an optical property of the sample, e.g. the refractive index, changes in the axial direction (Fig. 12). The light signal reflected from different depths interferes with the reference light signal, which travels a different path, generating frequency-dependent interferograms [129]. These interferograms can be transformed into intensity signals as a function of sample depth, providing the sample structure profile at any point. OCT provides simultaneous Doppler imaging, which can be used to additionally visualize the velocity profiles of observed particles [129].

OCT offers the possibility to monitor a large area (mm^2) in a short time [126, 3]. The use of relatively long-wavelength light means that OCT has a greater beam penetration in the studied surface than, for example, confocal microscopy, but the spatial resolution is limited to ∼10 µm [130, 127, 129]. It is sensitive to the optical path, i.e. the combination of the physical sample thickness, refractive index and total scattering cross-section of the sample. This is why scattering events play an important role as they lead to a loss of intensity. Scattering limits the scanning depth to ∼1 mm [127].

Additionally, OCT is not able to distinguish between different deposits formed on the membrane surface [131].

OCT measurements can be performed directly through a thin glass window, as in holographic interferometry. Processes with low pressures are preferable because of the potential failure of the glass window [129]. It is possible to scan multiple cross-sections at the same time, providing a 3D view that allows quantification of the foulant accumulation, porosity and spatial distribution [132, 38, 3, 133].

OCT has mainly been applied for biofouling monitoring [129, 127, 134, 130, 127, 126, 132, 128, 135, 38, 133] and the determination of the compressibility of biofilms [130, 135]. However, it has also been used to monitor scaling [136] and cake layer formation [129, 3, 137] and could potentially be applied to investigate concentration polarization [129]. Lee et al. [136] used OCT to investigate scaling by $CaSO_4$ and mixtures of $CaCO_3$, $CaSO_4$ and NaCl. They detected the growth and deposition of large aggregated crystals on the surface of a membrane while smaller crystals, which had sizes below the resolution limit, could not be detected. Gao et al. [129] applied simultaneously structural and Doppler imaging to demonstrate the ability of OCT to correlate localized fluid dynamics with the fouling process. Bentonite microparticles were used as foulants, also acting as tracers for Doppler imaging of flow patterns. In this way, OCT provided valuable information for the improvement of the spacer design. However, the response of OCT during turbulent flow has not yet been studied.

OCT monitoring directly related to organic fouling has only been reported recently. Park et al. [133] investigated the influence of organic matter composition on biofilm formation. They found that OCT monitoring was unable to detect a visual change in the membrane surface during the deposition of organic matter on the membrane. Fortunato et al. [131] studied fouling development in direct contact membrane distillation of seawater, and found that it was not possible to detect early-stage fouling caused by a mixture of organic compounds and salts as the thickness of the foulant layer was only about 50 to 70 nm. Trinh et al. [138] applied OCT to characterize membrane fouling by hexadecane oil droplets in water emulsion. They also studied relatively transparent particulate foulants. The fouling layer was found to consist of individual oil droplets that were seen as bright spots. Apart from direct visualization of foulant deposition on the membrane, OCT was also found to be able to detect the entry of foulants into the pores of the membrane. However, Trinh et al. also pointed out that the relation between the signal intensity and the variation in the composition of the surface may be non-linear when transparent particulate foulants such as oil droplets accumulate on the surface of the membrane. Changes in the liquid-foulant and foulant-polymer boundary layers may increase or decrease the reflectance at these interfaces, and thus increase or decrease the intensity of the OCT signal. More effective image processing algorithms are therefore needed to improve the accuracy of quantitative analysis using OCT. In addition, OCT may suffer from various optical artifacts, leading to a reduction in the spatial resolution and making the interpretation of the results more difficult [138].

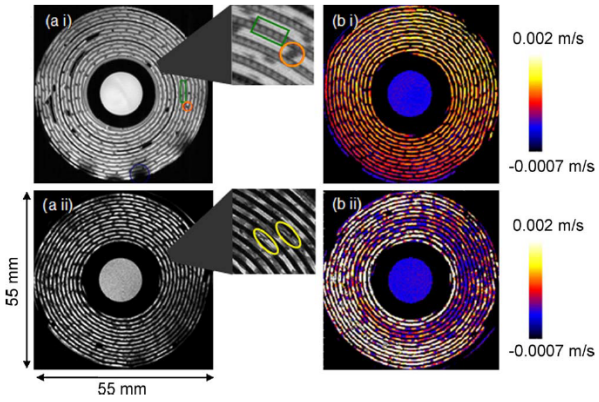

Figure 13: Example of the data obtained with MRI of in situ monitoring of membrane fouling [140].
Copyright 2010. Adapted with permission of Elsevier Science Ltd.

OCT is an established tool in medical diagnostics and emerging imaging technique in the non-destructive testing field, but the complexity and costs of current setups still limit its use [139]. However, its capability to provide information on foulant accumulation, distribution and porosity makes it an appealing technique for membrane fouling monitoring.

22. Magnetic resonance imaging

23. NMR/MRI

Nuclear magnetic resonance (NMR), also known as magnetic resonance imaging (MRI) in medical applications, utilizes the excitation and relaxation of atomic nuclei under the influence of an external magnetic field. We will refer to it as MRI as we would like to highlight the imaging ability of the technique. Atoms of the molecules are surrounded by electron clouds, and nuclear shielding affects the magnetic field felt by the nucleus. A change in the chemical environment of the atom causes a change in the energy level of the nucleus. This, in turn, changes the radio frequency required to excite the nucleus and results in a spin flip, the so-called excitation step. The excited nucleus returns to its normal state in the relaxation step, with the release of the energy absorbed during the excitation step. The relaxation signal can be recorded and transformed into an image that represents a variation within the sample matrix. MRI thus provides both chemical and structural information on a sample. The nuclei that can be studied with MRI include ^{1}H, ^{19}F, ^{31}P and ^{23}Na; and isotopes such as ^{2}H, ^{13}C and ^{15}N also have a magnetic moment. Images of local environments within a studied area can be obtained by varying the parameters of the pulse sequence and signal processing [17] (Fig. 13).

In MRI the distribution of mobile protons within the sample is usually scanned. Therefore, high signal intensities are obtained from regions filled with water [141]. It has been observed that the sample properties spin-lattice relaxation time (T_1) and spin-spin relaxation time (T_2) are especially

low for trapped water protons compared to the relaxation times of bulk water. This helps to distinguish, for example, between a biofilm and the bulk fluid. However, it should be noted that the values of T_1 and T_2 are affected by motion, and the MRI signal can be lost with increasing temperature [142, 13]. Spatially and time-resolved one- to three-dimensional flow velocity images allow the monitoring of flow fields of permeating water [143, 9, 144].

MRI can provide quantitative measurements of membrane fouling, the resulting impact on the hydrodynamic properties of the membrane module, and thus the mass transport [19]. The filtration module must be inserted inside the MRI magnetic coils, which usually limits the imaging to only one section of the module at a time [145]. Furthermore, a delay of several minutes can occur in the image during measurement, which may be due to limitations in spatial resolution and/or a transition from non-detectable concentration polarization to detectable particle deposition at a critical concentration in the boundary layer [143]. The mechanism governing this is still unclear and may be due to increased flow rates through the fouling layer, or structural changes in the fouling layer [145].

MRI has already been used to study the fouling tendency of hollow-fiber membranes. Adequate image contrast was achieved due to the significant differences in local particle concentration in the module. The signal from the bulk phase is lower than that from the permeate flow. The cake layer could be distinguished due to differences in the relaxation time of free water protons and protons bound to deposits [146, 143]. Çulfaz et al. [146] applied MRI to observe the deposition of two different silica sols and compared the results with SA adsorption on round and micro-structured hollow-fiber membranes. As the feed solutions had different particle sizes and ionic strengths, the proton relaxation times differed. Hence, only a quantitative comparison of the different intensities in MRI signal of the evolving cake layers was possible. However, spatial deposition analysis revealed that the smaller particle-sized solutions ended up in the grooves of the fiber surface. The solution with larger particles created a high resistance polarization layer that resulted in a self-regulating homogeneous spread-out of deposited throughout the surface. SA has also been used as a model foulant for the characterization of deposits in ceramic hollow-fiber membranes by compressed sensing rapid acquisition relaxation enhancement CS-RARE MRI [147]. A contrast agent was used to enhance the contrast between the deposit and the feed. It was shown that with CS-RARE MRI, a quantitative characterization of the fouling deposit is possible. Buetehorn et al.[143] have investigated the impact of set point permeate flux and solids concentration on the cake growth in hollow-fiber membranes. The effect of aeration pressure and duration on the cake-layer removal was also studied. They found that it is not feasible to use continuous or pulsed aeration during MRI, as the fluid motion had negative effects on the cake-to-bulk contrast. Arndt et al. [148, 149] used MRI to measure the influence of Ca^{2+} ions on fouling layer formation and the structure of the polysaccharide SA during dead-end filtration with ceramic hollow-fiber membranes. The growth of the fouling layer determined with MRI was correlated to classic filtration data: i.e. the addition of Ca^{2+} to SA led to the formation of a dense gel layer. In contrast, the absence of Ca^{2+} resulted in a concentration polarization layer, and both strongly influenced the flow profile in the hollow-fiber lumen.

Extensive studies on biofouling in spiral wound NF and RO membranes have been conducted [141, 150, 145, 140, 151, 19, 142, 152] but are only mentioned here as the main focus of this review was not on biofouling.

Although MRI allows the quantification of the spatial fouling distribution as well as being able to analyze the velocity field and its evolution during fouling, it suffers from major drawbacks, namely the high cost and limited resolution between the μm and nm range. An exception to this is the Earth's field (EF) NMR [152, 142]. As the name implies, EF-NMR employs a significantly weaker magnetic field than conventional high-field NMR systems, which means a lower total NMR signal and poorer resolution than in high-field NMR. It is a relatively simple, low-cost and portable alternative. In general, MRI is a more time-consuming and more complex method than other similar non-invasive in situ imaging techniques, such as optical coherence tomography [153].

NMR is one of the most versatile spectroscopic techniques available, and the widespread applications of MRI in the medical field have led to a significant development of commercially available MRI setups. MRI is used also in industrial sectors to monitor the flow of fluids in pipe lines, but holds still a great potential, especially in monitoring fluid transport in porous media such as membranes [154].

24. X-ray and neutron imaging

25. X-ray microimaging

X-ray microimaging (XMI) is an imaging technique based on the penetration of X-rays into material. The amplitude and phase of X-ray radiation passing through a sample is influenced by the imaginary and real parts of the refractive index of that material. Since the refractive index of a material is related to properties such as density and the velocity of light in the medium, the measured refractive index must be related to intrinsic properties of the sample. A distinct difference between the electron densities of the components of interest is necessary [12].

XMI allows the creation of 3D images of a sample with a significantly higher spatial resolution than in visible light microscopy (Fig. 14). Moreover, it is possible to study biological samples in water and samples embedded in a solid. However, X-ray beams with high spatial and temporal resolution are only available at synchrotron facilities. Only there, a spatial resolutions around 1 μm can be achieved, providing a higher resolution, than for example, MRI. If only low spatial resolution is required, polychromatic microfocus sources can be used in some cases.

We could not find any studies in the literature on in situ monitoring of organic membrane fouling by XMI, but are going to mention some interesting research that gives an in-

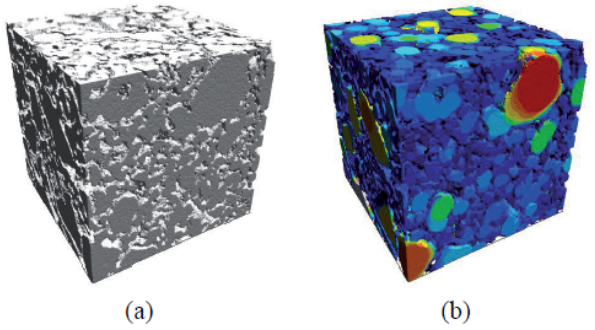

Figure 14: Example images of a fouled membrane obtained by X-ray microimaging: a) 3D reconstruction of imaged sample and b) solid granulometry visualization [155].
Copyright 2013. Adapted with permission by Philippe Moulin.

dication of what can be done with it. Yeo et al. [156] used phase-contrast XMI with synchrotron radiation to monitor external and internal cake layer deposition in a single hollow fiber using an iron hydroxide suspension as lumen feed. They reported that it was possible to observe the deposition of particles as a cake, and also fouling within the membrane pores on the order of 1 µm spatial resolution. Biofilm growth in a porous medium has been imaged with X-ray computed microtomography (micro-CT) by Davit et al. [157], who used a contrast agent to differentiate between the biofilm, the porous medium and the aqueous phase. Images of the system in 3D were obtained at the beginning and end of the study, providing information on the relationship between the topology of the porous medium and scale transport processes. However, imaging was restricted by long recording times of up to 1.5 h. Vicente et al. [155] characterized new and abraded ceramic MF membranes with XMI in two and three dimensions. In their study, the resolution was limited to 0.30 µm and mm-sized samples. They therefore concluded that XMI is limited to the characterization of MF membranes.

In conclusion, XMI appears to be a powerful technique for the characterization of membrane morphology [12], and in the future may also be applied for membrane fouling monitoring in fundamental scale. However, the technique currently requires expensive equipment and access to synchrotron accelerators is limited.

26. Small-angle scattering techniques

Small-angle scattering (SAS) techniques are based on small deflections, or scattering, of a collimated beam of radiation from its straight trajectory after interaction with objects that are much larger than the wavelength of the radiation. In most cases, it is assumed that no photon energy is lost, i.e. the scattering effects are purely elastic, and can therefore be treated as a pure wave interference effect. The scattered radiation is collected in an angle-discriminating detector, providing direct information on the inner structure of the sample. SAS can be used to obtain structural information on objects between 1 nm and 100 nm, over a small scattering volume with a thickness up to 100 µm [158]. This infor-

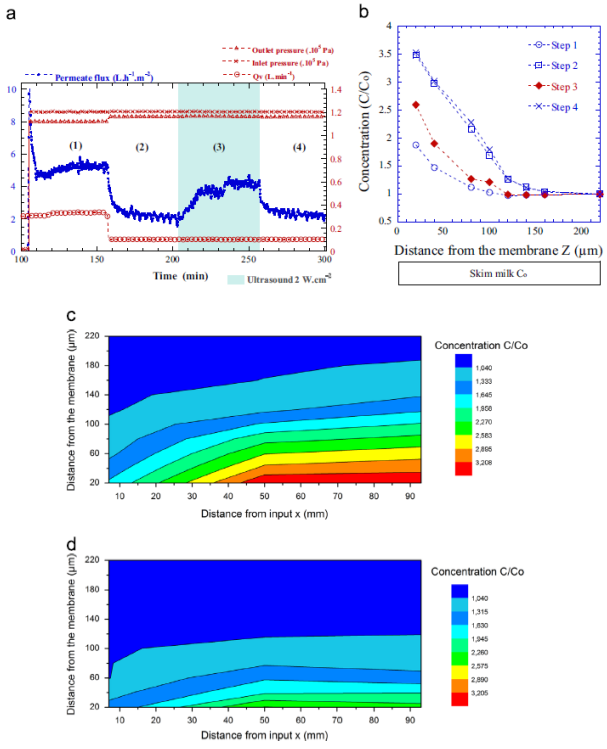

Figure 15: Example of the data obtained with SAXS from in situ real-time monitoring of membrane fouling [159].
Copyright 2014. Adapted with permission of Elsevier Science Ltd.

mation may be the size, the shape of macromolecules, or their spatial relationship. The sample does not have to be crystalline. Sufficiently high neutron and X-ray fluxes allow real-time measurements, but a synchrotron radiation source is needed for high-resolution research, making this technique very expensive and complicated. Unlike microscopic techniques, measurements with SAS become easier the smaller the investigated structure us. In contrast to MRI, the technique does not suffer from problems associated with macromolecules with a molecular weight >30 kDa. However, the information content in the scattered signal is low, hence data analysis is complex. Furthermore, spatial averaging leads to a loss of information compared, for example, to crystallography. SAS is typically used for the analysis of biological samples such as proteins and soft materials e.g polymers and colloids.

The two most common SAS techniques are small-angle X-ray scattering (SAXS) and small-angle neutron scattering (SANS). In SAXS, the elastic scattering of an X-ray beam hitting a sample and traveling through the material is observed as a function of the angle of incidence and scattering, while in SANS the elastic scattering of a neutron beam is observed. However, in contrast to SAXS, SANS is more sensitive to light elements and labeled isotopes can be used. Additionally, neutrons penetrate matter much more effectively than X-rays, and interact very differently with hydrogen and deuterium which can be used in so-called contrast variation.

This is especially useful when studying biological samples where the hydrogen can often be replaced by deuterium resulting in an increased contrast and allowing the identification of organic and inorganic compounds [160]. Different versions of both techniques exist. The common reflection mode of SAXS is grazing incidence small-angle X-ray scattering (GISAXS), which is especially suitable for measurements of ordered nanostructures and thin films.

SAS has been applied for the investigations of membrane fouling during milk filtration and water treatment. David et al. [158] used SAXS to observe the structural arrangement of a concentration polarization and deposition layer during UF of micelles of the milk protein casein. Especially at the early-stage of filtration, an exponential increase in casein micelle concentration at the membrane surface caused a considerable reduction in permeation flux. Structural changes in casein micelle deposition during membrane filtration have also been observed with GISAXS, where shape transformation of the proteins from spherical to ellipsoidal due to the filtration flow was seen. In contrast to the findings of other studies, the longitudinal axis of the deformed proteins was oriented perpendicularly and not parallel to the membrane surface [161]. The influence of the milk protein LG on the near-surface structure of casein micelles during MF has been studied with GISAXS by Steinhauer et al [162]. They found that LGs led to changes in the electron density and size of the casein micelles. The LG proteins clustered together on the surface of the casein micelles, causing a loss of their steric stabilization and agglomeration in mass-fractal structures. In comparison to the flux reduction due to casein micelle fouling alone, the combination of the two proteins led to the formation of pores between the fractal clusters that reduced the resistance caused by the deposits and thus increased the permeate flow. Jin et al. [159] investigated the effect of ultrasound on the structural organization of the concentration polarization layer during cross-flow UF of skim milk (soluble proteins, casein micelle proteins and mineral salts) with SAXS. No effect of the ultrasound treatment was observed on the internal structure of the casein micelles, but they were able to monitor the evolution of the concentration layer during filtration. It was found that the ultrasound treatment partially disrupted the concentration polarization layer resulting in an increase in the flux. However, this effect was reduced at higher feed concentrations.

Pipich et al. [163] applied SANS to assess the effect of BSA and lysozyme on calcium mineral formation during wastewater desalination. The aggregation of calcium phosphate and calcium carbonate, due to the presence of the proteins, was observed within a very short time. The aggregates formed were stable over several hours and did not increase further in size. Dahdal et al. [164] studied mineralization on BSA-coated citrate-capped gold nanoparticles as an advanced model for biofouled membranes. The BSA gold nanoparticles led to immediate mineralization of stable composite particles with sizes of about 0.2 µm when exposed to simulated wastewater. In a later study, Dahdal et al. [160] further investigated the potential of SA as a biomineralizing agent and scaling initiator with SANS. Grafted SA also induced the formation of 0.2 µm particles, which again formed stable composites within a few seconds. The most recent study using SANS explored the design of a RO pressure cell, where it was demonstrated that in situ SANS monitoring of fouling/scaling is possible in a RO setup. However, the interpretation of the data is difficult as scattering occurs in several parts of the setup. Furthermore, a relationship was found between the decline in permeability and the formation of large particles with fractal structures at the membrane surface [165].

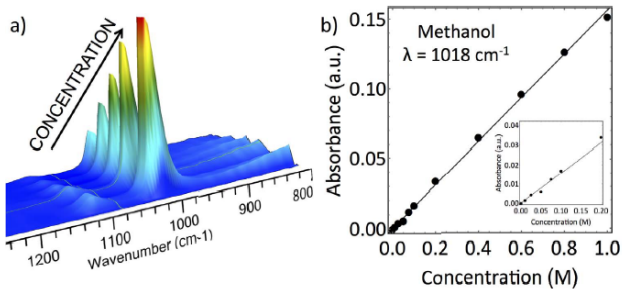

Figure 16: An example of the information obtained by in situ real-time monitoring of membrane fouling with ATR-FTIR spectroscopy [167].
Copyright 2018. Adapted with permission of Elsevier Science Ltd.

To summarize, SAS techniques offer unique insight into membrane fouling. However, accessibility to the equipment required is very limited due to limited numbers of research facilities, high complexity of the data and their analysis, and therefore also high costs. Online analysis has been performed, but the acquisition time and processable sample size are the limiting factors.

27. Vibrational spectroscopy and microspectroscopy

28. Infrared spectroscopy

A comprehensive review of time-resolved attenuated total reflectance Fourier-transform IR spectroscopy (ATR-FTIR) was presented by Elabd et al. in 2003 [166]. Since then, little research has been performed concerning the application of this technique to membrane processes. Real-time IR spectroscopy measurements during RO, NF, UF and MF membrane filtration are limited by interference from the broad O-H vibration bands of water. The absorption by water can be so great that it obscures the absorption of the analytes. It is therefore important to have a very thin layer of water between the path of the light and the sample.

The interactions between proteins and the resulting change in geometry have been studied by Kötting et al. [168], which can be useful when studying membrane fouling by proteins. Morita et al. [169] investigated water adsorption into poly(2-methoxyethyl acrylate) thin films with an ATR-FTIR cell. They could distinguish three different types of hydrated water: nonfreezing water, freezing bound water, and freezing water. The hydration and dehydration of Nafion^{TM} elec-

trolyte membranes has also been studied using an ATR-FTIR cell [170]. Holman et al. [171] combined chemical imaging of biofilms using open-channel microfluidics with synchrotron FTIR spectromicroscopy to monitor bacterial activity. They were able to follow the biochemistry in the biofilm at molecular level over a long period of time.

A rugged in-line FTIR spectrometer has recently been developed [172]. The spectrometer was validated by monitoring a fermentation and hydrolysis process, and the results were compared to those from HPLC analysis. It might be possible to further develop this in-line FTIR spectrometer in the future so that it can also be used for membrane fouling applications.

Overall, with further development, it may be possible to use ATR-FTIR to monitor not only the feed, retentate and permeate quality, but also the fouling layer composition in membrane processes.

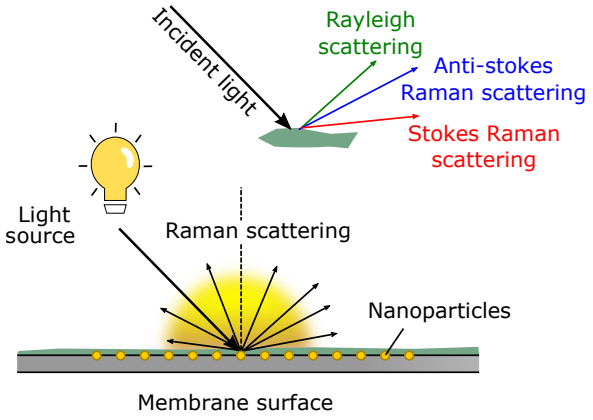

Figure 17: Schematic illustration of SERS for in situ real-time monitoring.

29. Raman spectroscopy

Raman spectroscopy is a form of vibrational spectroscopy that utilizes the energy of monochromatic light scattered from a probed sample (Fig. 17). It is used to obtain information on the vibrations of functional groups of molecules down to single molecules. It is a non-invasive technique. A drawback of Raman spectroscopy is that the signals for organic compounds are usually weak, and are difficult to separate from fluorescence emitted from the sample itself, limiting its use in the biotechnology, biorefinery and food sectors. However, with the appropriate setup, various Raman spectroscopy techniques can be used to distinguish different molecules with a very high detection sensitivity. Therefore, Raman spectroscopy could be a suitable technique for the characterization of the early stages of fouling processes, especially at low concentrations of the feed solution [173].

Several kinds of Raman spectroscopy have been applied to investigate membrane fouling, many of them in real-time applications. From the point of view of sample preparation, the most simple kind of Raman spectroscopy is normal Raman spectroscopy, where no enhancement of the scattering signal is implemented. However, the weak Raman scattering signal can be enhanced by modifying the surface to be analyzed with metallic NPs of silver or gold, as in surface-enhanced Raman spectroscopy (SERS). This is currently the most widely used technique in the field of membrane fouling. The scattering efficiency of SERS is improved by many orders of magnitude compared to normal Raman spectroscopy, especially in aqueous solutions. Moreover, in contrast to normal Raman spectroscopy, SERS suppresses the interfering Raman scattering resulting from the layer composition of most membranes. It thus has considerable potential as a highly selective and quantitative technique for the analysis of biological or chemical molecules in real time. However, the modification of the surface with NPs leads to some considerable drawbacks: (1) The cross-flow velocity over the membrane makes immobilization of the NPs difficult; (2) the applied pressure and vibrations in the membrane module resulting from a pump can disturb the probing system; and (3) the immobilization of the NPs affects the membrane performance and can significantly affect the permeability, pore size and morphology of the probed membrane [174]. As a conclusion it might affect how the surface is fouled. Finally, the SERS signal is bound to the surroundings of the NPs, and enhancement can only be achieved when the foulant is in very close proximity to them.

Normal Raman spectroscopy has been used to study organic fouling of an UF PES membrane by the model phenolic compound vanillin. With the help of principal component analysis and external calibration, Virtanen et al. [175, 176] revealed a time-dependent variation in the amount of vanillin adsorbed on the membrane surface during the fouling process.

Cui et al. [173] applied SERS to study reversible and irreversible adsorption of naturally occurring organic foulants such as the proteins myoglobin, ovalbumin and BSA on PVDF membranes. They found that SERS could be applied for the detection of early-stage fouling as no flux decline was measured at the beginning of the filtration process, while protein adsorption was already detected. Lamsal et al. [177] applied SERS and normal Raman spectroscopy to investigate fouling caused by naturally occurring organics. Normal Raman spectroscopy was reported to be suitable for the characterization of NF membranes, but was not sensitive enough to resolve the foulants. They found that SERS had greater potential in identifying the functional groups of the organic foulants adsorbed on the membranes. The same difference in detection sensitivity between normal Raman spectroscopy and SERS was also found in another study where the chemical variation in proteins, polysaccharides and lipids in a layer of EPS during biofilm formation was investigated [178]. Building on this, the formation and development of dual-species biofouling on cellulose MF membranes was studied with SERS [179], as well as the chemical variation in single-species biofouling during formation on polyamide NF membranes using layer-by-layer SERS [180].

Tip-enhanced Raman spectroscopy (TERS) is derived from SERS, and the Raman scattering signal is enhanced

using a sharp metal or metal-coated tip, often gold or silver, in the optical near-field of the probe. TERS has been applied for the chemical analysis of nanostructures in biofilms, mainly regarding the extracellular polysaccharides [81].

Raman spectroscopy has also been combined with other techniques. Virtanen et al. [70] characterized membrane foulant interactions between vanillin and a PES membrane with a combination of Raman spectroscopy, SPR and molecular dynamics. They observed a high pH dependence of the affinity of the PES surface for vanillin adsorption and found a stronger adsorption of vanilin at a lower pH.

Compared with other vibrational-based methods, Raman spectroscopy is able to simultaneously reveal the chemical structure of foulants and their temporal/spatial distributions without labeling, and with very high sensitivity. Recent and ongoing improvements in Raman spectroscopy techniques in the field of membrane science will lead to a better understanding of early-stage fouling on and in the membrane surface. Cheaper portable Raman spectrometers can be used with the appropriate setup. Kögler et al. [174] used a common portable Raman spectrometer for the real-time identification of biofouling. Moreover, the sensitivity could be significantly improved by using other, advanced Raman techniques, such as coherent anti-Stokes Raman spectroscopy or time-gated Raman spectroscopy, which enables the removal of interfering fluorescence. With further development, these advanced techniques will make a noticeable contribution to our understand of membrane fouling in real time.

30. Other Raman-based microspectroscopic methods

Stimulated Raman scattering (SRS) microscopy is an emerging vibrational spectroscopic imaging technique that employs a Stokes laser beam to stimulate Raman scattering, together with a pump laser beam of constant frequency. The technique offers a penetration depth of up to 200 μm [181], but it has low sensitivity [182]. Coherent anti-Stokes Raman scattering (CARS) is another novel vibrational spectroscopy technique. Compared to Raman spectroscopy, CARS produces a coherent signal that is orders of magnitude stronger than spontaneous Raman emission. This is because CARS employs multiple photons to address the molecular vibrations. As a result, CARS can produce spectra of proteins and carbohydrates with very short exposure times. In addition to the two laser beams in SRS, CARS incorporates a third, the so-called probe laser beam. A coherent optical signal is generated by the interaction of the three laser beams with the sample.

Chen et al. [181] recently investigated the evolution of membrane fouling by studying the adsorption of proteins such as BSA, polysaccharides such as dextran, and mixtures of the two onto MF membranes with SRS in a vibrational spectroscopic imaging approach. This chemical imaging revealed much severer fouling caused by the proteins than caused by the polysaccharides. Both foulants tended to penetrate into the membrane to a depth of about 10 μm. A combination of SRS and CARS has been applied to extract information on the orientation order of molecular bonds in biological samples [183]. Reliable information on the organization of the molecular bonds was obtained using SRS. However, CARS was found to be biased by a nonresonant contribution intrinsic to the CARS signal. If this nonresonant contribution can be determined, it can be corrected for the analysis.

Emerging Raman-based vibrational spectroscopy techniques promise substantial potential for membrane fouling characterization, however, their application to membrane fouling is currently limited by practical implementations such as low sensitivity and high costs [14].

31. Controlled-current techniques

32. Electrical impedance spectroscopy

Electrical impedance spectroscopy (EIS) is a technique that utilizes the change in the electrical resistance of a system resulting from a change in potential. The term impedance refers to the frequency dependent ability of a circuit to resist the changes in electrical current or voltage. The impedance can be determined over a defined frequency region by measuring the amplitude of the applied potential, the amplitude of the resulting alternating current, and the phase shift between these two sinusoidal signals. In EIS, the charge transfer in a system influenced by an alternating potential is modeled with equivalent circuits consisting of two circuit elements. The first element, an electrical resistor, allows for modeling of the frequency-independent charge transfer; while the other, a capacitor, is used to model the frequency-dependent charge transfer. When placed in parallel, these circuit elements provide information on the frequency-dependent and frequency-independent charge transfer across a layer of material. It is then possible to characterize the dielectric substructure of the system and the electrochemical diffusion processes. However, the resistance of the system is an area-specific extensive property. It must be borne in mind that it is only possible for intrinsically homogeneous material to use one specific material-dependent parameter describing the electrical conductivity [184]. As a result, a variation of this parameter with frequency allows a determination of layers such as the membrane skin, substrate and the polarization layer [185].

EIS has been applied to study fouling caused by BSA, molasses, silicate and a side-stream of a RO plant. Park et al. [186] characterized the fouling effects of BSA on ion-exchange membrane systems. A new method was developed to detect slight changes in the lumped measured impedance signal caused by fouling. Good agreement was found with general theoretical predictions. For example, Chilcott [187] suggested that the steady-state water flow that occurs via osmosis, is one of the effects interfering with the change in electrical impedance due to fouling. Cen et al. [188] investigated fouling of RO membranes by wastewater from the fermentation of cane molasses, and found that reversible fouling contributed to the electrical impedance spectrum in the low-frequency region and, that irreversible fouling contributed in the high-frequency region. They further investigated membrane fouling by BSA, silica and molasses wastewater in order to compare model and industrial organic foulants.

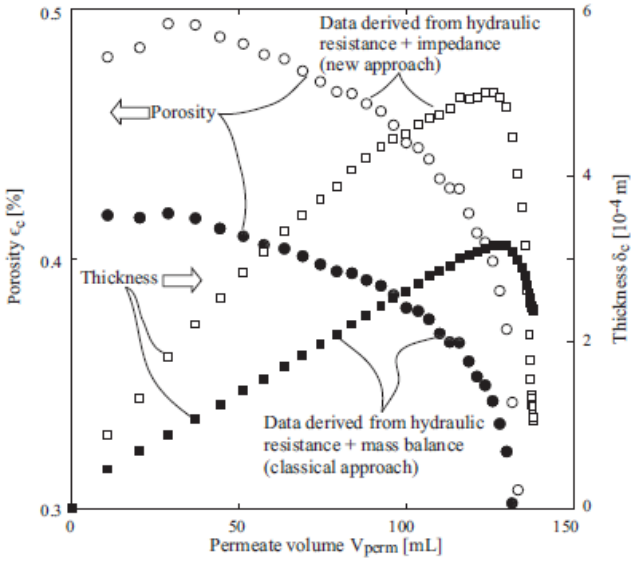

Figure 18: Example of data obtained using EIS for in situ real-time monitoring of membrane fouling [184].
Copyright 2016. Adapted with permission of Elsevier Science Ltd.

They found that EIS was more sensitive than measurements of the conductance or flux decline. Moreover, differences between macromolecular (BSA, molasses wastewater) and colloidal (silica) fouling were determined from the change in capacitance. The formation of gel layers due to organic fouling was observed as a decrease in capacitance while cake build-up as well as concentration polarization due to silica was observed as an increase in the low frequency capacitance [189]. Ho et al. [185] integrated a side-stream cell equipped with EIS monitoring setup into a RO plant to mimic the fouling conditions and to monitor the fouling behavior. A membrane autopsy showed colloidal inorganics and particulate matter as main foulants, while only modest amounts of organic matter were detected. Fouling by silica and BSA during RO has also been investigated [190]. Evidence was found for the build-up of a dense but thin fouling layer preventing the flow of NaCl. These results indicated that both the type and the concentration of the foulant in the mixture affected the fouling mechanism. Changes in BSA adsorption were detected within the first 5 minutes of contact.

Hydraulic EIS has recently been applied to identify possible correlations between characteristic impedance features, such as the evolution of the phase shift between flux and pressure, and the type of membrane fouling occurring, e.g. the build-up of external fouling layers and the occurrence of irreversible internal fouling [191]. This variant of EIS appears to be very suitable for sensitive monitoring of membrane fouling, especially at the beginning of the build-up process. In general, EIS provides an early indication of fouling, as well as an indication of the type of fouling.

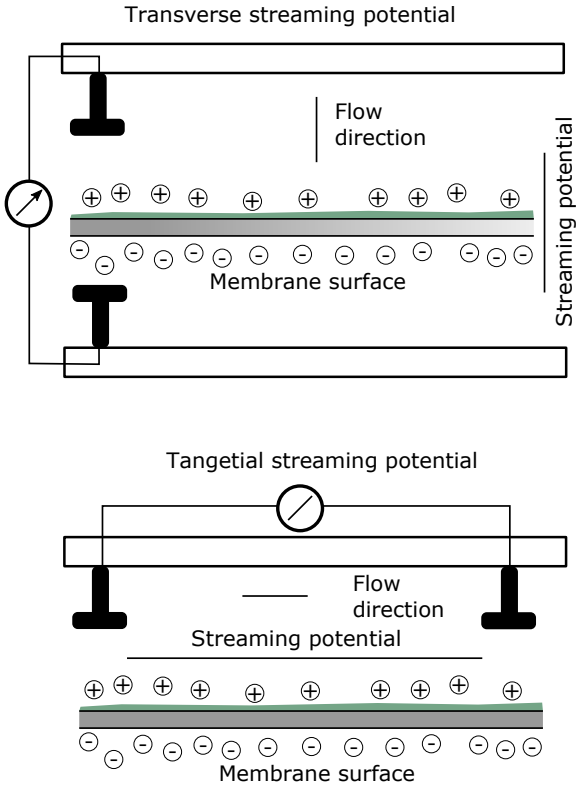

Figure 19: Schematic illustration of SP measurements for in situ real-time monitoring of membrane fouling.

33. Streaming potential

The streaming potential (SP) is the electrical potential difference caused by the electrokinetic flux between two sides of a porous material. It occurs when an electrolyte flows through a membrane due to a pressure difference across the membrane (transverse streaming potential), or when the electrolyte flows along a membrane (tangential streaming potential) (Fig. 19). The SP is the ratio between the electrical potential difference and the pressure difference through or along the membrane. It is related to the streaming current and zeta potential, i.e. the electrokinetic potential between an interfacial double layer on an interface and the bulk fluid, through the Helmholtz-Smoluchowski equation. This technique is subject to different limitations and advantages depending on the direction of flow (transverse or tangential). In transverse SP measurements, each membrane layer contributes to the measured zeta potential, although when studying membrane fouling, only the top layer is of the greatest interest. This kind of measurement is unsuitable for pore diameters smaller than the Debye length (thickness of double layer) as overlapping of the double layer on both sides of the pore occurs making the Helmholtz-Smoluchowski equation, invalid [15]. In tangential SP measurements, on the other hand, the pore size does not present a problem, and only the zeta potential of the uppermost layer of the membrane surface is determined [15].

The SP has been used to study the response of the zeta

potential to cake layer formation, cake compression and pore blocking. Teychene et al. [192] investigated whether electrokinetic properties could be used as an indicator of the formation of cake layers by developing a method applied at constant pressure. Three phases were used in monitoring. The first and third phases are used to stabilize the electrostatic charges inside the membrane, and to obtain the electrostatic properties of the pristine and fouled membrane, while the second phase is the actual filtration. They found that for a constant mass of particles deposited on the membrane (i.e. for a same thickness of the cake layer), the electrical potential is directly related to the transmembrane pressure. Furthermore, an increase in the mass deposited increased the electrical potential difference and varied as fouling rate varied. Lanteri et al. [193] also developed a method for monitoring cake formation during filtration under constant pressure. The general advantage of performing measurements at constant pressure is that variation in the measured streaming potential coefficients due to cake compression, resulting from pressure changes, can be avoided. They demonstrated that it was possible to monitor cake layer thicknesses greater than 15 μm. Based on these methods, Jia et al. [194] investigated the response of the zeta potential to local fouling such as pore blocking, cake formation and cake compression when filtering a yeast suspension in horizontal dead-end hollow-fiber membrane modules under constant pressure. They were able to distinguish local fouling from changes in the zeta potential, and observed a rapid decrease in zeta potential due to pore blocking, a gradual, linear decrease in zeta potential during cake formation, and almost no change in the zeta potential during cake compression.

Nakamura et al. [195] first developed an equation to estimate the degree of pore blocking and to relate the location of the pressure drop to the local zeta potential. They also quantitatively validated the equation by MF of humic acid and demonstrated a clear correlation between increasing filtration resistance and increasing potential difference [196]. Wang et al. [197] investigated the apparent zeta potential of fouling during the filtration of surface water using submerged hollow-fiber membranes and online coagulation UF. They observed a relation between the apparent zeta potential and the transmembrane pressure during filtration at constant flux.

Liu et al. [198] recently applied SP to determine the electrochemical properties of BSA and sodium humate as well as SA to identify the fouling potential of these compounds on PVDF membranes. No clear relationship between the zeta potential/particle size and the adsorption of the foulants on the membrane was observed, but the change in the SP was in accordance with the membrane fouling conditions during short-term filtration.

SP monitoring during protein filtration was performed by Chun et al. [199] in 2002 and is mentioned in a review by Li et al. [12]. From both studies state that SP has high sensitivity and is easy to use as an indicator for membrane fouling.

34. Voltammetry and chronopotentiometry

Voltammetry and chronopotentiometry are techniques based on measuring the relationship between a current and a corresponding voltage. A constant current or a current pulse is applied between a reference electrode and a working electrode and the resulting potential between the two electrodes is measured. These measurements result in voltammograms (current versus potential) and chronopotentiograms (potential versus time) reflecting the electrical properties of the membrane, and providing information on the electrochemical phenomena taking place on the surface of the membrane. [200, 201] The experiments are carried out in electrodialysis cells equipped with electrodes. Typical electrodes are platinum wire or plate electrodes, Ag/AgCl electrodes or electrodes in a Luggin capillary. The electrodes, or the tips of the capillaries, are placed above and below the membrane, and the distance between them can be varied. For example, a distance of 0.8 mm has been used to ensure that the electrodes are outside the laminar flow layer [202, 203], and a distance of 0.5 mm has been used to avoid contact between the electrode and the membrane [204]; however, even a distance as small as 0.2 mm has been shown to be possible [205].

The potential difference across the membrane is usually monitored with a multimeter. When the potential drops across the membrane and the current density is low, the value may oscillate significantly due to the instability of the equilibrium electroconvection. Oscillation of the measured values may also be seen in the early-stages of fouling, especially when a pulsed current is used and the stability of the fouling layer is low [206]. It has also been shown that a change in the position of the membrane may result in high variations of the potential drop due to the contribution of gravitational convection [202].

Voltammograms (Fig. 20) provide information on the limiting current density and phenomena such as water splitting (the formation of H^+ and OH^- ions), electroconvection and concentration polarization. They are divided into three regions, namely, the ohmic, limiting current and over-limiting current region. In the ohmic region, the current densities are low as ions can diffuse more freely in the boundary layer of the membrane. Also, the relation between current and voltage is linear, meaning that the flux of ions through the membrane increases proportionally as the electric field is increased. The first change in gradient of a voltammogram corresponds to the limiting current density. In this region, the potential increases sharply as the concentration of exchange ions approaches zero. Moreover, the current density remains stable as the flow of ions through the membrane is faster than the diffusion of ions from the medium to the boundary layer. The over-limiting current region is characterized by water splitting and electroconvection [200, 207, 208, 204].

The main drawback of voltammetry is that the interpretation of the results can be difficult [200]. Fouling can cause changes in the slopes of the ohmic and over-limiting current regions and alter the limiting current density, as well as the length of the limiting current region. In general, the length

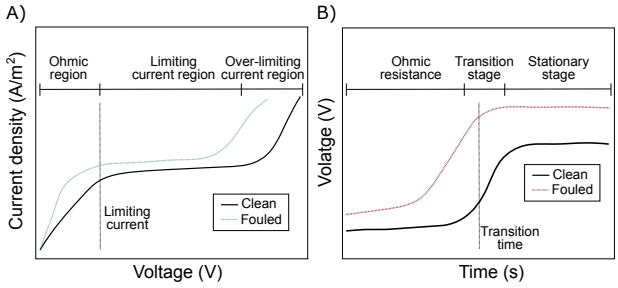

Figure 20: Typical voltammograms A) and choronopotentiograms B) of clean and fouled ion-exchange membranes.

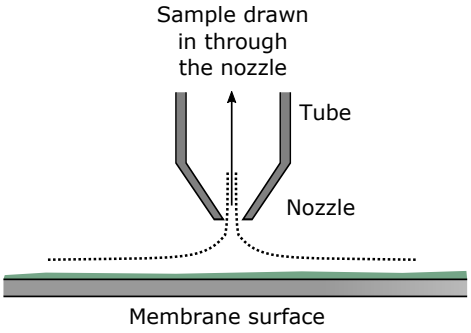

Figure 21: Schematic illustration of FDG for in situ real-time monitoring of membrane fouling. (After [218])

of the limiting current region is greater for membranes with high surface homogeneity and high antifouling properties [207]. The presence of weak electrolytes and buffering species can also affect the length of the limiting current region [209]. Changes in concentration and flow rate may also complicate the interpretation of the results, as the value of the limiting current increases with increasing concentration [209]. Water splitting and electroconvection also have complicated effects on voltammograms. The formation of H^+ and OH^- ions and electroconvection disrupts the diffusion layer, resulting in an increase in the current density. Water splitting leads to acidification or basification of the membrane interface (depending on the surface charge of the membrane) causing fouling and affecting the selectivity of the membrane. Fouling measurements using voltammograms can therefore be time consuming. Additionally, it is difficult to differentiate between the contributions of each electrochemical phenomenon [202].

Chronopotentiograms show changes in the potential difference as a function of time when the current is fixed, and also consist of three stages (Fig. 20). Initially, the potential increases slowly due to the ohmic resistance. During the transition stage, the potential increases sharply until the stationary stage is reached. A change in the gradient of the curve indicates the transition time. A decrease in the transition time indicates that the proportion of ion-permeable area has decreased as a result of fouling [210]. Chronopotentiograms can be used to monitor the development of fouling as a function of time and conditions as the amount of fouling can be related to the potential drop under constant current conditions [206]. This technique can thus be used to study the kinetics of membrane fouling.

Voltammetry and chronopotentiometry have been applied to study fouling of various kinds of ion-exchange membranes during electrodialysis of solutions containing protein-related compounds [205, 211, 204, 203, 210], surfactants [212, 213, 207, 214, 201, 215] and inorganic salts [208, 206, 216]. Studies on amino acid and protein fouling studies have focused on electrodialysis of alkylaromatic amino acid–sodium chloride solutions [205], the fouling caused by an aromatic amino acid solution at different current densities [211], the effect of pulsed electric fields and polarity reversal on amino acid and peptide fouling mitigation [203], and on the fouling potential of an anion-exchange membrane in the presence of BSA [210]. Analysis of the voltammetric characteristics of sodium chloride solutions containing phenylalanine, tyrosine or α-alanine at current densities higher than the limiting current density, revealed that the adsorption of amino acids reduced the length of the limiting current region [205]. Bukhovets et al. [211, 204] showed that amino acid fouling occurred at current densities close to the limiting values. The development of fouling during electrodialysis of phenylalanine–mineral salt solutions was observed as an increase in membrane voltage. In over-limiting current conditions, no significant increase was seen in membrane voltage over time, indicating that fouling was removed as the result of water splitting and electroconvection [204]. Suwal et al. [203] suggested that the application of a pulsed electric field and polarity reversal could prevent the formation of a concentration polarization layer and water splitting in the over-limiting current density region. Lee and Moon [210] demonstrated how irreversible fouling caused by BSA changed the shapes of voltammograms and chronopotentiograms.

Due to the versatility of voltammetric techniques, there have already been several applications in different industrial sectors, and thus the increasing adaptation of the techniques to membrane fouling studies can be expected.

35. Controlled stress techniques

36. Fluid dynamic gauging

Fluid dynamic gauging (FDG) is a technique employing fluid mechanics to determine the thickness of a soft, solid layer immersed in a liquid. Fluid is drawn in through a nozzle by the differential pressure applied across a the nozzle, which is governed by the distance between the nozzle and the liquid surface (Fig. 21). The differential pressure can be related to the increase or decrease in the thickness of the layer between the surface and the nozzle in the range of several µm. The cohesive and adhesive strength of the fouling layer can additionally be measured when FDG is used in combination with CFD [217]. In this method the cohesive and adhesive strength of the layer inferres with the maximum shear stress at which deformation (i.e. a decrease in thickness) is observed.

FDG is a relatively straightforward, inexpensive tech-

nique that can be almost fully automated. It is used to study opaque fluids and fouling layers [219], and requires only minimal sample preparation. The pressure and flow must be adjusted such that laminar flow is achieved in the gauge. The temperature is restricted only by the physical properties of the liquid and the equipment. The main constraint is that the fouling layer is assumed to be locally stiff, and thus does not change shape during the measurement [217]. It is a relatively recently developed technique, but has already undergone some development. FDG can be performed in two modes: the initial mode, where the pressure is set and the flow measured, and the pressure mode, where the flow is controlled and the pressure measured [220]. The latter has a number of advantages over the former. Controlling the gauging flow allows for more accurate control of the shear stress applied to the deposit, and allows the rate of fluid withdrawal from the system to be reduced, while at the same time preserving the bulk flow conditions [220]. This mode also allows FDG to be applied at a greater range of transmembrane pressures.

FDG has so far mainly been used to study model solutions with glass beads. However, studies have also been performed with yeast, humic acids, sugar molasses and Kraft lignin. Lewis et al. [220] applied pressure mode FDG to measure the thickness and cohesive strength of cake layers formed during cross-flow MF of inactive yeast suspensions. The resilience of the cake to fluid shear was found to be inversely proportional to the cake thickness below a thickness of 250 μm. Below a thickness of 100 μm a persistent fouling layer, capable of withstanding stresses outside of the operating limits of the gauge, was reached. Above a thickness of 250 μm, the cake layer was easily deformable, even at shear stresses below 10 Nm^{-2}. Furthermore, the asymptotic rate of cake growth corresponded well with the decreasing rate of flux decline.

Biofilm thickness and strength have been investigated by Suwarno et al. [221] during cross-flow MF under constant permeation. UF of a combination of fine TiO_2 particles and humic acids and the properties of the resulting fouling layer have been investigated by Du et al. [222]. They found that lower TiO_2/humic acid concentrations could lead to extremely severe membrane fouling, and the pH affectes cake layer formation, i.e. high pH leading to more compressed layers. Moreover, membrane fouling was controlled by shear stress under lower operational flux and low TiO_2/humic acid ratios. Jones et al. [219] applied FDG mainly to study membrane cleaning, but also for studying membrane fouling after MF of sugar beet molasses. Improved FDG equipment has been used to study soft cake fouling layers formed during cross-flow MF of Kraft lignin [223]. Very thin (40–70 μm) and highly resistance fouling layers were observed within the first hour of filtration. The cohesive strength of the layers closest to the membrane increased by up to 10 times compared to the uppermost layers.

Lewis et al. [224] developed FDG into an almost fully automated technique. They reprocessed their previous experimental data, performed new measurements and refined the operating procedures using a mixture of glass beads and Kraft lignin. In another study [225], they investigated how the fouling phenomena at the membrane surface and in a growing cake layer influenced the flux decline during cross-flow MF. They quantified the effects of membrane pore fouling and proposed a mechanism for the erosion of Kraft lignin cake layers under shear stress. They also compared their results to mathematical simulations based on the critical flux concept. In the most recent publication by Mattsson et al. [226] FDG was used to investigate the thickness and cohesive strength at different depths in Kraft lignin cake layers formed at different transmembrane pressures during cross-flow MF. They found that the thickness of the cake layer increased with increasing transmembrane pressure. Gravimetric analysis indicated that FDG underestimated the cake thickness, especially in the case of less dense cakes formed at lower transmembrane pressures.

FDG has also been developed into a surface imaging technique called scanning FDG (sFDG) [227], and used to image gelatin, polyvinyl alcohol and baked tomato puree deposits. This technique is based on fluid mechanics, and provides information on the submillimeter scale. Although sFDG has not yet been applied to real-time monitoring of membrane processes, it shows potential for the future.

FDG employs a very unique insides with a completely different approach from most of the other techniques presented in this review, and hereby allows new understanding into membrane fouling. Moreover, it is a very straight forwards and simple method.

37. Conclusions and future perspectives

The techniques discussed in this review offer good opportunities for in situ real-time monitoring of fouling in the biotechnology, biorefinery and food sectors. During the investigated period (2004–2018), exciting new monitoring techniques have been developed and already existing ones have been improved. It is now possible to investigate fouling layer thickness, distribution, composition, concentration and structural properties in high resolution and sensitivity. Moreover, various methods have been applied on many different experimental scales and types of membrane module. However, no single technique can provide all the information necessary to completely monitor all the interesting properties of the fouling development over time. Furthermore, each technique has its own advantages and disadvantages. Some of them can be found in Table 3 that presents an overview of the techniques discussed together with their major strengths and weaknesses. Overall, at least a combination of fouling layer thickness and composition analysis monitoring techniques is required for a better understanding of the occurring fouling and has to be tailored to the individual needs. However, no such combination exists today in a single tool .

In a recent work, a lack of real-time monitoring techniques for the pilot and industrial scale was identified, especially techniques for real-time composition analysis on an industrial scale are missing [7]. It was shown that there is

Table 3: Summary of the methods available for the monitoring of membrane fouling in the biotechnology, biorefinery and food sectors, together with their strengths and weaknesses.

Monitoring technique	**Strengths**	**Weaknesses**	**Section**
Direct observation	Simple and affordable	Only applicable to larger molecules, not proteins or polysaccharides	6
Laser-based techniques	Information on thickness of a fouling layer with resolution ~3 μm	Foulants must reflect laser light, interference from changes in a refractive index of solution	7
Image analysis	Both qualitative and quantitative information	Cannot be used as absolute fouling descriptor	8
Confocal laser scanning microscopy	Protein and carbohydrate differentiation possible	Foulants must be labeled with fluorophores	9
Multiphoton microscopy	Fluorescense excitation in UV region	Filtration must be stopped during imaging	10
Surface plasmon resonance	Information on early-stage fouling on model layers	Low molecular weight compounds are difficult to detect	12
Ellipsometry	Information on early-stage fouling during membrane filtration	Refractive index of fouling must be different from membrane	13
UV/Vis reflectance spectroscopy	Highly sensitive and rapid	Clear solution with low concentrations needed	14
Photointerrupt sensor	Fast, simple and affordable	Low concentration needed	14
Photoacoustic spectroscopy	Applicable in highly scattering, optically opaque media	Fouling signal must differ from membrane signal	16
Ultrasonic time-domain reflectometry	No constraints regarding module type or size	Density of fouling must differ from that of membrane	17
Quartz crystal microbalance with dissipation	Information on early-stage fouling on model layers	Sensitive to hydrodynamically coupled water, resulting in too high adsorbed mass	18
Holographic interferometry	Visualization of concentration polarization	Restricted to low flow rates	20
Optical coherence tomography	Applicable to opaque media layer	Scattering events lead to intensity loss and limit scan depth	21
Magnetic resonance imaging	Quantification of spatial fouling distribution	Low flow rates and small molecules required <30 kDa	23
X-ray microimaging	Not yet applied to in situ real-time monitoring	Distinct difference in electron density between components of interest needed	25
Small-angle scattering	Structural information on objects between 1 nm and 100 nm	Small scattering volume up to a thickness of 100 μm	26
Infrared spectroscopy	Quantification of chemical interaction between solutes and membrane	Measurements limited by interference from O–H vibrational bands from water	28
Raman spectroscopy	Both qualitative and quantitative information	Interference from fluorescence	29
Electrical impedance spectrocopy	Dielectric substructures of systems and electrochemical diffusion processes can be characterized	Conductive membrane and/or fouling needed	32
Streaming potential	Information on surface charge of fouling layer	Overlay of membrane and fouling layer zeta potential	33
Voltammetry and chronopotentiometry	Information on kinetics of ion-exchange membrane fouling	The interpretation of the results may be difficult	34
Fluid dynamic gauging	Information on cohesive/adhesive strength of fouling layer	Fouling layer is assumed to be locally stiff	36

a lack of communication between the industrial membrane users and the analytical tools suppliers as well as a lack of knowledge of the industrial membrane users on the available monitoring techniques that have to be overcome. As soon as this is achieved, It is believed that several of the monitoring tools discussed here will quickly be implemented in both pilot membrane plants and industrial membrane processes on a regular basis. As a results of this paper, one could identify UTDR as an especially interesting technique that will be relevant in industrial membrane applications in the near future. Another promising technique is FDG which offers unique information not available with any of the other techniques, and therefore has considerable potential. QCM-D appears to bear potential for membrane development and fundamental understanding of fouling layer build-up resulting from adsorption. MRI has potential to be applied especially to track changes in flow as a result of fouling. However, regarding the analysis of the composition of the fouling layer, all the available in situ monitoring techniques have limitations to overcome.

On the instrumental side, miniaturization and portability are increasingly important factors. Methods integrated in the membrane process should preferably be easy to use and cost-effective [7]. Due to this, simple optical tools such as photointerrupt sensors and sensors based on UV/Vis reflectance spectroscopy or fluorescence emission may be emerging in the near future. The strengths of UV/Vis reflectance spectroscopy and fluorescence-based methods is that they can provide both qualitative and quantitative information. Fiber optical sensors developed for pipewall fouling monitoring are also interesting and could potentially work in membrane fouling monitoring. Fiber optical devices that combine fluorescence, scattering, transmission and refraction measurements have been shown to be able to detect biofilm growth and differentiate it from inorganic scaling [228, 229]. The pipewall deposit sensors based on the measurement of thermal transfer from a sensor, through a deposit to water phase [230] or sensors utilizing electrical capacitance tomography [231] could potentially also be applicable to membrane fouling monitoring.

Besides the techniques presented in this work, there are numerous monitoring techniques that are in development stage or have applications in non-destructive testing and medical fields, as well as in research laboratories. For example, there are laser-based optical techniques such as sum frequency generation and second harmonic generation that can be applied to study solid-liquid interfaces [13, 232], and could potentially be able to detect membrane fouling. In addition to the development of novel instruments, attention should also be paid to automation, an essential requirement for a more widespread use of online monitoring techniques [7]. Extraction of information from data requires mathematical or statistical treatment and thus development of more effective data processing algorithms and chemometrical methods is needed as well.

Overall, in situ real-time monitoring techniques have a great potential to deepen the understanding of membrane fouling in the biotechnology, biorefinery and food sectors. As this paper showed, many monitoring techniques have already been widely used in research and development. Although, a further improvement of the individual techniques and their usage can be expected in the near future and many more applications using in situ real-time monitoring techniques for membrane processes will be seen soon.

List of abbreviations

AFM	Atomic force microscopy
ATR	Attenuated total reflectance
BSA	Bovine serum albumin
CARS	Coherent anti-Stokes Raman scattering
CFD	Computational fluid dynamics
CLSM	Confocal laser scanning microscopy
CS-RARE	Compressed sensing rapid acquisition relaxation enhancemen
DO	Direct observation
DOTM	Direct observation through the membrane
DVO	Direct visualization on the membrane
EARS	Ellipsometry of angle-resolved scattering
EF	Earth field
EIS	Electrical impedance spectroscopy
EPS	Extracellular polymeric substances
FDG	Fluid dynamic gauging
FTIR	Fourier-transform infrared spectroscopy
GISAXS	Grazing incidence small-angle X-ray scattering
IR	Infrared
LG	β-Lactoglobulin
LSGI	Laser sheet at grazing incidence
MBR	Membrane bioreactor
MF	Microfiltration
micro-CT	Microtomography
MPM	Multiphoton microscopy
MRI	Magnetic resonance imaging
NF	Nanofiltration
NMR	Nuclear magnetic resonance
NP	Nanoparticle
OCT	Optical coherence tomography
PAS	Photoacoustic spectroscopy
PES	Polyethersulfone
PS	Polysulfone
PVDF	Polyvinylidene fluoride
QCM-D	Quartz crystal microbalance with dissipation
RGB	Red-green-blue
RO	Reverse osmosis
SA	Sodium alginate
SAM	Self-assembled monolayer
SANS	Small-angle neutron scattering
SAS	Small-angle scattering
SAXS	Small-angle X-ray scattering
SERS	Surface-enhanced Raman spectroscopy
sFDG	Scanning fluid dynamic gauging
SP	Streaming potential
SPR	Surface plasmon resonance
SRS	Stimulated Raman scattering
TERS	Tip-enhanced Raman spectroscopy

UF	Ultrafiltration
UTDR	Ultrasonic time-domain reflectometry
UV/Vis	Ultraviolet-visible light
XMI	X-ray microimaging

Acknowledgments

The Academy of Finland (Grant No. 292253 and No. 288619) is gratefully acknowledged for financial support. Special thanks to Dr. Helen Sheppard for her excellent commentary and language revision.

References

[1] W. J. Koros, Y. H. Ma, T. Shimidzu, Terminology for membranes and membrane processes (IUPAC Recommendation 1996), J. Membrane Sci. 120 (2) (1996) 149–159. doi:10.1016/0376-7388(96)82861-4.

[2] C. Güell, M. Ferrando, F. López, Monitoring and Visualizing Membrane-Based Processes, WILEY-VCH Verlag GmbH & Co. KGaA, Weinheim, 2009.

[3] W. Li, X. Liu, Y.-N. Wang, T. H. Chong, C. Y. Tang, A. G. Fane, Analyzing the evolution of membrane fouling via a novel method based on 3D optical coherence Tomography Imaging, Environ. Sci. Technol. 50 (13) (2016) 6930–6939. doi:10.1021/acs.est.6b00418.

[4] M. A. Saad, Early discovery of RO membrane fouling and real-time monitoring of plant performance for optimizing cost of water, Desalination 165 (2004) 183–191. doi:10.1016/j.desal.2004.06.021.

[5] K. Cobry, Integrated sensors for real-time monitoring of filtration performance during membrane-based liquid separations, Ph.D. thesis, University of Colorado at Boulder (2011).

[6] G. Rudolph, J. Thuvander, A.-S. Jönsson, F. Lipnizki, Fouling and cleaning of membranes in biorefineries, in: The 7th Nordic Wood Biorefinery Conference, Research Institutes of Sweden, 2017, pp. 196–196.

[7] G. Rudolph, T. Virtanen, M. Kallioinen, F. Lipnizki, Focus on fouling monitoring, Filtr. Sep. 56 (3) (2019) 25–27.

[8] R. Chan, V. Chen, Characterization of protein fouling on membranes: Opportunities and challenges, J. Membrane Sci. 242 (1-2) (2004) 169–188. doi:10.1016/j.memsci.2004.01.029.

[9] V. Chen, H. Li, A. G. Fane, Non-invasive observation of synthetic membrane processes - a review of methods: A review of methods, J. Membrane Sci. 241 (1) (2004) 23–44. doi:10.1016/j.memsci.2004.04.029.

[10] J. C. Chen, Q. Li, M. Elimelech, In situ monitoring techniques for concentration polarization and fouling phenomena in membrane filtration, Adv. Colloid. Interface. Sci. 107 (2-3) (2004) 83–108. doi:10.1016/j.cis.2003.10.018.

[11] S. Suwal, A. Doyen, L. Bazinet, Characterization of protein, peptide and amino acid fouling on ion-exchange and filtration membranes: Review of current and recently developed methods, J. Membrane Sci. 496 (2015) 267–283. doi:10.1016/j.memsci.2015.08.056.

[12] X. Li, Y. Mo, J. Li, W. Guo, H. H. Ngo, In-situ monitoring techniques for membrane fouling and local filtration characteristics in hollow fiber membrane processes: A critical review, J. Membrane Sci. 528 (2017) 187–200. doi:10.1016/j.memsci.2017.01.030.

[13] F. Zaera, Probing liquid/solid interfaces at the molecular level, Chem. Rev. 112 (5) (2012) 2920–2986. doi:10.1021/cr2002068.

[14] W. Chen, C. Qian, K.-G. Zhou, H.-Q. Yu, Molecular spectroscopic characterization of membrane fouling: A critical review, Chem 4 (7) (2018) 1492–1509. doi:10.1016/j.chempr.2018.03.011.

[15] D. J. Johnson, D. L. Oatley-Radcliffe, N. Hilal, State of the art review on membrane surface characterisation: Visualisation, verification and quantification of membrane properties, Desalination 434 (2018) 12–36. doi:10.1016/j.desal.2017.03.023.

[16] M. F. A. Goosen, S. S. Sablani, H. Al-Hinai, S. Al-Obeidani, R. Al-Belushi, D. Jackson, Fouling of reverse osmosis and ultrafiltration membranes: A critical review, Sep. Sci. Technol. 39 (10) (2005) 2261–2297. doi:10.1081/SS-120039343.

[17] R. A. Al-Juboori, T. Yusaf, Biofouling in RO system: Mechanisms, monitoring and controlling, Desalination 302 (2012) 1–23. doi:10.1016/j.desal.2012.06.016.

[18] L. N. Sim, T. H. Chong, A. H. Taheri, S. Sim, L. Lai, W. B. Krantz, A. G. Fane, A review of fouling indices and monitoring techniques for reverse osmosis, Desalination 434 (2018) 169–188. doi:10.1016/j.desal.2017.12.009.

[19] M. C. M. van Loosdrecht, L. Bereschenko, A. Radu, J. C. Kruithof, C. Picioreanu, M. L. Johns, H. S. Vrouwenvelder, New approaches to characterizing and understanding biofouling of spiral wound membrane systems, Water Sci. Technol. 66 (1) (2012) 88–94. doi:10.2166/wst.2012.096.

[20] T. Nguyen, F. A. Roddick, L. Fan, Biofouling of water treatment membranes: a review of the underlying causes, monitoring techniques and control mea-

sures, Membranes 2 (4) (2012) 804–840. doi:10.3390/membranes2040804.

[21] A. Drews, Membrane fouling in membrane bioreactors—Characterisation, contradictions, cause and cures, J. Membrane Sci. 363 (1-2) (2010) 1–28. doi:10.1016/j.memsci.2010.06.046.

[22] F. Meng, B. Liao, S. Liang, F. Yang, H. Zhang, L. Song, Morphological visualization, componential characterization and microbiological identification of membrane fouling in membrane bioreactors (MBRs), J. Membrane Sci. 361 (1-2) (2010) 1–14. doi:10.1016/j.memsci.2010.06.006.

[23] A. W. Mohammad, C. Y. Ng, Y. P. Lim, G. H. Ng, Ultrafiltration in food processing industry: Review on application, membrane fouling, and fouling control, Food Bioprocess Technol. 5 (4) (2012) 1143–1156. doi:10.1007/s11947-012-0806-9.

[24] A. Bokhary, A. Tikka, M. Leitch, B. Liao, Membrane fouling prevention and control strategies in pulp and paper industry applications: A review, J. Membrane Sci. Res. 4 (4) (2018) 181–197. doi:10.22079/jmsr.2018.83337.1185.

[25] Y. He, D. M. Bagley, K. T. Leung, S. N. Liss, B.-Q. Liao, Recent advances in membrane technologies for biorefining and bioenergy production, Biotechnol. Adv. 30 (4) (2012) 817–858. doi:10.1016/j.biotechadv.2012.01.015.

[26] H. Li, V. Chen, Membrane fouling and cleaning in food and bioprocessing, in: Membrane Technology, Butterworth-Heinemann, Oxford, 2010, pp. 213 – 254. doi:10.1016/B978-1-85617-632-3.00010-0.

[27] M. Bücking, M. Kotthoff, On-line monitoring tools for food processing, Food Safety Magazine.

[28] Y. Dixit, M. P. Casado-Gavalda, R. Cama-Moncunill, X. Cama-Moncunill, M. Markiewicz-Keszycka, P. J. Cullen, C. Sullivan, Developments and Challenges in Online NIR Spectroscopy for Meat Processing, Compr. Rev. Food Sci. Food Saf. 16 (6).

[29] Y. Marselina, P. Le-Clech, R. Stuetz, V. Chen, Detailed characterisation of fouling deposition and removal on a hollow fibre membrane by direct observation technique, Desalination 231 (1) (2008) 3–11. doi:10.1016/j.desal.2007.11.033.

[30] F. Meng, B. Liao, S. Liang, F. Yang, H. Zhang, L. Song, Morphological visualization, componential characterization and microbiological identification of membrane fouling in membrane bioreactors (MBRs), J. Membrane Sci. 361 (1–2) (2010) 1–14. doi:10.1016/j.memsci.2010.06.006.

[31] I. S. Ngene, R. G. Lammertink, M. Wessling, W. van der Meer, A microfluidic membrane chip for in situ fouling characterization, J. Membrane Sci. 346 (1) (2010) 202–207. doi:10.1016/j.memsci.2009.09.035.

[32] J. Vrouwenvelder, J. van Paassen, L. Wessels, A. van Dam, S. Bakker, The membrane fouling simulator: A practical tool for fouling prediction and control, J. Membrane Sci. 281 (1–2) (2006) 316–324. doi:10.1016/j.memsci.2006.03.046.

[33] J. Vrouwenvelder, S. Bakker, M. Cauchard, R. Le Grand, M. Apacandié, M. Idrissi, S. Lagrave, L. Wessels, J. van Paassen, J. Kruithof, M. van Loosdrecht, The membrane fouling simulator: a suitable tool for prediction and characterisation of membrane fouling, Water Sci. Tech. 55 (8–9) (2007) 197–205. doi:10.2166/wst.2007.259.

[34] S. Lorenzen, Y. Ye, V. Chen, M. L. Christensen, Direct observation of fouling phenomena during cross-flow filtration: Influence of particle surface charge, J. Membrane Sci. 510 (2016) 546–558. doi:10.1016/j.memsci.2016.01.046.

[35] F. Zamani, A. Ullah, E. Akhondi, H. J. Tanudjaja, E. R. Cornelissen, A. Honciuc, A. G. Fane, J. W. Chew, Impact of the surface energy of particulate foulants on membrane fouling, J. Membrane Sci. 510 (2016) 101–111. doi:10.1016/j.memsci.2016.02.064.

[36] P. Le-Clech, Y. Marselina, Y. Ye, R. M. Stuetz, V. Chen, Visualisation of polysaccharide fouling on microporous membrane using different characterisation techniques, J. Membrane Sci. 290 (1) (2007) 36–45. doi:10.1016/j.memsci.2006.12.012.

[37] P. Le-Clech, Y. Marselina, R. Stuetz, V. Chen, Fouling visualisation of soluble microbial product models in MBRs, Desalination 199 (1) (2006) 477–479. doi:10.1016/j.desal.2006.03.110.

[38] C. Li, S. Felz, M. Wagner, S. Lackner, H. Horn, Investigating biofilm structure developing on carriers from lab-scale moving bed biofilm reactors based on light microscopy and optical coherence tomography, Bioresource Technol. 200 (2016) 128–136. doi:10.1016/j.biortech.2015.10.013.

[39] W. J. T. Lewis, Advanced studies of membrane fouling: Investigation of cake fouling using fluid dynamic gauging, Ph.D. thesis, University of Bath, Bath (2014).

[40] J. Mendret, C. Guigui, P. Schmitz, C. Cabassud, In situ dynamic characterisation of fouling under different pressure conditions during dead-end filtration: Compressibility properties of particle cakes, J. Membrane Sci. 333 (1–2) (2009) 20–29. doi:10.1016/j.memsci.2009.01.035.

[41] P. Loulergue, C. Andre, D. Laux, J.-Y. Ferrandis, C. Guigui, C. Cabassud, In-situ characterization of fouling layers: which tool for which measurement?, Desalin. Water Treat. 34 (1–3) (2011) 156–162. doi:10.5004/dwt.2011.2898.

[42] M. Palencia, T. Lerma, V. Palencia, Description of fouling, surface changes and heterogeneity of membranes by color-based digital image analysis, J. Membrane Sci. 510 (2016) 229–237. doi:10.1016/j.memsci.2016.02.057.

[43] M. Marroquin, T. Bruce, J. Pellegrino, S. R. Wickramasinghe, S. M. Husson, Characterization of asymmetry in microporous membranes by cross-sectional confocal laser scanning microscopy, J. Membrane Sci. 379 (1) (2011) 504–515. doi:10.1016/j.memsci.2011.06.024.

[44] M. Marroquin, A. Vu, T. Bruce, R. Powell, S. R. Wickramasinghe, S. M. Husson, Location and quantification of biological foulants in a wet membrane structure by cross-sectional confocal laser scanning microscopy, J. Membrane Sci. 453 (2014) 282–291. doi:10.1016/j.memsci.2013.11.011.

[45] F. Gao, J. Wang, H. Zhang, M. A. Hang, Z. Cui, G. Yang, Interaction energy and competitive adsorption evaluation of different NOM fractions on aged membrane surfaces, J. Membrane Sci. 542 (2017) 195–207. doi:10.1016/j.memsci.2017.08.020.

[46] M. L. Hir, Y. Wyart, G. Georges, L. S. Lamoine, P. Sauvade, P. Moulin, Effect of salinity and nanoparticle polydispersity on UF membrane retention fouling, J. Membrane Sci. 563 (2018) 405–418. doi:10.1016/j.memsci.2018.05.077.

[47] J. Kromkamp, F. Faber, K. Schroen, R. Boom, Effects of particle size segregation on crossflow microfiltration performance: Control mechanism for concentration polarisation and particle fractionation, J. Membrane Sci. 268 (2) (2006) 189–197. doi:10.1016/j.memsci.2005.06.012.

[48] G. Brans, A. van Dinther, B. Odum, C. Schroën, R. Boom, Transmission and fractionation of micro-sized particle suspensions, J. Membrane Sci. 290 (1) (2007) 230–240. doi:10.1016/j.memsci.2006.12.045.

[49] L. A. Bereschenko, A. J. M. Stams, G. J. W. Euverink, M. C. M. van Loosdrecht, Biofilm formation on reverse osmosis membranes is initiated and dominated by sphingomonas spp., Appl. Environ. Microbiol. 76 (8) (2010) 2623–2632. doi:10.1128/AEM.01998-09.

[50] S. Beaufort, S. Alfenore, C. Lafforgue, Use of fluorescent microorganisms to perform in vivo and in situ local characterization of microbial deposits, J. Membrane Sci. 369 (1) (2011) 30–39. doi:10.1016/j.memsci.2010.11.023.

[51] L. Vanysacker, P. Declerck, I. Vankelecom, Development of a high throughput cross-flow filtration system for detailed investigation of fouling processes, J. Membrane Sci. 442 (2013) 168–176. doi:10.1016/j.memsci.2013.04.033.

[52] I. B. Hassan, C. Lafforgue, A. Ayadi, P. Schmitz, In situ 3D characterization of monodispersed spherical particle deposition on microsieve using confocal laser scanning microscopy, J. Membrane Sci. 454 (2014) 283–297. doi:10.1016/j.memsci.2013.12.003.

[53] I. B. Hassan, C. Lafforgue, A. Ayadi, P. Schmitz, in situ 3D characterization of bidisperse cakes using confocal laser scanning microscopy, J. Membrane Sci. 466 (2014) 103–113. doi:10.1016/j.memsci.2014.04.041.

[54] I. Ben Hassan, C. Lafforgue, C. Ellero, A. Ayadi, P. Schmitz, Coupling of local visualization and numerical approach for particle microfiltration optimization, Microsyst. Technol. 21 (3) (2015) 509–517. doi:10.1007/s00542-013-1906-9.

[55] H. Di, G. J. Martin, D. E. Dunstan, A microfluidic system for studying particle deposition during ultrafiltration, J. Membrane Sci. 532 (2017) 68–75. doi:10.1016/j.memsci.2017.03.017.

[56] H. Di, G. J. Martin, Q. Sun, D. Xie, D. E. Dunstan, Detailed, real-time characterization of particle deposition during crossflow filtration as influenced by solution properties, J. Membrane Sci. 555 (2018) 115–124. doi:10.1016/j.memsci.2018.03.021.

[57] D. Hughes, U. Tirlapur, R. Field, Z. Cui, Multiphoton microscopy – new insights into membrane fouling, Desalination 199 (1) (2006) 23–25. doi:10.1016/j.desal.2006.03.135.

[58] D. J. Hughes, Z. Cui, R. W. Field, U. K. Tirlapur, In situ three-dimensional characterization of membrane fouling by protein suspensions using multiphoton microscopy, Langmuir 22 (14) (2006) 6266–6272. doi:10.1021/la053388q.

[59] D. Hughes, U. K. Tirlapur, R. Field, Z. Cui, In situ 3D characterization of membrane fouling by yeast suspensions using two-photon femtosecond near infrared non-linear optical imaging, J. Membrane Sci. 280 (1) (2006) 124–133. doi:10.1016/j.memsci.2006.01.017.

[60] H. D. J., C. Zhanfeng, F. R. W., T. U. K., Membrane fouling by cell-protein mixtures: In situ characterisation using multi-photon microscopy, Biotechnol. Bioeng. 96 (6) (2006) 1083–1091. doi:10.1002/bit.21113.

[61] I. Lundström, Real-time biospecific interaction analysis, Biosens. Bioelectron. 9 (1994) 725–736.

[62] C. Zhou, J.-M. Friedt, A. Angelova, K.-H. Choi, W. Laureyn, F. Frederix, L. A. Francis, A. Campitelli, Y. Engelborghs, G. Borghs, Human immunoglobulin adsorption investigated by means of quartz crystal microbalance dissipation, atomic force microscopy, surface acoustic wave, and surface plasmon resonance techniques, Langmuir 20 (14) (2004) 5870–5878. doi:10.1021/la036251d.

[63] E. Servoli, D. Maniglio, M. R. Aguilar, A. Motta, J. San Roman, L. A. Belfiore, C. Migliaresi, Quantitative analysis of protein adsorption via atomic force microscopy and surface plasmon resonance, Macromol. Biosci. 8 (12) (2008) 1126–1134. doi:10.1002/mabi.200800110.

[64] R. H. Peiris, N. Ignagni, H. Budman, C. Moresoli, R. L. Legge, Characterizing natural colloidal/particulate-protein interactions using fluorescence-based techniques and principal component analysis, Talanta 99 (2012) 457–463. doi:10.1016/j.talanta.2012.06.010.

[65] Q. Liu, A. Singh, R. Lalani, L. Liu, Ultralow fouling polyacrylamide on gold surfaces via surface-initiated atom transfer radical polymerization, Biomacromolecules 13 (4) (2012) 1086–1092. doi:10.1021/bm201814p.

[66] Y.-W. Huang, V. K. Gupta, A SPR and AFM study of the effect of surface heterogeneity on adsorption of proteins, J. Chem. Phys. 121 (5) (2004) 2264–2271. doi:10.1063/1.1768155.

[67] G. Diaconu, T. Schäfer, Study of the interactions of proteins with a solid surface using complementary acoustic and optical techniques, Biointerphases 9 (2) (2014) 029015–1–029015–6. doi:10.1116/1.4874736.

[68] A. L. Hook, H. Thissen, N. H. Voelcker, Surface plasmon resonance imaging of polymer microarrays to study protein-polymer interactions in high throughput, Langmuir 25 (16) (2009) 9173–9181. doi:10.1021/la900735n.

[69] H. Minehara, K. Dan, Y. Ito, H. Takabatake, M. Henmi, Quantitative evaluation of fouling resistance of PVDF/PMMA-g-PEO polymer blend membranes for membrane bioreactor, J. Membrane Sci. 466 (2014) 211–219. doi:10.1016/j.memsci.2014.04.039.

[70] T. Virtanen, P. Parkkila, A. Koivuniemi, J. Lahti, T. Viitala, M. Kallioinen, M. Mänttäri, A. Bunker, Characterization of membrane–foulant interactions with novel combination of Raman spectroscopy, surface plasmon resonance and molecular dynamics simulation, Sep. Purif. Technol. 205 (2018) 263–272. doi:10.1016/j.seppur.2018.05.050.

[71] G. Diaconu, T. Schäfer, Sensing techniques involving thin films for studying biomolecular interactions and membrane fouling phenomena, in: A. Gugliuzza (Ed.), Smart Membranes and Sensors, Scrivener Publishing LLC, 2014, pp. 145–160.
URL https://doi.org/10.1002/9781119028642.ch5

[72] Y. Wyart, G. Georges, C. Deumié, C. Amra, P. Moulin, Membrane characterization by optical methods: Ellipsometry of the scattered field, J. Membrane Sci. 318 (1-2) (2008) 145–153. doi:10.1016/j.memsci.2008.02.039.

[73] W. Ogieglo, H. Wormeester, K.-J. Eichhorn, M. Wessling, N. E. Benes, In situ ellipsometry studies on swelling of thin polymer films: A review, Prog. Polym. Sci. 42 (2015) 42–78. doi:10.1016/j.progpolymsci.2014.09.004.

[74] Z. Yang, V. V. Tarabara, M. L. Bruening, Adsorption of anionic or cationic surfactants in polyanionic brushes and its effect on brush swelling and fouling resistance during emulsion filtration, Langmuir 31 (43) (2015) 11790–11799. doi:10.1021/acs.langmuir.5b01938.

[75] M. Rückel, S. Nied, G. Schürmann, An experimental approach to explore cleaner systems for desalination membranes, Desalination Water Treat. 31 (1-3) (2012) 285–290. doi:10.5004/dwt.2011.2351.

[76] C. Hippius, S. Nied, G. Schürmann, A. Feßenbecker, Surface analysis for the identification of effective strategies to fight marine biofouling, Desalination Water Treat. 51 (4-6) (2013) 1004–1013. doi:10.1080/19443994.2012.715131.

[77] Y. Wyart, R. Tamime, L. Siozade, I. Baudin, K. Glucina, C. Deumié, P. Moulin, Morphological analysis of flat and hollow fiber membranes by optical and microscopic methods as a function of the fouling, J. Membrane Sci. 472 (2014) 241–250. doi:10.1016/j.memsci.2014.08.012.

[78] K. Hinrichs, D. Aulich, L. Ionov, N. Esser, K.-J. Eichhorn, M. Motornov, M. Stamm, S. Minko, Chemical and structural changes in a pH-responsive mixed polyelectrolyte brush studied by infrared ellipsometry, Langmuir 25 (18) (2009) 10987–10991. doi:10.1021/la901219f.

[79] F. Gao, J. Wang, H. Zhang, H. Jia, Z. Cui, G. Yang, Role of ionic strength on protein fouling during ultrafiltration by synchronized UV–vis spectroscopy and electrochemical impedance spectroscopy, J. Membrane Sci. 563 (2018) 592–601. doi:10.1016/j.memsci.2018.06.030.

[80] K.-L. Tung, H.-R. Damodar, R.-A. Damodar, T.-T. Wu, Y.-L. Li, N.-J. Lin, C.-J. Chuang, S.-J. You, K.-J. Hwang, Online monitoring of particle fouling in a

submerged membrane filtration system using a photointerrupt sensor array, J. Membrane Sci. 407–408 (2012) 58–70. doi:10.1016/j.memsci.2012.03.013.

[81] T. Schmid, A. Messmer, B.-S. Yeo, W. Zhang, R. Zenobi, Towards chemical analysis of nanostructures in biofilms II: Tip-enhanced Raman spectroscopy of alginates, Anal. Bioanal. Chem. 391 (5) (2008) 1907–1916. doi:10.1007/s00216-008-2101-1.

[82] Y. Segal, R. Linker, C. G. Dosoretz, Quantitative estimation of protein fouling of ultra-filtration membranes by photoacoustic spectroscopy, Desalination 271 (1-3) (2011) 231–235. doi:10.1016/j.desal.2010.12.037.

[83] S. Stade, M. Kallioinen, M. Mänttäri, T. Tuuva, High precision UTDR measurements by sonic velocity compensation with reference transducer, Sensors 14 (7) (2014) 11682–11690. doi:10.3390/s140711682.

[84] S. Stade, T. Hakkarainen, M. Kallioinen, M. Mänttäri, T. Tuuva, A Double Transducer for High Precision Ultrasonic Time-Domain Reflectometry Measurements, Sensors 15 (7) (2015) 15090–15100. doi:10.3390/s150715090.

[85] E. Kujundzic, K. Cobry, A. R. Greenberg, M. Hernandez, Use of ultrasonic sensors for characterization of membrane fouling and cleaning, J. Eng. Fiber. Fabr. 3 (2) (2008) 155892500800300. doi:10.1177/155892500800300211.

[86] R. D. Sanderson, J. Li, D. K. Hallbauer, S. K. Sikder, Fourier wavelets from ultrasonic spectra: A new approach for detecting the onset of fouling during microfiltration of paper mill effluent, Environ. Sci. Technol. 39 (18) (2005) 7299–7305. doi:10.1021/es050414y.

[87] S. K. Sikder, M. B. Mbanjwa, D. A. Keuler, D. S. McLachlan, F. J. Reineke, R. D. Sanderson, Visualisation of fouling during microfiltration of natural brown water by using wavelets of ultrasonic spectra, J. Membrane Sci. 271 (1-2) (2006) 125–139. doi:10.1016/j.memsci.2005.07.018.

[88] Y.-H. Lin, K.-L. Tung, S.-H. Wang, Q. Zhou, K. K. Shung, Distribution and deposition of organic fouling on the microfiltration membrane evaluated by high-frequency ultrasound, J. Membrane Sci. 433 (2013) 100–111. doi:10.1016/j.memsci.2013.01.020.

[89] E. Kujundzic, A. C. Fonseca, E. A. E., M. Peterson, A. R. Greenberg, M. Hernandez, Ultrasonic monitoring of early-stage biofilm growth on polymeric surfaces, J. Microbiol. Methods. 68 (3) (2007) 458–467. doi:10.1016/j.mimet.2006.10.005.

[90] E. Kujundzic, A. R. Greenberg, R. Fong, M. Hernandez, Monitoring protein fouling on polymeric membranes using ultrasonic frequency-domain reflectometry, Membranes 1 (3) (2011) 195–216. doi:10.3390/membranes1030195.

[91] L.-H. Cheng, Y.-C. Yang, J. Chen, Y.-H. Lin, S.-H. Wang, A new view of membrane fouling with 3D ultrasonic imaging techniques: Taking the canola oil with phospholipids for example, J. Membrane Sci. 372 (1-2) (2011) 134–144. doi:10.1016/j.memsci.2011.01.062.

[92] S. Sim, T. H. Chong, W. B. Krantz, A. G. Fane, Monitoring of colloidal fouling and its associated metastability using Ultrasonic Time Domain Reflectometry, J. Membrane Sci. 401-402 (2012) 241–253. doi:10.1016/j.memsci.2012.02.010.

[93] J. Chen, Y.-C. Yang, T.-Y. Wei, Application of wavelet analysis and decision tree in UTDR data for diagnosis of membrane filtration, Chemometr. Intell. Lab. Syst. 116 (2012) 102–111. doi:10.1016/j.chemolab.2012.04.012.

[94] J. Chen, J.-Y. Huang, Texture analysis of UTDR images for enhancement of monitoring and diagnosis of membrane filtration, Chemometr. Intell. Lab. Syst. 138 (2014) 142–152. doi:10.1016/j.chemolab.2014.08.001.

[95] J. Li, R. D. Sanderson, G. Y. Chai, A focused ultrasonic sensor for in situ detection of protein fouling on tubular ultrafiltration membranes, Sens. Actuators B Chem. 114 (1) (2006) 182–191. doi:10.1016/j.snb.2005.04.041.

[96] X. Xu, J. Li, H. Li, Y. Cai, Y. Cao, B. He, Y. Zhang, Non-invasive monitoring of fouling in hollow fiber membrane via UTDR, J. Membrane Sci. 326 (1) (2009) 103–110. doi:10.1016/j.memsci.2008.09.042.

[97] X. Xu, J. Li, N. Xu, Y. Hou, J. Lin, Visualization of fouling and diffusion behaviors during hollow fiber microfiltration of oily wastewater by ultrasonic reflectometry and wavelet analysis, J. Membrane Sci. 341 (1-2) (2009) 195–202. doi:10.1016/j.memsci.2009.06.009.

[98] X. Li, J. Li, J. Wang, H. Zhang, Y. Pan, In situ investigation of fouling behavior in submerged hollow fiber membrane module under sub-critical flux operation via ultrasonic time domain reflectometry, J. Membrane Sci. 411-412 (2012) 137–145. doi:10.1016/j.memsci.2012.04.024.

[99] X. Li, J. Li, J. Wang, H. Wang, B. He, H. Zhang, Ultrasonic visualization of sub-critical flux fouling in the double-end submerged hollow fiber membrane module, J. Membrane Sci. 444 (2013) 394–401. doi:10.1016/j.memsci.2013.05.052.

[100] S. Sim, W. B. Krantz, T. H. Chong, A. G. Fane, Online monitor for the reverse osmosis spiral wound module

— Development of the canary cell, Desalination 368 (2015) 48–59. doi:10.1016/j.desal.2015.04.014.

[101] K.-L. Tung, H.-C. Teoh, C.-W. Lee, C.-H. Chen, Y.-L. Li, Y.-F. Lin, C.-L. Chen, M.-S. Huang, Characterization of membrane fouling distribution in a spiral wound module using high-frequency ultrasound image analysis, J. Membrane Sci. 495 (2015) 489–501. doi:10.1016/j.memsci.2015.08.035.

[102] A. Mierczynska-Vasilev, P. A. Smith, Adsorption of wine constituents on functionalized surfaces, Molecules 21 (10). doi:10.3390/molecules21101394.

[103] R. I. J. Iturri, S. Stahl, R. P. Richter, S. E. Moya, Water content and buildup of poly(diallyldimethylammonium chloride)/ poly(sodium 4-styrenesulfonate) and poly(allylamine hydrochloride)/ poly(sodium 4-styrenesulfonate) polyelectrolyte multilayers studied by an in situ combination of a quartz crystal microbalance with dissipation monitoring and spectroscopic ellipsometry, Macromolecules 43 (21) (2010) 9063–9070. doi:10.1021/ma1015984.

[104] D. L. Ferrando Chavez, A. Nejidat, M. Herzberg, Viscoelastic properties of extracellular polymeric substances can strongly affect their washing efficiency from reverse osmosis membranes, Environ. Sci. Technol. 50 (17) (2016) 9206–9213. doi:10.1021/acs.est.6b01458.

[105] M. Hashino, K. Hirami, T. Ishigami, Y. Ohmukai, T. Maruyama, N. Kubota, H. Matsuyama, Effect of kinds of membrane materials on membrane fouling with BSA, J. Membrane Sci. 384 (1-2) (2011) 157–165. doi:10.1016/j.memsci.2011.09.015.

[106] M. Hashino, K. Hirami, T. Katagiri, N. Kubota, Y. Ohmukai, T. Ishigami, T. Maruyama, H. Matsuyama, Effects of three natural organic matter types on cellulose acetate butyrate microfiltration membrane fouling, J. Membrane Sci. 379 (1-2) (2011) 233–238. doi:10.1016/j.memsci.2011.05.068.

[107] J. T. Kim, N. Weber, G. H. Shin, Q. Huang, S. X. Liu, The study of beta-lactoglobulin adsorption on polyethersulfone thin film surface using QCM-D and AFM, J. Food Sci. 72 (4) (2007) E214–21. doi:10.1111/j.1750-3841.2007.00344.x.

[108] S. X. Liu, J.-T. Kim, Application of Kevin–Voigt model in quantifying whey protein adsorption on polyethersulfone using QCM-D, J. Lab. Autom. 14 (4) (2009) 213–220. doi:10.1016/j.jala.2009.01.003.

[109] A. E. Contreras, Z. Steiner, J. Miao, R. Kasher, Q. Li, Studying the role of common membrane surface functionalities on adsorption and cleaning of organic foulants using QCM-D, Environ. Sci. Technol. 45 (15) (2011) 6309–6315. doi:10.1021/es200570t.

[110] P. Roach, D. Farrar, C. C. Perry, Interpretation of protein adsorption: Surface-induced conformational changes, J. Am. Chem. Soc. 127 (22) (2005) 8168–8173. doi:10.1021/ja042898o.

[111] H. Z. Shafi, Z. Khan, R. Yang, K. K. Gleason, Surface modification of reverse osmosis membranes with zwitterionic coating for improved resistance to fouling, Desalination 362 (2015) 93–103. doi:10.1016/j.desal.2015.02.009.

[112] A. E. Contreras, A. Kim, Q. Li, Combined fouling of nanofiltration membranes: Mechanisms and effect of organic matter, J. Membrane Sci. 327 (1-2) (2009) 87–95. doi:10.1016/j.memsci.2008.11.030.

[113] W. Ying, N. Siebdrath, W. Uhl, V. Gitis, M. Herzberg, New insights on early stages of RO membranes fouling during tertiary wastewater desalination, J. Membrane Sci. 466 (2014) 26–35. doi:10.1016/j.memsci.2014.04.027.

[114] T. Wang, Y.-J. Yen, Y.-K. Hsieh, J. Wang, Size effect of calcium-humic acid non-rigid complexes on the fouling behaviors in nanofiltration: An LA-ICP-MS study, Colloids Surf. A Physicochem. Eng. Asp. 513 (2017) 335–347. doi:10.1016/j.colsurfa.2016.10.062.

[115] M. Piatkovsky, H. Acar, A. B. Marciel, M. Tirrell, M. Herzberg, A zwitterionic block-copolymer, based on glutamic acid and lysine, reduces the biofouling of UF and RO membranes, J. Membrane Sci. 549 (2018) 507–514. doi:10.1016/j.memsci.2017.12.042.

[116] R. Hamamoto, H. Ito, M. Hirohara, R. Chang, T. Hongo-Hirasaki, T. Hayashi, Interactions between protein molecules and the virus removal membrane surface: Effects of immunoglobulin G adsorption and conformational changes on filter performance, Biotechnol. Prog. 34 (2) (2018) 379–386. doi:10.1002/btpr.2586.

[117] X. Wang, D. Huang, B. Cheng, L. Wang, New insight into the adsorption behaviour of effluent organic matter on organic-inorganic ultrafiltration membranes: a combined QCM-D and AFM study, R. Soc. Open Sci. 5 (8) (2018) 180586. doi:10.1098/rsos.180586.

[118] Quartz Crystal Microbalance with Dissipation Monitoring: the first scientific QCM entirely Open Source (2017).
URL https://openqcm.com/

[119] C. Rodrigues, P. Garcia-Algado, V. Semião, M. N. de Pinho, V. Geraldes, Concentration boundary layer visualization in nanofiltration by holographic interferometry with light deflection correction, J. Membrane Sci. 447 (2013) 306–314. doi:10.1016/j.memsci.2013.07.035.

[120] J. Fernández-Sempere, F. Ruiz-Beviá, R. Salcedo-Díaz, P. García-Algado, M. García-Rodríguez, Digital holographic interferometry visualization of PEG-10000 accumulation on an acetate cellulose membrane: assessment of polarization layer and adsorption phenomenon, Desalin. Water Treat. 42 (1–3) (2012) 49–56. doi:10.1080/19443994.2012.683105.

[121] J. Fernández-Sempere, F. Ruiz-Beviá, P. García-Algado, R. Salcedo-Díaz, Experimental study of concentration polarization in a crossflow reverse osmosis system using digital holographic interferometry, Desalination 257 (1–3) (2010) 36–45. doi:10.1016/j.desal.2010.03.010.

[122] J. Fernández-Sempere, F. Ruiz-Beviá, R. Salcedo-Díaz, P. García-Algado, Measurement of concentration profiles by holographic interferometry and modelling in unstirred batch reverse osmosis, Ind. Eng. Chem. Res. 45 (21) (2006) 7219–7231. doi:10.1021/ie060417z.

[123] J. Fernández-Sempere, F. Ruiz-Beviá, P. García-Algado, R. Salcedo-Díaz, Visualization and modelling of the polarization layer and a reversible adsorption process in PEG-10000 dead-end ultrafiltration, J. Membrane Sci. 342 (1–2) (2009) 279–290. doi:10.1016/j.memsci.2009.06.046.

[124] J. Fernández-Sempere, F. Ruiz-Beviá, R. Salcedo-Díaz, Measurements by holographic interferometry of concentration profiles in dead-end ultrafiltration of polyethylene glycol solutions, J. Membrane Sci. 229 (1–2) (2004) 187–197. doi:10.1016/j.memsci.2003.10.029.

[125] E. Petrovic, I. Ćirić, J. Milisavljevic-Syed, P. Djekic, Holographic interferometry for vibration analysis of mechanical systems, in: 28th Danubia – Adria Symposium on Advances in Experimental Mechanics, 2011.

[126] L. Fortunato, A. Qamar, Y. Wang, S. Jeong, T. Leiknes, In-situ assessment of biofilm formation in submerged membrane system using optical coherence tomography and computational fluid dynamics, J. Membrane Sci. 521 (2017) 84–94. doi:10.1016/j.memsci.2016.09.004.

[127] C. Haisch, R. Niessner, Visualisation of transient processes in biofilms by optical coherence tomography, Water Res. 41 (11) (2007) 2467–2472. doi:10.1016/j.watres.2007.03.017.

[128] S. West, M. Wagner, C. Engelke, H. Horn, Optical coherence tomography for the in situ three-dimensional visualization and quantification of feed spacer channel fouling in reverse osmosis membrane modules, J. Membrane Sci. 498 (2016) 345–352. doi:10.1016/j.memsci.2015.09.047.

[129] Y. Gao, S. Haavisto, W. Li, C. Y. Tang, J. Salmela, A. G. Fane, Novel approach to characterizing the growth of a fouling layer during membrane filtration via optical coherence tomography, Environ. Sci. Technol. 48 (24) (2014) 14273–14281. doi:10.1021/es503326y.

[130] C. Dreszer, A. Wexler, S. DrusovÃą, T. Overdijk, A. Zwijnenburg, H.-C. Flemming, J. Kruithof, J. Vrouwenvelder, In-situ biofilm characterization in membrane systems using optical coherence tomography: Formation, structure, detachment and impact of flux change, Water Res. 67 (2014) 243–254. doi:10.1016/j.watres.2014.09.006.

[131] L. Fortunato, Y. Jang, J.-G. Lee, S. Jeong, S. Lee, T. Leiknes, N. Ghaffour, Fouling development in direct contact membrane distillation: Non-invasive monitoring and destructive analysis, Water Res. 132 (2018) 34–41. doi:10.1016/j.watres.2017.12.059.

[132] L. Fortunato, S. Bucs, R. V. Linares, C. Cali, J. S. Vrouwenvelder, T. Leiknes, Spatially-resolved in-situ quantification of biofouling using optical coherence tomography (OCT) and 3D image analysis in a spacer filled channel, J. Membrane Sci. 524 (2017) 673–681. doi:10.1016/j.memsci.2016.11.052.

[133] S. Park, T. Nam, J. Park, S. Kim, Y. Ahn, S. Lee, Y. M. Kim, W. Jung, K. H. Cho, Investigating the influence of organic matter composition on biofilm volumes in reverse osmosis using optical coherence tomography, Desalination 419 (2017) 125–132. doi:10.1016/j.desal.2017.06.002.

[134] C. Dreszer, H.-C. Flemming, A. Wexler, A. Zwijnenburg, J. Kruithof, J. Vrouwenvelder, Development and testing of a transparent membrane biofouling monitor, Desalin. Water Treat. 52 (10–12) (2014) 1807–1819. doi:10.1080/19443994.2013.874708.

[135] R. V. Linares, A. Wexler, S. Bucs, C. Dreszer, A. Zwijnenburg, H.-C. Flemming, J. Kruithof, J. Vrouwenvelder, Compaction and relaxation of biofilms, Desalin. Water Treat. 57 (28) (2016) 12902–12914. doi:10.1080/19443994.2015.1057036.

[136] J.-G. Lee, Y. Jang, L. Fortunato, S. Jeong, S. Lee, T. Leiknes, N. Ghaffour, An advanced online monitoring approach to study the scaling behavior in direct contact membrane distillation, J. Membrane Sci. 546 (Supplement C) (2018) 50–60. doi:10.1016/j.memsci.2017.10.009.

[137] Q. Han, W. Li, T. A. Trinh, A. G. Fane, J. W. Chew, Effect of the surface charge of monodisperse particulate foulants on cake formation, J. Membrane Sci. 548 (2018) 108–116. doi:10.1016/j.memsci.2017.11.017.

[138] T. A. Trinh, W. Li, Q. Han, X. Liu, A. G. Fane, J. W. Chew, Analyzing external and internal membrane fouling by oil emulsions via 3D optical coherence tomography, J. Membrane Sci. 548 (2018) 632–640. doi:10.1016/j.memsci.2017.10.043.

[139] R. Dsouza, H. M. Subhash, K. Neuhaus, J. Hogan, C. Wilson, M. Leahy, 3D nondestructive testing system with an affordable multiple reference optical-delay-based optical coherence tomography, Appl. Opt. 54 (18) (2015) 5634–5638. doi:10.1364/AO.54.005634.

[140] S. A. Creber, T. Pintelon, D. Graf von der Schulenburg, J. S. Vrouwenvelder, M. van Loosdrecht, M. L. Johns, Magnetic resonance imaging and 3D simulation studies of biofilm accumulation and cleaning on reverse osmosis membranes, Food Bioprod. Process. 88 (4) (2010) 401–408. doi:10.1016/j.fbp.2010.08.010.

[141] D. Graf von der Schulenburg, J. S. Vrouwenvelder, S. A. Creber, M. C. M. van Loosdrecht, M. L. Johns, Nuclear magnetic resonance microscopy studies of membrane biofouling, J. Membrane Sci. 323 (1) (2008) 37–44. doi:10.1016/j.memsci.2008.06.012.

[142] E. O. Fridjonsson, S. J. Vogt, J. S. Vrouwenvelder, M. L. Johns, Early non-destructive biofouling detection in spiral wound RO membranes using a mobile earth's field NMR, J. Membrane Sci. 489 (2015) 227–236. doi:10.1016/j.memsci.2015.03.088.

[143] S. Buetehorn, L. Utiu, M. Küppers, B. Blümich, T. Wintgens, M. Wessling, T. Melin, NMR imaging of local cumulative permeate flux and local cake growth in submerged microfiltration processes, J. Membrane Sci. 371 (1-2) (2011) 52–64. doi:10.1016/j.memsci.2011.01.018.

[144] M. Wiese, C. Malkomes, B. Krause, M. Wessling, Flow and filtration imaging of single use sterile membrane filters, J. Membrane Sci. 552 (2018) 274–285. doi:10.1016/j.memsci.2018.02.002.

[145] S. A. Creber, J. S. Vrouwenvelder, M. van Loosdrecht, M. L. Johns, Chemical cleaning of biofouling in reverse osmosis membranes evaluated using magnetic resonance imaging, J. Membrane Sci. 362 (1-2) (2010) 202–210. doi:10.1016/j.memsci.2010.06.052.

[146] P. Z. Çulfaz, S. Buetehorn, L. Utiu, M. Kueppers, B. Bluemich, T. Melin, M. Wessling, R. G. H. Lammertink, Fouling behavior of microstructured hollow fiber membranes in dead-end filtrations: Critical flux determination and NMR imaging of particle deposition, Langmuir 27 (5) (2011) 1643–1652. doi:10.1021/la1037734.

[147] S. Schuhmann, N. Schork, K. Beller, H. Nirschl, T. Oerther, G. Guthausen, In-situ characterization of deposits in ceramic hollow fiber membranes by compressed sensing RARE-MRI, AIChE J. 64 (11) (2018) 4039–4046. doi:10.1002/aic.16201.

[148] F. Arndt, U. Roth, H. Nirschl, S. Schütz, G. Guthausen, New insights into sodium alginate fouling of ceramic hollow fiber membranes by NMR imaging, AIChE J. 62 (7) (2016) 2459–2467. doi:10.1002/aic.15226.

[149] F. Arndt, S. Schuhmann, G. Guthausen, S. Schütz, H. Nirschl, In situ MRI of alginate fouling and flow in ceramic hollow fiber membranes, J. Membrane Sci. 524 (2017) 691–699. doi:10.1016/j.memsci.2016.11.079.

[150] J. S. Vrouwenvelder, D. A. Graf von der Schulenburg, J. C. Kruithof, M. L. Johns, M. C. M. van Loosdrecht, Biofouling of spiral-wound nanofiltration and reverse osmosis membranes: A feed spacer problem, Water Res. 43 (3) (2009) 583–594. doi:10.1016/j.watres.2008.11.019.

[151] J. S. Vrouwenvelder, C. Picioreanu, J. C. Kruithof, M. van Loosdrecht, Biofouling in spiral wound membrane systems: Three-dimensional CFD model based evaluation of experimental data, J. Membrane Sci. 346 (1) (2010) 71–85. doi:10.1016/j.memsci.2009.09.025.

[152] R. Valladares Linares, L. Fortunato, N. M. Farhat, S. S. Bucs, M. Staal, E. O. Fridjonsson, M. L. Johns, J. S. Vrouwenvelder, T. Leiknes, Mini-review: Novel non-destructive in situ biofilm characterization techniques in membrane systems, Desalination Water Treat. 57 (48-49) (2016) 22894–22901. doi:10.1080/19443994.2016.1180483.

[153] S. West, H. Horn, W. Hijnen, C. Castillo, M. Wagner, Confocal laser scanning microscopy as a tool to validate the efficiency of membrane cleaning procedures to remove biofilms, Sep. Purif. Technol. 122 (2014) 402–411. doi:10.1016/j.seppur.2013.11.032.

[154] D. Bonn, S. Rodts, M. Groenink, S. RafaÃf, N. Shahidzadeh-Bonn, P. Coussot, Some applications of magnetic resonance imaging in fluid mechanics: Complex flows and complex fluids, Annu. Rev. Fluid Mech. 40 (1) (2008) 209–233. doi:10.1146/annurev.fluid.40.111406.102211.

[155] J. Vicente, Y. Wyart, P. Moulin, Characterization (two-dimensional-three-dimensional) of ceramic microfiltration membrane by synchrotron radiation: new and abraded membranes, J. Porous Media 16 (6) (2013) 537–545. doi:10.1615/JPorMedia.v16.i6.50.

[156] A. Yeo, P. Yang, A. Fane, T. White, H. Moser, Non-invasive observation of external and internal deposition during membrane filtration by X-ray microimaging (XMI), J. Membrane Sci. 250 (1-2) (2005) 189–193. doi:10.1016/j.memsci.2004.10.035.

[157] Y. Davit, G. Iltis, G. Debenest, S. Veran-Tissoires, D. Wildenschild, M. Gerino, M. Quintard, Imaging biofilm in porous media using X-ray computed microtomography, J. Microsc. 242 (1) (2011) 15–25. doi:10.1111/j.1365-2818.2010.03432.x.

[158] C. David, F. Pignon, T. Narayanan, M. Sztucki, G. Gésan-Guiziou, A. Magnin, Spatial and temporal in situ evolution of the concentration profile during casein micelle ultrafiltration probed by small-angle X-ray scattering, Langmuir 24 (9) (2008) 4523–4529. doi:10.1021/la703256s.

[159] Y. Jin, N. Hengl, S. Baup, F. Pignon, N. Gondrexon, M. Sztucki, G. Gésan-Guiziou, A. Magnin, M. Abyan, M. Karrouch, D. Blésès, Effects of ultrasound on cross-flow ultrafiltration of skim milk: Characterization from macro-scale to nano-scale, J. Membrane Sci. 470 (2014) 205–218. doi:10.1016/j.memsci.2014.07.043.

[160] Y. N. Dahdal, V. Pipich, H. Rapaport, Y. Oren, R. Kasher, D. Schwahn, Small-angle neutron scattering studies of alginate as biomineralizing agent and scale initiator, Polymer 85 (2016) 77–88. doi:10.1016/j.polymer.2016.01.012.

[161] R. Gebhardt, T. Steinhauer, P. Meyer, J. Sterr, J. Perlich, U. Kulozik, Structural changes of deposited casein micelles induced by membrane filtration, Faraday Discuss. 158 (1–2) (2012) 77. doi:10.1039/c2fd20022h.

[162] T. Steinhauer, U. Kulozik, R. Gebhardt, Structure of milk protein deposits formed by casein micelles and beta-lactoglobulin during frontal microfiltration, J. Membrane Sci. 468 (2014) 126–132. doi:10.1016/j.memsci.2014.05.027.

[163] V. Pipich, Y. Dahdal, H. Rapaport, R. Kasher, Y. Oren, D. Schwahn, Effects of biological molecules on calcium mineral formation associated with wastewater desalination as assessed using small-angle neutron scattering, Langmuir 29 (25) (2013) 7607–7617. doi:10.1021/la4001889.

[164] Y. N. Dahdal, V. Pipich, H. Rapaport, Y. Oren, R. Kasher, D. Schwahn, Small-angle neutron scattering studies of mineralization on BSA coated citrate capped gold nanoparticles used as a model surface for membrane scaling in RO wastewater desalination, Langmuir 30 (50) (2014) 15072–15082. doi:10.1021/la502706k.

[165] D. Schwahn, H. Feilbach, T. Starc, V. Pipich, R. Kasher, Y. Oren, Design and test of a reverse osmosis pressure cell for in-situ small-angle neutron scattering studies, Desalination 405 (2017) 40–50. doi:10.1016/j.desal.2016.11.026.

[166] Y. A. Elabd, M. G. Baschetti, T. A. Barbari, Time-resolved Fourier transform infrared/attenuated total reflection spectroscopy for the measurement of molecular diffusion in polymers, J. Polym. Sci. B Polym. Phys. 41 (22) (2003) 2794–2807. doi:10.1002/polb.10661.

[167] B. S. Beckingham, N. A. Lynd, D. J. Miller, Monitoring multicomponent transport using in situ ATR FTIR spectroscopy, J. Membrane Sci. 550 (2018) 348–356. doi:10.1016/j.memsci.2017.12.072.

[168] C. Kötting, K. Gerwert, Proteins in action monitored by time-resolved FTIR spectroscopy, Chemphyschem 6 (5) (2005) 881–888. doi:10.1002/cphc.200400504.

[169] S. Morita, M. Tanaka, Y. Ozaki, Time-Resolved in situ ATR-IR observations of the process of sorption of water into a Poly(2-methoxyethyl acrylate) film, Langmuir 23 (7) (2007) 3750–3761. doi:10.1021/la0625998.

[170] R. K. Singh, K. Kunimatsu, K. Miyatake, T. Tsuneda, Experimental and theoretical infrared spectroscopic study on hydrated nafion membrane, Macromolecules 49 (17) (2016) 6621–6629. doi:10.1021/acs.macromol.6b00999.

[171] H.-Y. N. Holman, R. Miles, Z. Hao, E. Wozei, L. M. Anderson, H. Yang, Real-time chemical imaging of bacterial activity in biofilms using open-channel microfluidics and synchrotron FTIR spectromicroscopy, Anal. Chem. 81 (20) (2009) 8564–8570. doi:10.1021/ac9015424.

[172] J. Speed, Vibration-resistant FT-IR for in-process monitoring of an industrial fermentation process, Spectroscopy 21 (8) (2016) 38.

[173] L. Cui, M. Yao, B. Ren, K. Zhang, Sensitive and versatile detection of the fouling process and fouling propensity of proteins on polyvinylidene fluoride membranes via surface-enhanced Raman spectroscopy, Anal. Chem. 83 (5) (2011) 1709–1716. doi:10.1021/ac102891g.

[174] M. Kögler, B. Zhang, L. Cui, Y. Shi, M. Yliperttula, T. Laaksonen, T. Viitala, K. Zhang, Real-time Raman based approach for identification of biofouling, Sens. Actuators B Chem. 230 (2016) 411–421. doi:10.1016/j.snb.2016.02.079.

[175] T. Virtanen, S.-P. Reinikainen, M. Kögler, M. Mänttäri, T. Viitala, M. Kallioinen, Real-time fouling monitoring with Raman spectroscopy, J. Membrane Sci. 525 (2017) 312–319. doi:10.1016/j.memsci.2016.12.005.

[176] T. Virtanen, S.-P. Reinikainen, J. Lahti, M. Mänttäri, M. Kallioinen, Visual tool for real-time monitoring of membrane fouling via Raman spectroscopy and

process model based on principal component analysis, Sci. Rep. 8 (1) (2018) 11057. doi:10.1038/s41598-018-29268-y.

[177] R. Lamsal, S. G. Harroun, C. L. Brosseau, G. A. Gagnon, Use of surface enhanced Raman spectroscopy for studying fouling on nanofiltration membrane, Sep. Purif. Technol. 96 (2012) 7–11. doi:10.1016/j.seppur.2012.05.019.

[178] Y. Chao, T. Zhang, Surface-enhanced Raman scattering (SERS) revealing chemical variation during biofilm formation: From initial attachment to mature biofilm, Anal. Bioanal. Chem. 404 (5) (2012) 1465–1475. doi:10.1007/s00216-012-6225-y.

[179] P. Chen, L. Cui, K. Zhang, Surface-enhanced Raman spectroscopy monitoring the development of dual-species biofouling on membrane surfaces, J. Membrane Sci. 473 (2015) 36–44. doi:10.1016/j.memsci.2014.09.007.

[180] L. Cui, P. Chen, B. Zhang, D. Zhang, J. Li, F. L. Martin, K. Zhang, Interrogating chemical variation via layer-by-layer SERS during biofouling and cleaning of nanofiltration membranes with further investigations into cleaning efficiency, Water Res. 87 (2015) 282–291. doi:10.1016/j.watres.2015.09.037.

[181] W. Chen, C. Qian, W.-L. Hong, J.-X. Cheng, H.-Q. Yu, Evolution of membrane fouling revealed by label-free vibrational spectroscopic imaging, Environ. Sci. Technol. 51 (17) (2017) 9580–9587. doi:10.1021/acs.est.7b02775.

[182] W. J. Tipping, M. Lee, A. Serrels, V. G. Brunton, A. N. Hulme, Stimulated Raman scattering microscopy: an emerging tool for drug discovery, Chem. Soc. Rev. 45 (8) (2016) 2075–2089. doi:10.1039/c5cs00693g.

[183] J. Duboisset, P. Berto, P. Gasecka, F.-Z. Bioud, P. Ferrand, H. Rigneault, S. Brasselet, Molecular orientational order probed by coherent anti-Stokes Raman scattering (CARS) and stimulated Raman scattering (SRS) microscopy: a spectral comparative study, J. Phys. Chem. B 119 (7) (2015) 3242–3249. doi:10.1021/jp5113813.

[184] S. Bannwarth, T. Trieu, C. Oberschelp, M. Wessling, On-line monitoring of cake layer structure during fouling on porous membranes by in situ electrical impedance analysis, J. Membrane Sci. 503 (2016) 188–198. doi:10.1016/j.memsci.2016.01.009.

[185] J. S. Ho, L. N. Sim, R. D. Webster, B. Viswanath, H. G. L. Coster, A. G. Fane, Monitoring fouling behavior of reverse osmosis membranes using electrical impedance spectroscopy: A field trial study, Desalination 407 (2017) 75–84. doi:10.1016/j.desal.2016.12.012.

[186] J.-S. Park, T. C. Chilcott, H. G. L. Coster, S.-H. Moon, Characterization of BSA-fouling of ion-exchange membrane systems using a subtraction technique for lumped data, J. Membrane Sci. 246 (2) (2005) 137–144. doi:10.1016/j.memsci.2004.07.022.

[187] T. C. Chilcott, Origin of resonant electrical impedances in membranes induced by osmosis: Analytical solutions of the AC Nernst–Planck, Poisson and continuity equations as functions of water velocity, J. Membrane Sci. 438 (2013) 65–76. doi:10.1016/j.memsci.2013.03.022.

[188] J. Cen, J. Kavanagh, H. Coster, G. Barton, Fouling of reverse osmosis mebranes by cane molasses fermentation wastewater: detection by electrical impedance spectroscopy techniques, Desalination Water Treat. 51 (2013) 969–975.

[189] J. Cen, M. Vukas, G. Barton, J. Kavanagh, H. G. L. Coster, Real time fouling monitoring with Electrical Impedance Spectroscopy, J. Membrane Sci. 484 (2015) 133–139. doi:10.1016/j.memsci.2015.03.014.

[190] L. N. Sim, Z. J. Wang, J. Gu, H. G. L. Coster, A. G. Fane, Detection of reverse osmosis membrane fouling with silica, bovine serum albumin and their mixture using in-situ electrical impedance spectroscopy, J. Membrane Sci. 443 (2013) 45–53. doi:10.1016/j.memsci.2013.04.047.

[191] M. C. Martí-Calatayud, S. Schneider, M. Wessling, On the rejection and reversibility of fouling in ultrafiltration as assessed by hydraulic impedance spectroscopy, J. Membrane Sci. 564 (2018) 532–542. doi:10.1016/j.memsci.2018.07.021.

[192] B. Teychene, P. Loulergue, C. Guigui, C. Cabassud, Development and use of a novel method for in line characterisation of fouling layers electrokinetic properties and for fouling monitoring, J. Membrane Sci. 370 (1-2) (2011) 45–57. doi:10.1016/j.memsci.2010.12.014.

[193] Y. Lanteri, P. Fievet, C. Magnenet, S. Déon, A. Szymczyk, Electrokinetic characterisation of particle deposits from streaming potential coupled with permeate flux measurements during dead-end filtration, J. Membrane Sci. 378 (1-2) (2011) 224–232. doi:10.1016/j.memsci.2011.05.002.

[194] H. Jia, H. Zhang, J. Wang, H. Zhang, X. Zhang, Response of zeta potential to different types of local membrane fouling in dead-end membrane filtration with yeast suspension, RSC Adv. 5 (96) (2015) 78738–78744. doi:10.1039/C5RA12668A.

[195] K. Nakamura, T. Orime, K. Matsumoto, Response of zeta potential to cake formation and pore blocking

during the microfiltration of latex particles, J. Membrane Sci. 401-402 (2012) 274–281. doi:10.1016/j.memsci.2012.02.013.

[196] K. Nakamura, T. Orime, K. Matsumoto, Zeta potential monitoring during microfiltration of humic acid, J. Chem. Eng. Jpn. 45 (8) (2012) 583–589.

[197] J. Wang, S. Yang, W. Guo, H.-H. Ngo, H. Jia, J. Yang, H. Zhang, X. Zhang, Characterization of fouling layers for in-line coagulation membrane fouling by apparent zeta potential, RSC Adv. 5 (128) (2015) 106087–106093. doi:10.1039/C5RA18826A.

[198] J. Liu, J. Xiong, X. Ju, B. Gao, L. Wang, M. Sillanpää, Streaming potential for identification of foulants adsorption on PVDF membrane surface, J. Membrane Sci. 566 (2018) 428–434. doi:10.1016/j.memsci.2018.09.024.

[199] M.-S. Chun, H. Il Cho, I. K. Song, Electrokinetic behavior of membrane zeta potential during the filtration of colloidal suspensions, Desalination 148 (1-3) (2002) 363–368. doi:10.1016/S0011-9164(02)00731-2.

[200] S. Mikhaylin, L. Bazinet, Fouling on ion-exchange membranes: Classification, characterization and strategies of prevention and control, Adv. Colloid Interface Sci. 229 (2016) 34–56. doi:10.1016/j.cis.2015.12.006.

[201] H.-J. Lee, M.-K. Hong, S.-D. Han, J. Shim, S.-H. Moon, Analysis of fouling potential in the electrodialysis process in the presence of an anionic surfactant foulant, J. Membrane Sci. 325 (2) (2008) 719–726. doi:10.1016/j.memsci.2008.08.045.

[202] E. Volodina, N. Pismenskaya, V. Nikonenko, C. Larchet, G. Pourcelly, Ion transfer across ion-exchange membranes with homogeneous and heterogeneous surfaces, J. Colloid Interface Sci. 285 (1) (2005) 247–258. doi:10.1016/j.jcis.2004.11.017.

[203] S. Suwal, J. Amiot, L. Beaulieu, L. Bazinet, Effect of pulsed electric field and polarity reversal on peptide/amino acid migration, selectivity and fouling mitigation, J. Membrane Sci. 510 (2016) 405 – 416. doi:10.1016/j.memsci.2016.03.010.

[204] A. Bukhovets, T. Eliseeva, N. Dalthrope, Y. Oren, The influence of current density on the electrochemical properties of anion-exchange membranes in electrodialysis of phenylalanine solution, Electrochim. Acta 56 (27) (2011) 10283–10287. doi:10.1016/j.electacta.2011.09.025.

[205] T. V. Eliseeva, A. Y. Kharina, Voltammetric and transport characteristics of anion-exchange membranes during electrodialysis of solutions containing alkylaromatic amino acid and a mineral salt, Russ. J. Electrochem. 51 (1) (2015) 63–69. doi:10.1134/S1023193515010048.

[206] M. Andreeva, V. Gil, N. Pismenskaya, L. Dammak, N. Kononenko, C. Larchet, D. Grande, V. Nikonenko, Mitigation of membrane scaling in electrodialysis by electroconvection enhancement, pH adjustment and pulsed electric field application, J. Membrane Sci. 549 (2018) 129–140. doi:10.1016/j.memsci.2017.12.005.

[207] E. Güler, W. van Baak, M. Saakes, K. Nijmeijer, Monovalent-ion-selective membranes for reverse electrodialysis, J. Membrane Sci. 455 (2014) 254–270. doi:10.1016/j.memsci.2013.12.054.

[208] J.-H. Chang, A. V. Ellis, C.-H. Tung, W.-C. Huang, Copper cation transport and scaling of ionic exchange membranes using electrodialysis under electroconvection conditions, J. Membrane Sci. 361 (1) (2010) 56–62. doi:10.1016/j.memsci.2010.06.012.

[209] R. Zerdoumi, K. Oulmi, S. Benslimane, Electrochemical characterization of the CMX cation exchange membrane in buffered solutions: Effect on concentration polarization and counterions transport properties, Desalination 340 (2014) 42–48. doi:10.1016/j.desal.2014.02.014.

[210] H.-J. Lee, S.-H. Moon, Analyses of fouling potentials in electrodialysis process using electrochemical methods, in: Asian Pacific Confederation of Chemical Engineering congress program and abstracts Asian Pacific Confederation of Chemical Engineers congress program and abstracts, 2004, pp. 761–761.

[211] A. Bukhovets, T. Eliseeva, Y. Oren, Fouling of anion-exchange membranes in electrodialysis of aromatic amino acid solution, J. Membrane Sci. 364 (1) (2010) 339–343. doi:10.1016/j.memsci.2010.08.030.

[212] Z. Zhao, S. Shi, H. Cao, Y. Li, Electrochemical impedance spectroscopy and surface properties characterization of anion exchange membrane fouled by sodium dodecyl sulfate, J. Membrane Sci. 530 (2017) 220–231. doi:10.1016/j.memsci.2017.02.037.

[213] Z. Zhao, S. Shi, H. Cao, B. Shan, Y. Sheng, Property characterization and mechanism analysis on organic fouling of structurally different anion exchange membranes in electrodialysis, Desalination 428 (2018) 199–206. doi:10.1016/j.desal.2017.11.021.

[214] Y. Jin, Y. Zhao, H. Liu, A. Sotto, C. Gao, J. Shen, A durable and antifouling monovalent selective anion exchange membrane modified by polydopamine and sulfonated reduced graphene oxide, Sep. Purif. Technol. 207 (2018) 116–123. doi:10.1016/j.seppur.2018.06.053.

[215] H. Guo, L. Xiao, S. Yu, H. Yang, J. Hu, G. Liu, Y. Tang, Analysis of anion exchange membrane fouling mechanism caused by anion polyacrylamide in electrodialysis, Desalination 346 (2014) 46–53. doi:10.1016/j.desal.2014.05.010.

[216] M. Martí-Calatayud, D. Buzzi, M. García-Gabaldón, A. Bernardes, J. Tenório, V. Pérez-Herranz, Ion transport through homogeneous and heterogeneous ion-exchange membranes in single salt and multicomponent electrolyte solutions, J. Membrane Sci. 466 (2014) 45–57. doi:10.1016/j.memsci.2014.04.033.

[217] T. Gu, Y. J. M. Chew, W. R. Paterson, D. I. Wilson, Experimental and CFD studies of fluid dynamic gauging in duct flows, Chem. Eng. Sci. 64 (2) (2009) 219–227. doi:10.1016/j.ces.2008.09.032.

[218] Y. J. M. Chew, W. R. Paterson, D. I. Wilson, Fluid dynamic gauging: A new tool to study deposition on porous surfaces 296 (1-2) (2007) 29–41. doi:10.1016/j.memsci.2007.03.009.

[219] S. A. Jones, Y. J. M. Chew, D. I. Wilson, M. R. Bird, Fluid dynamic gauging of microfiltration membranes fouled with sugar beet molasses, J. Food Eng. 108 (1) (2012) 22–29. doi:10.1016/j.jfoodeng.2011.08.001.

[220] W. J. T. Lewis, Y. J. M. Chew, M. R. Bird, The application of fluid dynamic gauging in characterising cake deposition during the cross-flow microfiltration of a yeast suspension, J. Membrane Sci. 405-406 (2012) 113–122. doi:10.1016/j.memsci.2012.02.065.

[221] S. R. Suwarno, W. Huang, Y. J. M. Chew, S. H. H. Tan, A. E. Trisno, Y. Zhou, On-line biofilm strength detection in cross-flow membrane filtration systems, Biofouling 34 (2) (2018) 123–131. doi:10.1080/08927014.2017.1409892.

[222] X. Du, F. Qu, H. Liang, K. Li, H. Chang, G. Li, Cake properties in ultrafiltration of TiO2 fine particles combined with HA: in situ measurement of cake thickness by fluid dynamic gauging and CFD calculation of imposed shear stress for cake controlling, Environ. Sci. Pollut. R. 23 (9) (2016) 8806–8818. doi:10.1007/s11356-015-5984-3.

[223] T. Mattsson, W. J. T. Lewis, Y. J. M. Chew, M. R. Bird, In situ investigation of soft cake fouling layers using fluid dynamic gauging, Food Bioprod. Process. 93 (2015) 205–210. doi:10.1016/j.fbp.2014.09.003.

[224] W. J. T. Lewis, A. Agg, A. Clarke, T. Mattsson, Y. J. M. Chew, M. R. Bird, Development of an automated, advanced fluid dynamic gauge for cake fouling studies in cross-flow filtrations, Sens. Actuators A Phys. 238 (2016) 282–296. doi:10.1016/j.sna.2015.12.019.

[225] W. J. T. Lewis, T. Mattsson, Y. J. M. Chew, M. R. Bird, Investigation of cake fouling and pore blocking phenomena using fluid dynamic gauging and critical flux models, J. Membrane Sci. 533 (2017) 38–47. doi:10.1016/j.memsci.2017.03.020.

[226] T. Mattsson, W. J. T. Lewis, Y. J. M. Chew, M. R. Bird, The use of fluid dynamic gauging in investigating the thickness and cohesive strength of cake fouling layers formed during cross-flow microfiltration, Sep. Purif. Technol. 198 (2018) 25–30. doi:10.1016/j.seppur.2017.01.040.

[227] P. W. Gordon, A. D. M. Brooker, Y. J. M. Chew, D. I. Wilson, D. W. York, A scanning fluid dynamic gauging technique for probing surface layers, Meas. Sci. Technol. 21 (8) (2010) 085103. doi:10.1088/0957-0233/21/8/085103.

[228] M. Strathmann, K.-H. Mittenzwey, G. Sinn, W. Papadakis, H.-C. Flemming, Simultaneous monitoring of biofilm growth, microbial activity, and inorganic deposits on surfaces with an in situ, online, real-time, non-destructive, optical sensor, Biofouling 29 (5) (2013) 573–583. doi:10.1080/08927014.2013.791287.

[229] M. Fischer, M. Wahl, G. Friedrichs, Design and field application of a UV-LED based optical fiber biofilm sensor, Biosens. Bioelectron. 33 (1) (2012) 172–178. doi:10.1016/j.bios.2011.12.048.

[230] U. Borchers, J. Gray, K. Thompson, Water Contamination Emergencies: Managing the Threats, Royal Society of Chemistry, Cambridge, UK, 2013.

[231] I. L. S. Mei, I. Ismail, A. Shafquet, B. Abdullah, Real-time monitoring and measurement of wax deposition in pipelines via non-invasive electrical capacitance tomography, Meas. Sci. Technol. 27 (2) (2015) 1–11. doi:10.1088/0957-0233/27/2/025403.

[232] Q. Shi, S. Ye, C. Kristalyn, Y. Su, Z. Jiang, Z. Chen, Probing molecular-level surface structures of solyethersulfone/pluronic F127 blends using sum-frequency generation vibrational spectroscopy, Langmuir 24 (15) (2008) 7939–7946. doi:10.1021/la800570a.